

Investigating the interaction of Hepatitis C virus non-structural protein NS5A with the methyltransferase SMYD3

Doctoral thesis at the Medical University of Vienna for obtaining the
academic degree

Doctor of Philosophy (PhD)

Submitted by

Carol-Ann Eberle, B.A. (hons.)

Supervisor:

Prof. Giulio Superti-Furga

CeMM - Research Center for Molecular Medicine of the Austrian
Academy of Sciences

Lazarettgasse 14, AKH BT 25.3, 1090, Vienna, Austria

Vienna, December 2014

TABLE OF CONTENTS

DECLARATION.....	i
ACKNOWLEDGEMENTS	ii
ABSTRACT.....	iii
ZUSAMMENFASSUNG	iv
LIST OF FIGURES.....	vi
ABBREVIATIONS	vii
1. INTRODUCTION.....	1
1.1 Hepatitis C – a general overview.....	1
1.1.1 Epidemiology.....	1
1.1.2 Classification and genetic diversity	1
1.1.3 Current treatment options.....	2
1.2 Molecular biology of HCV	3
1.2.1 Genome and proteome organization	3
1.2.2 The viral life cycle	5
1.3 The non-structural protein NS5A	7
1.3.1 Structure and function.....	7
1.3.2 NS5A phosphorylation	9
1.4 <i>In vitro</i> models for HCV	9
1.4.1 HCV replicon systems	10
1.4.2 Cell-culture derived HCV.....	11
1.4.3 HCV-like virus particles	12
1.4.4 Permissive cell lines.....	13
1.5 The biology of lysine methylation and protein lysine methyltransferases	13
1.6 The SET- and MYND domain containing lysine methyltransferase SMYD3	16
1.6.1 Structural features.....	16
1.6.2 Functional features.....	17
2. AIMS.....	19
3. RESULTS.....	20
3.1 Prologue manuscript: The lysine methyltransferase SMYD3 interacts with hepatitis C virus NS5A and is a negative regulator of viral particle production.	20
3.1.1 The lysine methyltransferase SMYD3 interacts with hepatitis C virus NS5A and is a negative regulator of viral particle production.....	22
3.2 Prologue: Generating a SMYD3-binding mutant virus and identification of NS5A post-translational methylation sites.....	38
3.2.1 Mapping the SMYD3 binding site.....	39
3.2.2 Effect of P417/P418 on the viral life cycle	40
3.2.3 Proteomic approach to Identify putative methylation sites in NS5A.....	43

3.2.4 Functional validation of K240.....	46
4. CONCLUDING DISCUSSION	49
4.1 Identification of NS5A-binding proteins using a proteomic approach.....	49
4.2 SMYD3 interacts with NS5A and negatively regulates HCV virion assembly.....	50
4.2.1 SMYD3 overexpression inhibits infectious particle assembly.....	51
4.2.2 Infectious particle assembly is impaired in a SMYD3-binding mutant virus.....	51
4.3 Identification of K240 as a putative NS5A post-translational methylation site.....	53
5. MATERIALS AND METHODS.....	55
5.1 Materials	55
5.1.1 Buffers and solutions.....	55
5.1.2 Antibodies.....	56
5.1.3 Plasmids.....	57
5.1.4 Primer sequences.....	58
5.2 Methods.....	61
5.2.1 Cloning.....	61
5.2.2 <i>In vitro</i> transcription.....	62
5.2.3 Cell biology.....	63
5.2.4 SDS-PAGE and Western blot.....	66
5.2.5 Virological methods.....	67
6. BIBLIOGRAPHY.....	69
7. APPENDIX.....	81

DECLARATION

The following thesis includes the projects developed in the last four years by the author herself. The manuscript has been written in the cumulative format and includes one first author publication. In addition, the thesis includes experimental work as part of the project but not included in the published article.

Work contributed by other parties include: analysis of mass spectral data was performed by Dr. Alexey Stukalov and Dr. Florian Breitwieser. Due to the lack of an appropriate biosafety level 3 laboratory in Vienna, all experiments involving infectious genotype 2a Jc1 genotypes were conducted by the author herself during a total of 3 research stays at the laboratory of Prof. Ralf Bartenschlager in Heidelberg (April – June 2012; August – October 2012; March and April 2014)

ACKNOWLEDGEMENTS

The four years I spent at CeMM in the laboratory of Prof. Giulio Superti-Furga were truly unique and I would not have liked to miss a single minute of them. They have shaped me in a professional, personal as well as athletic way. I would like to take this opportunity to extend my gratitude to everybody who has supported me throughout the pursuit of my PhD:

First and foremost, I would like to thank my supervisor Prof. Giulio Superti-Furga for giving me the opportunity to join such an outstanding research institution. I am very grateful for his advice and constant support. Even in difficult times and when facing difficult decisions regarding my future career, I knew I could always rely on his support. Without him I would not be where I am now.

I would also like to extend my gratitude to Prof. Ralf Bartenschlager for hosting me in his laboratory and his support and contributions allowing me to publish my paper. I also have to thank Dr. Margarita Zayas for mentoring me during my time in Heidelberg and from whom I have learned a lot. Margara has impressed me in many ways and I will miss working with her.

Moreover, I would like to mention Dr. Andreas Pichlmair and Dr. Andreas Bergthaler for their constant guidance throughout my PhD. I sincerely hope we will stay in contact in future. I would also like to thank Anita Ender and Catherine Lloyd; Anita for her advice and willingness to help, and Catherine for guiding me throughout the compilation of this thesis. Furthermore, I would like to thank Roberto Giambruno, Eilis Carroll and Moritz Körber for their input and critical proofreading of my thesis.

I also have to extend a special thank you to all the former and current members of the Superti-Furga and the Bergthaler lab for their scientific and mental support, their fruitful discussion and all the fun-times outside of CeMM.

I would also like to acknowledge my thesis committee members Prof. Sylvia Knapp and Prof Franz-Xaver Heinz for their support and advice. Along the line I would also like to say thank you to my fellow CCHD colleagues, with whom I had an amazing four years.

Last but not least, I owe sincere and earnest thankfulness to my family and friends, for their support, their understanding for long working hours and just being there when I needed them.

ABSTRACT

Hepatitis C virus (HCV) is one of the major causes of chronic hepatitis and the most common indication for liver transplantation. With ~3% of the world's population being infected, HCV constitutes a global health as well as economic burden. Recent progress in the development of antiviral treatment strategies has led to the approval of a set of very efficient direct-acting antivirals. Given in combination with pegylated interferon α (pegIFN α) and ribavirin, these drugs have significantly improved the cure rates of HCV. However, the high cost, severe side effects and the development of viral resistance remain a major challenge. Hence a better understanding of the yet enigmatic biology of the HCV life cycle is vital for improving current HCV treatment options.

The HCV non-structural protein NS5A is a multifunctional protein and essential for regulating viral replication and particle assembly. A previous large-scale proteomic screen to map virus-host interactions identified the lysine methyltransferase SMYD3 as a novel NS5A binding protein. In the first part of this thesis I confirm the interaction and show that SMYD3 binds to two highly conserved prolines (P417 and P418) in domain III of NS5A via its MYND domain. Furthermore, both proteins also interact in the context of viral infection, with a preference of SMYD3 for the hyperphosphorylated form of NS5A. Functional studies using subgenomic HCV replicons as well as infectious cell-culture systems indicate that SMYD3 negatively regulates infectious virus particle production, while having no impact on viral RNA replication.

In the second part I investigated the possibility of NS5A being regulated by post-translational methylation. Re-analysis of available NS5A mass-spectrometry data revealed lysine K240 as a potential methylation site. With few exceptions, K240 is highly conserved across all genotypes. Introducing an alanine at this site induced a band shift observable by immunoblot resembling NS5A hyperphosphorylation. In addition, comparing wild type subgenomic replicon activity with replication of various point mutants suggested that this residue influences replication in a genotype-dependent manner. Overall, my results highlight how changing the same residue in distinct genotypes can have profoundly different outcomes, emphasizing the difficulties in identifying pan-anti-HCV direct-acting antivirals. At the same time, my data also highlight the need for caution when using mass-spectrometry for the identification of post-translational methylation sites.

ZUSAMMENFASSUNG

Das Hepatitis C Virus (HCV) gilt als eine der Hauptursachen für chronische Hepatitis und als häufigste Indikation für Lebertransplantationen. Mit ~ 3% Infizierten in der Weltbevölkerung stellt HCV ein globales Gesundheitsproblem sowie ein wirtschaftliches Problem dar. Aktuelle Fortschritte in der Entwicklung von antiviralen Behandlungsmethoden haben die Zulassung einer Reihe von effizienten direkt-wirkenden antiviralen Substanzen ermöglicht. Gegeben in Kombination mit pegyliertem Interferon α (pegIFN α) und Ribavirin führen diese Medikamente bei HCV-Infektionen zu einer signifikant erhöhten Heilungsrate. Allerdings bleiben die hohen Kosten, schwere Nebenwirkungen und die Entwicklung resistenter Virenstämme weiterhin als ungelöste Probleme bestehen. Deshalb ist ein besseres Verständnis der noch immer weitgehend unerklärten Biologie des HCV Lebenszyklus wichtig für die Weiterentwicklung aktueller Behandlungsmethoden.

Das HCV nicht-strukturelle Protein NS5A ist ein multifunktionales Protein und essentiell zur Regulierung der viralen Replikation sowie des Viruspartikelbaus. Eine vorherige proteom-weite Studie zur Untersuchung der Virus-Wirt-Interaktion identifizierte die Lysin-Methyltransferase SMYD3 als ein neuartiges NS5A Bindungsprotein. Im ersten Teil dieser Arbeit wird die Interaktion nachgewiesen sowie aufgezeigt, dass SMYD3 sich an zwei hochkonservierte Proline (P417 and P418) in Domäne III des NS5A via seiner MYND Domäne bindet. Außerdem interagieren beide Proteine auch im Kontext einer viralen Infektion, wobei die Präferenz des SMYD3 in der hyperphosphorlierten Form des NS5A liegt. Funktionale Studien, welche das subgenome HCV Replikon- sowie das infektiöse Zellkultursystem einsetzten, zeigten, dass SMYD3 die virale Partikelproduktion negativ reguliert, ohne jedoch Einfluss auf die virale RNA Replikation zu haben.

Im zweiten Teil der Arbeit wird untersucht, ob NS5A von posttranslationaler Methylierung reguliert wird. Eine wiederholte Analyse der verfügbaren NS5A Massenspektrometriedaten zeigte, dass Lysin K240 als mögliche Methylierungsstelle denkbar ist. Mit wenigen Ausnahmen ist K240 über alle Genotypen hoch konserviert. Eine Westernblot-Analyse zeigte, dass die Einführung eines Alanin an dieser Stelle eine Verschiebung der Proteinbanden induzierte, welches der NS5A Hyperphosphorylierung gleicht. Zudem legte der Vergleich der Aktivität wildtypischer subgenomischer Replikone mit der Replikation verschiedener Mutanten nahe, dass das Residuum die Replikation in einer vom Genotyp abhängigen Manier beeinflusst. Insgesamt stellen die Ergebnisse heraus, wie die Veränderung desselben Residuums zu unterschiedlichen Genotyp-spezifischen Resultaten führen kann. Dies betont die Problematik während der Identifikation von pan-anti-HCV direkt-agierend antiviraler Medikamente. Gleichzeitig geht aus den gewonnenen Daten hervor, dass

bei der Verwendung eines Massenspektrometers zur Identifikation posttranslationalen Methylierungsstellen Vorsicht geboten ist

LIST OF FIGURES

- Figure 1: Global distribution and prevalence of the different HCV genotypes
- Figure 2: HCV genome and proteome organization
- Figure 3: Overview of the Hepatitis C virus life cycle
- Figure 4: NS5A domain structure
- Figure 5: Overview of commonly used HCV replicons
- Figure 6: Posttranslational lysine modification
- Figure 7: SMYD3 structure
- Figure 8: Conserved proline-motifs in DIII of NS5A
- Figure 9: SMYD3 interacts with NS5A through prolines 417 and 418
- Figure 10: Effect of NS5A P417/418A on the viral life cycle
- Figure 11: NS5A possesses two putative lysine methylation sites
- Figure 12: Conservation of K240 and K378
- Figure 13: Effect of K240, R240 and A240 on viral replication
- Figure 14: Protein levels of wild type and mutant NS5A

ABBREVIATIONS

(+)ssRNA	Positive single-stranded RNA
BSL-3	Biosafety level 3
CIP	Calf intestinal phosphatase
CKI- α , CKII- α	Casein Kinases I- α and II- α
CLDN1	Claudin-1
EGFR	Epidermal growth factor receptor
EPH	Ephrin receptor A2
ER	Endoplasmatic reticulum
EZ	Enhancer of Zeste
HCV	Hepatitis C virus
HCVcc	Cell-cultured derived HCV
HIV	Human immunodeficiency virus
hpe	Hours post electroporation
HTLV-1	Human T-cell leukemia virus type 1
IRES	Internal ribosome entry site
JFH-1	Japanese fulminant hepatitis-1
JmjC	Jumonji C
JNK	Jun N-terminal kinase
KDM	Lysine demethylase
KMT	Lysine methyltransferase
LCS	Low complexity sequence
LDL	Low-density lipoprotein
LSD	Lysine-specific demethylase
LVP	Lipoviroparticle
MAP3K2	Mitogen-Activated Protein Kinase Kinase Kinase 2
MS	Mass spectrometry
MYND	Myeloid-Nervy-DEAF-1
NEO	Neomycin
NPC1L1	Niemann–Pick C1-like 1
NS5A	Non-structural protein 5A
OCLN	Occludin
pegIFN α	Pegylated interferon α

PI4KIII α	Phosphatidylinositol 4-kinase
PI4P	Phosphatidylinositol-4-phosphate
PIP	Phosphatidylinositolphosphate
PKMT	Protein lysine methyltransferase
PPIase	Peptidyl-prolyl isomerase
PTM	Post-translational modification
Rb	Retinoblastoma protein
RC	Replication complex
RIZ	Retinoblastoma-interacting zinc-finger
RLU	Relative light units
SAM	S-adenosyl-L-methionine
SET	SU(var), Enhancer of Zeste and Trithorax
sg	subgenomic
SILAC	Stable isotope labeling by amino acids in cell culture
SMYD2	SET- and MYND-domain containing protein 2
SMYD3	SET- and MYND-domain containing protein 3
SR-BI	Scavenger receptor class B member 1
STAT1	Signal Transducers and Activators of Transcription
TAP-MS	Tandem-affinity-mass spectrometry
TFR1	Transferrin receptor 1
VEGFR1	Vascular endothelial growth factor receptor 1
VELOS	LTQ Orbitrap Velos mass-spectrometer
VLDL	Very-low-density lipoprotein

1. INTRODUCTION

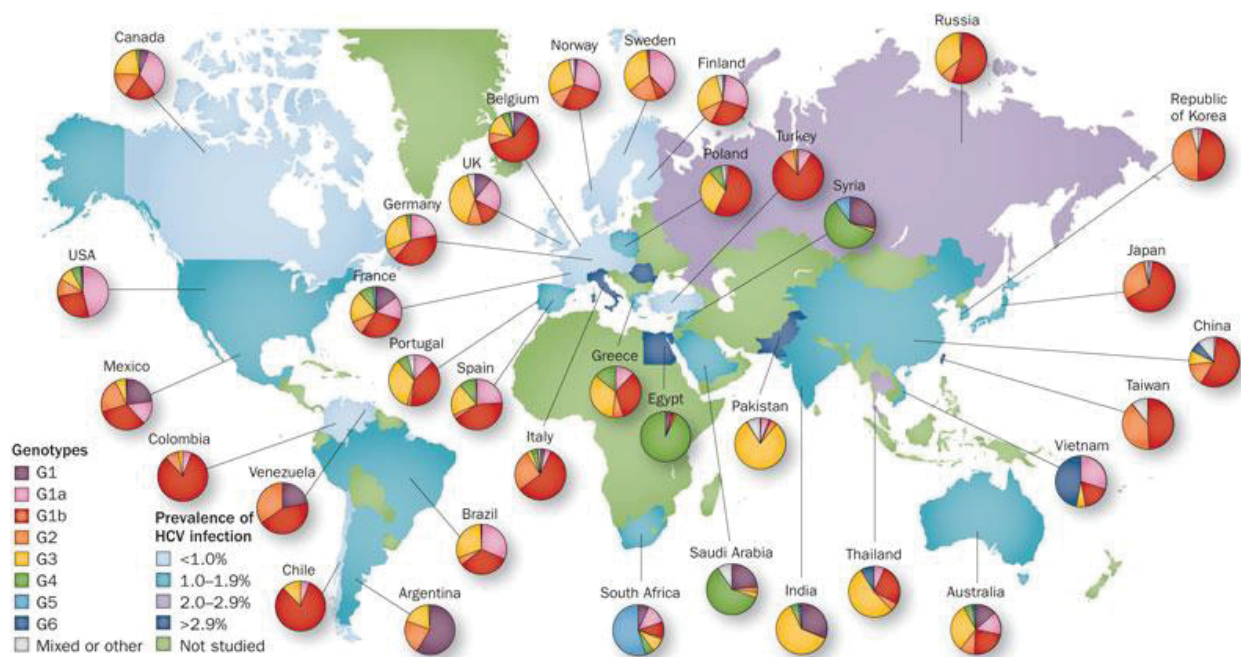
1.1 Hepatitis C – a general overview

1.1.1 Epidemiology

Hepatitis C virus (HCV) is a blood-borne virus and one of the major causes of chronic liver disease. Common routes of transmission include injection drug use, blood transfusions and unsafe medical practices, such as the re-use of needles and multi-dose vials. Other routes, such as mother-to-infant or sexual transmission, can occur, but are rare events (Thursz and Fontanet, 2013). Acute infection, which refers to the first six months post exposure, is usually asymptomatic or mild and cleared by 20-25% of patients without intervention. However, in the majority of cases the virus persists and as the infection often goes undetected, the disease remains untreated. Over the course of 20-30 years, chronically infected individuals commonly develop severe liver disease, characterized by fibrosis, steatosis, cirrhosis and, in the worst case, hepatocellular carcinoma. In fact, it is thought that chronic infection accounts for 25% of liver cancers and up to 30% of liver transplants (Kim et al., 2009; Perz et al., 2006). To date, the Centers for Disease Control and Prevention (CDC) estimate that approximately 2-3% of the world's population is chronically infected. Considering the silent nature and slow disease progression of chronic HCV, this number is likely to increase in the coming years, making HCV a serious global health and economic burden (Khoury et al., 2011).

1.1.2 Classification and genetic diversity

HCV is a hepacivirus which belongs to the family of flaviviridae, a class of positive, single-stranded RNA viruses (Houghton, 1996). Other members of this family include Dengue, Yellow Fever and West Nile virus, all of which can cause severe disease in humans. Based on its genetic diversity, HCV is classified into seven different genotypes (1-7) and numerous subgroups (a, b, c, etc), which can differ up to 35% and 25% in their nucleotide sequence, respectively (Moradpour et al., 2007; Simmonds, 2013). Genotypes 1a and b are the most common strains and broadly distributed across the world, closely followed by genotypes 2 and 3. In contrast, genotypes 4, 5 and 6 are restricted to certain areas in Africa, the Middle East and Asia (**Fig. 1**) (Hajarizadeh et al., 2013). Besides differences in geographic distribution, HCV genotypes also vary in epidemiology and response to antiviral treatment. The genetic diversity is explained by the high rate of viral replication (10^{12} virions per day) and the error-prone nature of the RNA polymerase, rapidly giving rise to a heterogeneous viral sub-population (quasi-species). As consequence, resistant strains emerge, which greatly hamper the development of effective vaccines and antiviral treatment strategies (Neumann et al., 1998).



Hajarizadeh et al., 2013

Figure 1: Global distribution and prevalence of the different HCV genotypes.

World map representing genotype distribution (pie charts) and global prevalence (country color code) of the different HCV genotypes. The highest prevalence is observed in Egypt and Cameroon (>10%) and vast parts of Asia. Genotype 1 is the most common (46% of cases), followed by genotypes 3 (22%) and 2 (13%). While genotypes 1, 2 and 3 are evenly spread across the globe, 4, 5 and 6 are restricted to the Middle East, South Africa and Southeast Asia, respectively (Gower et al., 2014; Hajarizadeh et al., 2013). Taken from Hajarizadeh et al, 2013.

1.1.3 Current treatment options

Until recently, standard-of-care involved a 48-week course of pegylated interferon α in combination with ribavirin (pegIFN α /ribavirin). However, this regimen is associated with severe side effects and an average response rate of ~50%. In 2011, a triple combination treatment consisting of one of two viral protease inhibitors, Telaprevir or Boceprevir, and conventional pegIFN α /ribavirin was approved by the FDA and is now used for the treatment of HCV genotype 1 infections (Cox, 2011a; 2011b). Although the success rate for the difficult-to-treat genotype 1 increased from 45% to 75%, severe side effects and a low barrier to resistance are still an important issue (Scheel and Rice, 2013). At the end of 2013, the FDA approved two more direct-acting antiviral drugs (DAAs), the nucleotide inhibitor Sofosbuvir (Sovaldi[®], Gilead Sciences) and the protease inhibitor Simeprevir (OLYSIO[™], Johnson&Johnson) (Reardon, 2014). Compared to existing treatment options, these drugs possess higher response rates, tend to be better tolerated and require shorter treatment times (12-24

weeks). Nevertheless, they come at a high price, with 84.000\$ and 66.000\$ per 12-week treatment course, respectively. For patients infected with genotype 3, who require a 24-week regimen, prices can be as high as 168.000\$. In addition, a broader genotype coverage and poor success rates of ~10% for previous non-responders, remain ongoing challenges to treatment (Hill and Cooke, 2014; Scheel and Rice, 2013)

1.2 Molecular biology of HCV

1.2.1 Genome and proteome organization

The HCV genome consists of one positive-sense, single-stranded RNA ((+)ssRNA) molecule (~9.6 kb in length) containing a single long open reading frame (ORF) which is flanked by untranslated regions (UTRs) at the 5' and 3'-end. Together with the first 16 codons of the protein coding sequence, the 5'UTR folds into an internal ribosome entry site (IRES) for cap-independent initiation of translation and contains two bindings sites for micro-RNA 122, which stabilizes the RNA genome and further facilitates translation (Conrad et al., 2013; Kim et al., 2002; Tsukiyama-Kohara et al., 1992). The 3'UTR contains a variable region, a polyU/UC tract and a highly conserved RNA element termed X-tail and is required for initiating RNA replication and enhancing polyprotein translation (Friebe et al., 2005; Song et al., 2006; You and Rice, 2008) (**Fig. 2**).

The ORF encodes a single ~3000 amino acid long precursor polyprotein, which is co- and posttranslationally processed by host and viral proteases into the structural proteins Core, E1 and E2, the viroporin p7 and the non-structural proteins NS2, NS3, NS4A, NS5A and NS5B. Based on the designated functions of the individual viral proteins, the polyprotein can be subdivided into an N-terminal "assembly unit" and a C-terminal "replication unit" (Bartenschlager et al., 2013). The assembly unit consists of Core, the envelope glycoproteins E1 and E2, which make up the physical virion, the viroporin p7 and the nonstructural protein NS2 which are important for the actual assembly process (Jones et al., 2007). NS2 is a cysteine protease which, in addition to its role in viral assembly, cleaves the junction between NS2 and NS3, thus separating the two functional modules (Grakoui et al., 1993). On the other hand, the replication unit consists of the non-structural proteins NS3, NS4A, NS4B, NS5A and NS5B. Similar to other positive strand RNA viruses, these proteins are sufficient for RNA replication, even in the absence of the structural proteins (Lohmann, 1999). NS3 is a multifunctional protein with N-terminal protease activity and a C-terminal nucleic acid-binding DExH/D-box helicase domain. Together with its co-factor NS4A, the NS3-4A protease is responsible for processing the polyprotein upstream of the NS2-NS3 junction. In addition, NS3-4A can cleave the host adaptor proteins MAVS and TRIF, thus blocking the induction of antiviral immune responses (Meylan et al., 2005). The NS3 helicase most likely facilitates replication by unwinding local RNA secondary structures, separating template from nascent RNA strands and translocating RNA-binding

proteins (Scheel and Rice, 2013). NS4B is an integral membrane protein, with a core of four membrane-spanning segments. The N- and C-terminal parts are helical in nature and oriented towards the cytosol (Bartenschlager et al., 2013). The best-described function of NS4B is the rearrangement of ER-derived membranes into multilayered, vesicular structures which are thought to serve as platforms for the subsequent assembly of viral replication complexes (RCs) (Egger et al., 2002). Although NS4B is the main driver, other host and viral proteins are also involved in this process (Romero-Brey et al., 2012). Some reports also suggest a more direct role of NS4B in RNA replication and assembly, but this is still under investigation (Jones et al., 2009). NS5A is an ER-membrane-bound protein with key roles in viral RNA replication, as well as infectious particle assembly and will be described in more detail below. The RNA-dependent RNA polymerase NS5B catalyzes the replication of viral RNA. With the support of the other viral replicase proteins and various host factors, such as the cyclophilin A and miRNA-122, NS5B first produces a negative-sense RNA strand, which it then uses as template for the production of multiple copies of nascent positive-strand RNA molecules (Lohmann, 2013).

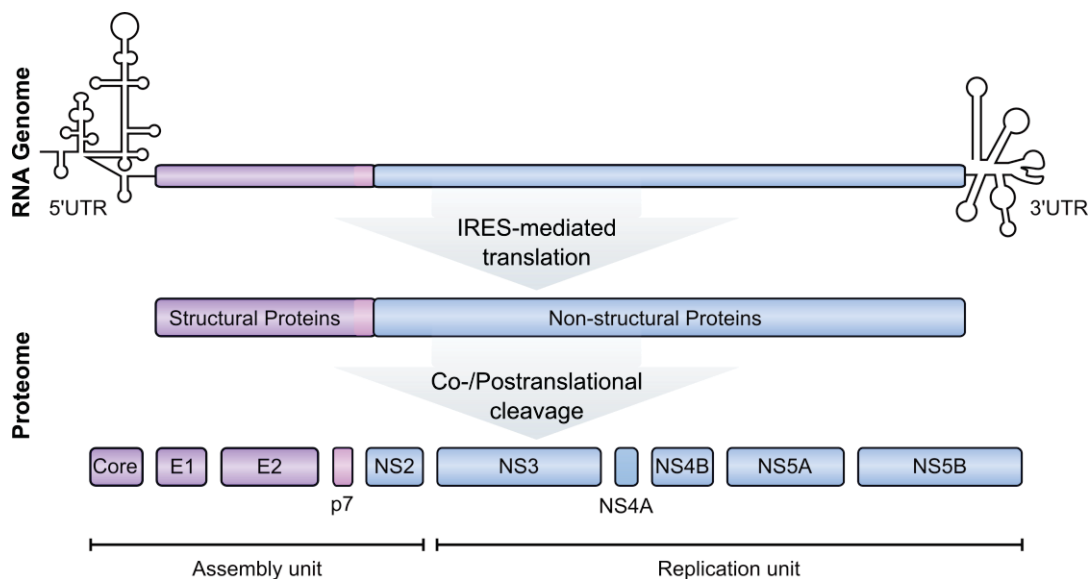


Figure 2: HCV genome and proteome organization.

Schematic representation of the HCV genome, the precursor polyprotein and the processed mature proteins. The ssRNA molecule (top) is flanked by highly structured UTRs, both of which are required for efficient replication and translation. The single, long ORF encodes a precursor polyprotein, which is co- and posttranslationally cleaved into the viral structural and non-structural proteins. The viral proteins can be functionally subdivided into an assembly and a replication unit. Core, E1 and E2 form the viral capsid, while the viroporin p7 and the autoprotease NS2 facilitate assembly. Although NS3-

5B contribute to the assembly process to a certain extent, their main task remains the synthesis of (+)ssRNA and interference with host signaling pathways.

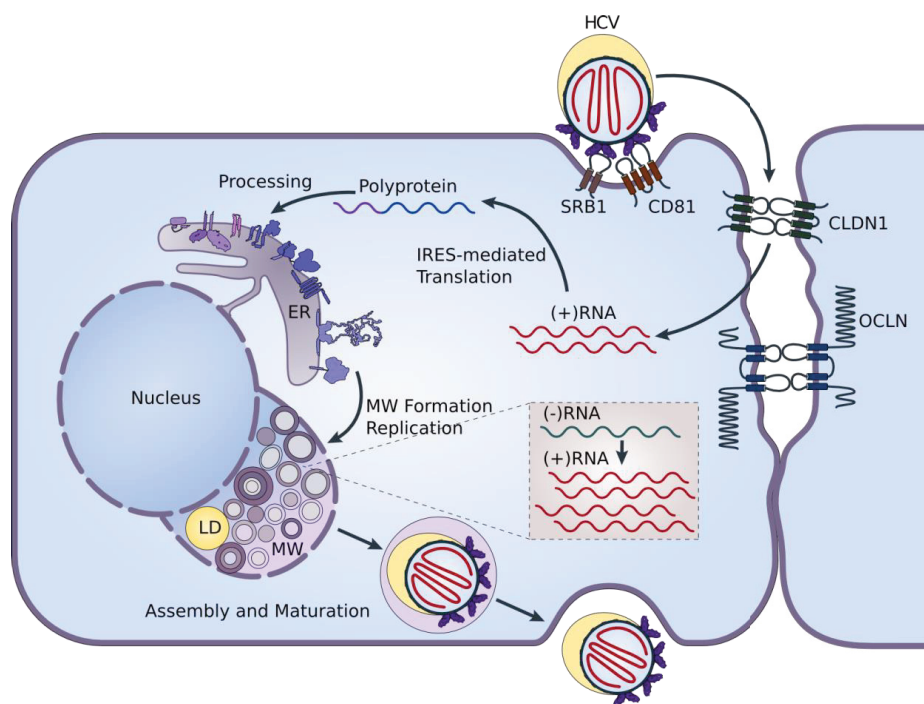
1.2.2 The viral life cycle

A distinctive feature of HCV virions is their close resemblance to different classes of lipoproteins, such as very-low and low-density lipoproteins (VLDLs and LDLs). More precisely, HCV exists as hybrid lipid-virus particles (LVPs), consisting of triglycerides, cholesterol and different apolipoproteins (Chang et al., 2007; Merz et al., 2011). As a result, HCV LVPs are rather heterogeneous, ranging in size (40-80nm in diameter), composition and buoyant density. In fact, the lipid content positively correlates with a higher infectivity of the virus particle (Lindenbach et al., 2006). The association with lipoproteins probably facilitates entry into hepatocytes and protects the circulating virions from antibody neutralization (Lindenbach and Rice, 2013). The actual virus particle is composed of the nucleocapsid, an assembly of Core protein and a single copy of the RNA genome, and a host membrane-derived envelope in which the glycoproteins E1 and E2 are embedded (Moradpour et al., 2007).

Viral entry is a complex process involving multiple host cell factors. It is believed that circulating HCV virions initially attach to hepatocytes via low affinity interactions between LVP-associated apolipoproteins and glycans with LDL receptors and glycosaminoglycans on the cell surface (Agnello et al., 1999; Barth et al., 2003). The attachment and entry process is then initiated through the sequential interactions of E2 with the Scavenger receptor class B member 1 (SR-BI) and the tetraspanin cluster of differentiation 81 (CD81). Cell surface-bound virus particles translocate to sites of cell-to-cell contact, where the tight junction proteins claudin-1 (CLDN1) and occludin (OCLN) facilitate clathrin-mediated endocytosis (Blanchard et al., 2006; Evans et al., 2007; Pileri et al., 1998; Ploss et al., 2009; Scarselli et al., 2002) (**Fig. 3**). Recently, additional proteins have been identified which contribute to the various stages of viral entry. These include the receptor tyrosine kinases epidermal growth factor receptor (EGFR) and ephrin (EPH) receptor A2, the transferring receptor 1 (TFR1) and Niemann–Pick C1–like 1 (NPC1L1) (Lupberger et al., 2011; Sainz et al., 2012). How these factors facilitate entry is still under investigation, but it most likely involves the modulation of pathways required for cell-surface translocation, inhibition of antiviral immune responses and structural modification of the attached LVPs (Lindenbach and Rice, 2013).

Acidification of endosomes triggers fusion of the viral envelope with the endosomal membrane and the release of viral RNA into the cytoplasm. 5'-IRES-mediated translation of the viral genome is then initiated at the rough ER (Tsukiyama-Kohara et al., 1992) (**Fig. 3**). The non-structural proteins assemble into RCs located inside vesicular compartments that arise as part of the membranous web formation (Egger et al., 2002). Newly synthesized RNA is then either translated into viral proteins, or

packaged into virus particles (Scheel and Rice, 2013) (**Fig. 3**). In fact, each RC is thought to contain only a single template negative (-)ssRNA molecule and two – ten newly synthesized (+)ss RNA strands at a given time, while the non-structural proteins are present in excess, presumably stabilizing the surrounding vesicle (Quinkert et al., 2005). The later stages of the HCV life cycle, including viral assembly, maturation and release are still poorly understood. The current model suggests that, prior to assembly, Core resides on the surface of cellular lipid droplets, while E1 and E2 exist as a membrane-bound dimer, facing the ER-lumen (Dubuisson et al., 1994; Miyanari et al., 2007a). Assembly is initiated with packaging of Core and viral RNA into nucleocapsids, a process that requires the activity of NS5A (Appel et al., 2008; Miyanari et al., 2007a). The nucleocapsid then acquires its envelope by budding into the ER. As the virion is released via the secretory pathway, it matures into fully infectious LVPs (reviewed in Bartenschlager et al., 2011). It is generally believed that HCV co-opts and depends on the VLDL pathway for assembly, maturation and release. First of all, lipid droplets, the precursor of VLDLs, and other host factors involved in lipoprotein synthesis, are essential for infectious particle production (Gastaminza et al., 2008; Huang et al., 2007a; Miyanari et al., 2007a). In addition, viral envelopes are enriched in cholesterol and sphingolipids, suggesting that assembly occurs in specialized lipid rafts in the ER membrane (Aizaki et al., 2008).



adapted from Bartenschlager et al, 2011

Figure 3: Overview of the Hepatitis C virus life cycle

Circulating HCV LVPs sequentially bind to first SR-BI and then CD81 on the basolateral membrane of polarized hepatocytes. Cell-surface attached virions translocate to lateral tight junctions, where

clathrin-mediated endocytosis is facilitated by the late entry factors CLDN1 and OCLN. Additional cellular entry factors have been identified (not shown), but their precise role in the entry process remains unclear. Upon pH-induced membrane fusion, viral RNA is released into the cytoplasm and IRES-mediated translation is initiated at the rough ER. The produced polyprotein is cleaved into the individual structural and non-structural proteins. Non-structural proteins NS3-5B assemble into replication complexes that are located in virus-induced membranous vesicles. RNA replication is catalyzed by the RNA-dependent RNA polymerase NS5B which synthesizes (+)ssRNA from a single (-)ssRNA molecule. Nucleocapsid formation and loading with viral RNA is initiated in close proximity to cellular lipid droplets, requiring the aid of NS5A. By co-opting the VLDL-pathway, the RNA-loaded nucleocapsid buds into the ER lumen where it acquires the viral glycoproteins and lipid envelope and continues to mature as it travels along the VLDL-secretory pathway before being released. Image was adapted from Bartenschlager et al., 2011.

1.3 The non-structural protein NS5A

The NS5A protein is absolutely essential for HCV RNA replication and virion assembly. It is an RNA-binding, monotopic membrane protein, which is anchored to the cytosolic leaflet of the ER via an N-terminal amphipathic α -helix (Brass et al., 2002; Penin et al., 2004). The remainder of the protein is composed of three domains (DI, DII and DIII), separated by protease-sensitive low-complexity sequences (LCS I and LCS II) (**Fig. 4A**) (Tellinghuisen et al., 2004). Domain DI harbors a zinc-binding motif, which when mutated, completely abolishes viral replication (Tellinghuisen et al., 2004). Crystal structure-based studies suggest that DI from two adjacent NS5A proteins dimerise, forming a basic RNA-binding groove (Tellinghuisen et al., 2005). Additional *in silico* modeling of NS5A dimer suggested they may oligomerize, forming a long channel-like structure for shuttling nascent RNA and protecting it from degradation and detection by immune sensors (Bartenschlager et al., 2011; Verdegem et al., 2011). In contrast to DI, DII and DIII are intrinsically disordered and lack stable secondary and tertiary structures, conferring a high degree of structural flexibility (**Fig. 4B**) (Hanouille et al., 2009b; Liang et al., 2006). These unfolded regions are common features of hub proteins, where they increase the number of binding partners and facilitate low-affinity, yet specific interactions, respectively (Kosol et al., 2013).

1.3.1 Structure and function

While DI and a small part of DII are required for replication, DIII mediates infectious particle production, presumably through its interaction with Core on lipid droplets and the shuttling of nascent RNA to the sites of assembly (Appel et al., 2008; Masaki et al., 2008; Miyanari et al., 2007b; Ross-Thriepfand et al., 2013; Tellinghuisen et al., 2008b). Besides its direct role in the viral life cycle,

NS5A has been shown to modulate various cellular pathways, a prime example being the antiviral innate immune response. NS5A inhibits the dsRNA-dependent protein kinase R (PKR), an important IFN-inducible antiviral effector protein (Gale et al., 1998). Furthermore, NS5A interferes with Signal Transducers and Activators of Transcription 1 (STAT1) phosphorylation and downstream induction of IFN-stimulated genes (Kumthip et al., 2012). Another critical pathway affected by NS5A is the phosphatidylinositolphosphate (PIP) synthesis pathway. Phosphatidylinositol-4-phosphate (PI4P) is a phospholipid commonly found in Golgi membranes. In HCV-infected cells, levels of PI4P are increased at the site of replication, a phenomenon attributed to the recruitment and activation of the PIP kinase PI4KIII α by NS5A. This local enrichment of PI4P is critical for replication as it presumably stabilizes the integrity of the replication complex (Reiss et al., 2011).

Despite the efforts made towards understanding the mechanisms underlying NS5A function, it is still not clear how NS5A co-ordinates its multiple tasks. Given its different states of phosphorylation and its structural flexibility, it is commonly thought that this and possibly other post-translational modifications as well as differential protein-protein interactions play a major role in regulating NS5A function.

The paramount role of NS5A in the HCV life cycle is further emphasized by the discovery of a set of very potent small molecules targeting NS5A that inhibit HCV replication in the low- to subpicomolar range (Gao et al., 2010). Although several of these compounds are already being tested in phase II and III clinical trials, a low barrier to viral resistance and genotype-dependent treatment response rates remain common problems (Scheel and Rice, 2013).

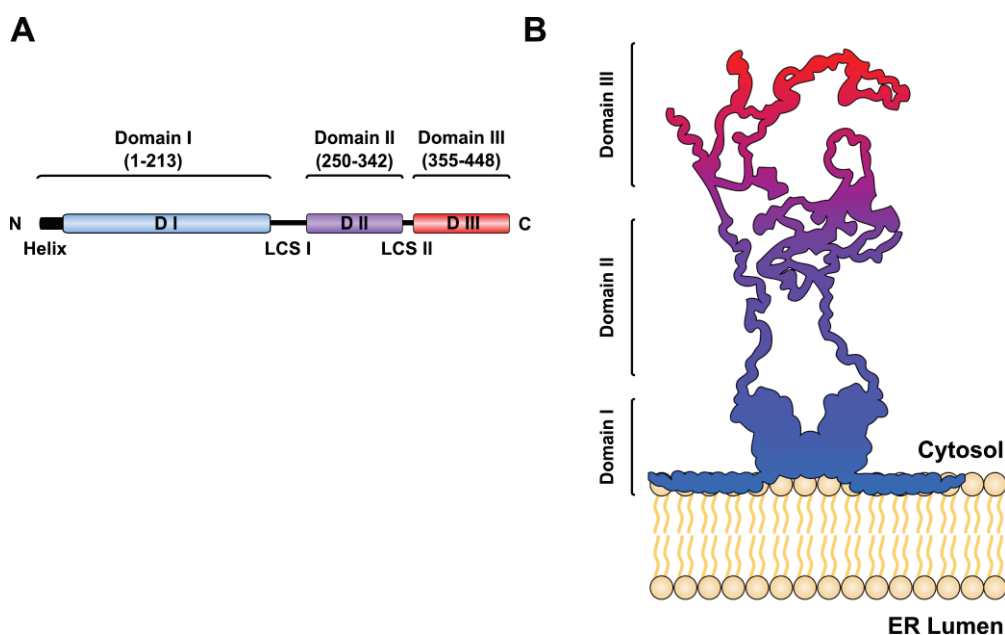


Figure 4: NS5A domain structure.

A) Schematic domain layout of NS5A. Depending on the genotype, NS5A consists of 448-466 amino acids and is composed of three domains (DI, DII and DIII), which are linked by protease-sensitive, low-complexity sequences. The N-terminus of DI forms an amphipathic α -helix, which tethers NS5A to the cytosolic leaflet of ER membranes. Residue numbers correspond to NS5A from the genotype 1b isolate Con1. B) Proposed structure of the NS5A dimer embedded in the ER-membrane. Shown is the DI dimer as proposed by Tellinghuisen et al. (Tellinghuisen et al., 2005) (PDB accession: 1ZH1) and the intrinsically unfolded nature of DII and DIII. The NS5A structure outline was adopted from Bartenschlager et al. and modified accordingly (Bartenschlager et al., 2013).

1.3.2 NS5A phosphorylation

NS5A is phosphorylated on different serine and threonine residues and generally exists in two different phosphorylation states: a basal- (NS5A p56) and a hyperphosphorylated form (NS5A p58) (Kaneko et al., 1994; Reed et al., 1997). The best-characterized kinases that phosphorylate NS5A are the casein kinases CKI- α and CKII- α . CKI- α is responsible for hyperphosphorylating NS5A and is required for viral replication, while CKII- α contributes to basal phosphorylation and infectious particle assembly (Quintavalle et al., 2007; Tellinghuisen et al., 2008b). However, additional kinases with activity towards NS5A have been identified. Although it is widely accepted that NS5A is a substrate for other kinases, their precise role in the regulation of NS5A is still under investigation (Chen et al., 2010; Huang et al., 2007b; Reed et al., 1997). Although hyperphosphorylation is a common feature of all HCV genotypes, isolate-specific differences exist (Ross-Thriepland and Harris, 2014). For instance, NS5A from the genotype 1a H77 exists in both phosphoforms when transiently overexpressed in various different cell lines such as HeLA cells or the human hepatoma cell line Huh7 (Reed et al., 1997). NS5A p58 from genotype 1b isolates, on the other hand, is only observed when the other NS proteins are present (Asabe et al., 1997; Koch and Bartenschlager, 1999; Liu et al., 1999; Neddermann et al., 1999). In these strains even small perturbations, such as point mutations in NS3 and NS4B, ablate the formation of NS5A p58 (Appel et al., 2005). Interestingly, mutations that enhance HCV replication were found to inversely correlate with NS5A hyperphosphorylation suggesting that this modification may provide some sort of switch between replication and assembly (Appel et al., 2005; Pietschmann et al., 2009; Tellinghuisen et al., 2008a).

1.4 *In vitro* models for HCV

Ever since its discovery in 1989, HCV research has been hampered by the inability to efficiently culture serum-derived virus *in vitro* and the lack of a small animal model. As a consequence, efficient

serologic and nucleic acid-based tools for the routine screening of donated blood were developed within two years of its discovery, resulting in the near eradication of transfusion-transmitted hepatitis. However, the development of efficient treatment strategies and preventive vaccines lagged behind (Alter and Klein, 2008). It took 10 years to identify a first set of susceptible host cells and develop a sufficient HCV cell culture system. The most widely used models nowadays include non-infectious subgenomic replicons, a cell-culture infectious system (HCVcc) based on the genotype 2a isolate JFH-1 and HCV-like virus particles.

1.4.1 HCV replicon systems

Subgenomic replicons are HCV RNA molecules capable of replicating autonomously in certain permissive cell lines. The most commonly used replicons are bicistronic constructs, which were first developed by Lohmann et al. The first cistron consists of the HCV IRES, which is driving translation of a reporter gene, a selection marker, or both (**Fig. 5B and C**). The second cistron encodes the viral replicase proteins NS3-5B, which are placed under the control of an encephalomyocarditis virus (EMCV) IRES (Krieger et al., 2001a; Lohmann, 1999).

Commonly used reporter genes include Firefly (F-luc) or Renilla (R-luc) luciferase (Krieger et al., 2001a). Since their activity directly correlates with RNA replication efficiency of the respective replicon, they provide an easy and sensitive readout for transient replication assays (Krieger et al., 2001a). Replicons encoding selection markers, such as the neomycin phosphotransferase, are used for the generation of cell lines harboring persistently replicating replicons. As these replicons can persist for long periods of time, these cell lines are used for studying the molecular effects of chronic infection. More sophisticated replicons containing both a selection marker and a reporter (**Fig. 5C**) provide useful tools for the identification of antiviral compounds and other (high-throughput) screening activities (Tai et al., 2009; Zhao et al., 2012). It is important to note, that patient-derived strains generally replicate poorly, or not at all *in vitro*. In order to achieve efficient replication, a set of genotype-specific cell-culture adaptive mutations has to be introduced (Krieger et al., 2001b; Lohmann, 1999; Lohmann et al., 2003). Amongst the most efficient replicons is the adapted genotype 1b isolate Con1/ET. It contains three point mutations, namely E1202G, T1280I, K1846T (located in NS3 and NS4B, respectively) and replicates up to 200-fold better than the wild type genome (Lohmann et al., 2003). While these mutations greatly enhance replication *in vitro*, the majority inhibits the production of infectious particles when introduced into the respective full-length genomes, thus limiting their use to the study of viral replication. Mutations in NS3 and NS5A were in particular shown to block the assembly processes (Lohmann et al., 2003; Pietschmann et al., 2009). To date, robust replicons are only available for genotypes 1a, 1b and 2a, but progress is being made

towards the generation of replicons covering the remaining genotypes (Lohmann and Bartenschlager, 2013).

1.4.2 Cell-culture derived HCV

Due to the aforementioned adaptive mutations, full-length replicons generally do not support the other steps of the viral life cycle, such as entry and infectious virion production. However, this obstacle was overcome with the discovery of a unique genotype 2a strain, isolated from a patient with a rare case of fulminant hepatitis. This isolate, designated JFH-1, is capable of replicating to very high levels *in vitro* without the acquisition of adaptive mutations (Kato et al., 2003). What is more, full-length JFH1 was also found to release infectious particles into the supernatant of transfected cells, thus giving rise to the currently used infectious, cell-culture derived HCV model system (Lindenbach et al., 2005; Wakita et al., 2005). Currently used constructs involve full-length JFH-1 genomes, or the optimized intragenotypic chimeric strain Jc1 (**Fig. 5D**) (Pietschmann et al., 2006). Jc1 consists of the JFH1 replicase, which is fused to the Core-NS2 region of the genotype 2a isolate J6CF and produces virus titers 100- to 1,000-fold higher compared to the parental JFH1 strain (Pietschmann et al., 2006; Yanagi et al., 1999). In addition, a set of infectious reporter viruses has become available. Similar to the reporter replicons, they allow fast and easy quantification of viral replication as well as infectious particle production (**Fig. 5E**). However, it is important to note that in Europe, HCV is classified as a level 3 infectious agent and as such must be handled in appropriate facilities only.

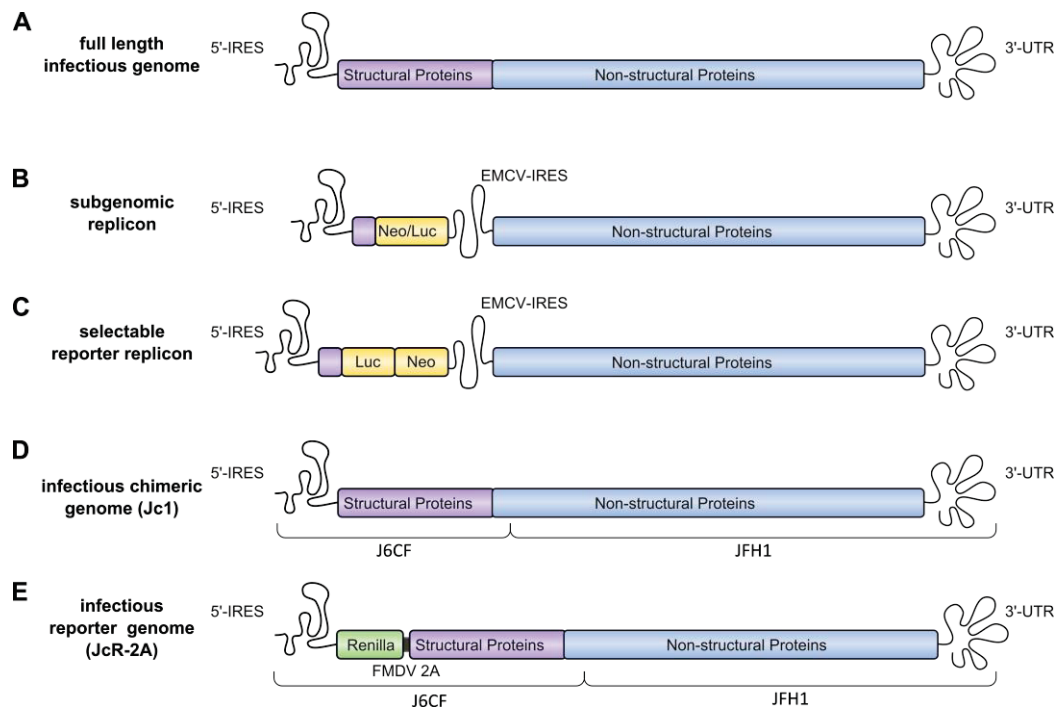


Figure 5: Overview of commonly used HCV replicons

A) Schematic view of the full length, wild type HCV genome. Shown are the 5' IRES, the 3'-UTR and the regions coding the structural and non-structural proteins. In subgenomic replicons, the structural genes are replaced by an antibiotic-resistance gene, a reporter gene (B) or a combination of both (C). The HCVcc system was optimized by generating intragenomic chimeric genomes, which release higher titers compared to the parental JFH1 strain. Jc1 (D), the most efficient chimera, consists of the J6CF structural region and the JFH1 NS-proteins. JcR-2A (E) is a Jc-1-derived reporter virus. The R-luc gene is fused to the N-terminus of Core via a Foot-and-mouth disease virus (FMDV) 2A; a short, self-cleaving peptide (Reiss et al., 2011).

1.4.3 HCV-like virus particles

Prior to the development of HCVcc, the viral entry, assembly and release pathways were investigated using HCV pseudoparticles (HCVpp) or trans-complemented hepatitis C virus particles (HCVtcp), respectively (Woerz et al., 2009). HCVpp are lenti- or retroviral-based virus particles surrounded by a lipid envelope into which the HCV E1 and E2 glycoproteins are incorporated. The retroviral core generally encodes a reporter gene such as F-luc or green fluorescent protein (GFP) to measure infectivity (Bartenschlager et al., 2013). HCVtcps on the other hand contain subgenomic replicons that are packaged into HCV-like particles when the viral structural proteins are supplemented in *trans* (Woerz et al., 2009). Both models have been indispensable for studying virus – host receptor interactions, viral entry processes and the identification and characterization of neutralizing antibodies. As none of these systems are capable of producing infectious progeny, no BSL-3 facilities are required.

1.4.4 Permissive cell lines

Another important factor determining the efficiency of HCV replication *in vitro* is the choice of suitable cell lines. Although a number of different hepatic as well as non-hepatic cell lines are somewhat susceptible to HCV infection and replication, only the human hepatoma cell line Huh7 supports high levels of replication (Date et al., 2004; Kato et al., 2005; Windisch et al., 2005). Further optimization led to the generation of even more permissive Huh7 subclones, the most widely used being Huh7.5, Huh7.5.1 and Huh7-Lunet cells. All three clones were generated by treating Huh7 cells harboring particularly high levels of persistent HCV replicons with IFN α , thus "curing" them from replicating HCV RNA (Blight et al., 2002). Huh7-Lunet cells support high levels of replication, but lack CD81 and are thus refractory to infection (Koutsoudakis et al., 2006). Huh7.5 and Huh7.5.1 cells harbor a point mutation in the antiviral gene RIG-I and, in contrast to Huh7-Lunet cells, they express all HCV surface receptors and are highly susceptible to HCV infection (Blight et al., 2002; Friebe et al., 2005).

Although the developed replicon and cell-culture infectious systems have led to major advances towards the understanding of the biology of HCV and the development of more effective treatment strategies, it is important to keep in mind that these systems do not fully represent HCV found in infected patients. First of all, cell-culture adapted genomes are not infectious in chimpanzees, the only other susceptible host. Secondly, despite the fact that JFH1 does not require adaptive mutations, it is isolated from a rare case of fulminant hepatitis and thus may not completely represent conventional HCV. Likewise, Huh7 cells and derivatives lack many important key features of human hepatocytes, including a functional type I IFN system, the formation of polarized monolayers and the production of serum lipoproteins (Steenbergen et al., 2013). Thus, culture-derived virions exhibit different biophysical properties compared to the LVPs found in patient sera (Pietschmann et al., 2009). Hence, efforts to develop similar efficient infectious systems covering the remaining genotypes are still ongoing.

1.5 The biology of lysine methylation and protein lysine methyltransferases

Lysine is a polar amino acid, which possesses a positively charged ϵ -amino group (or primary amine) and is frequently found in catalytic sites as well as protein-binding regions. In addition, lysines are often involved in the formation of salt bridges and thereby stabilize protein structure (Betts and Russell, 2003). The primary amine is highly reactive and amenable to numerous different post-translational modifications (PTM), each being capable of eliciting different functional outcomes. These modifications range from the addition of small functional groups to the covalent attachment

of entire proteins, such as ubiquitin and ubiquitin-like proteins (**Fig. 6A**) (Lanouette et al., 2014 and references therein). Lysine methylation is catalyzed by lysine methyltransferases (KMTs), which can transfer up to three methyl-groups to the receptor lysine using S-adenosyl-L-methionine (SAM) as methyl-donor (**Fig. 6B**). As for many other modifications, methylation is a reversible process and the methyl-groups are readily removed by two distinct classes of lysine demethylases (KDMs), the lysine-specific (LSD) demethylases and the Jumonji C (JmjC) domain containing proteins. In contrast to KMTs, these enzymes employ different reaction mechanisms. While LSD proteins remove methylgroups by amine oxidation, JmjC-KDMs hydroxylate their target lysines (Helin and Dhanak, 2013).

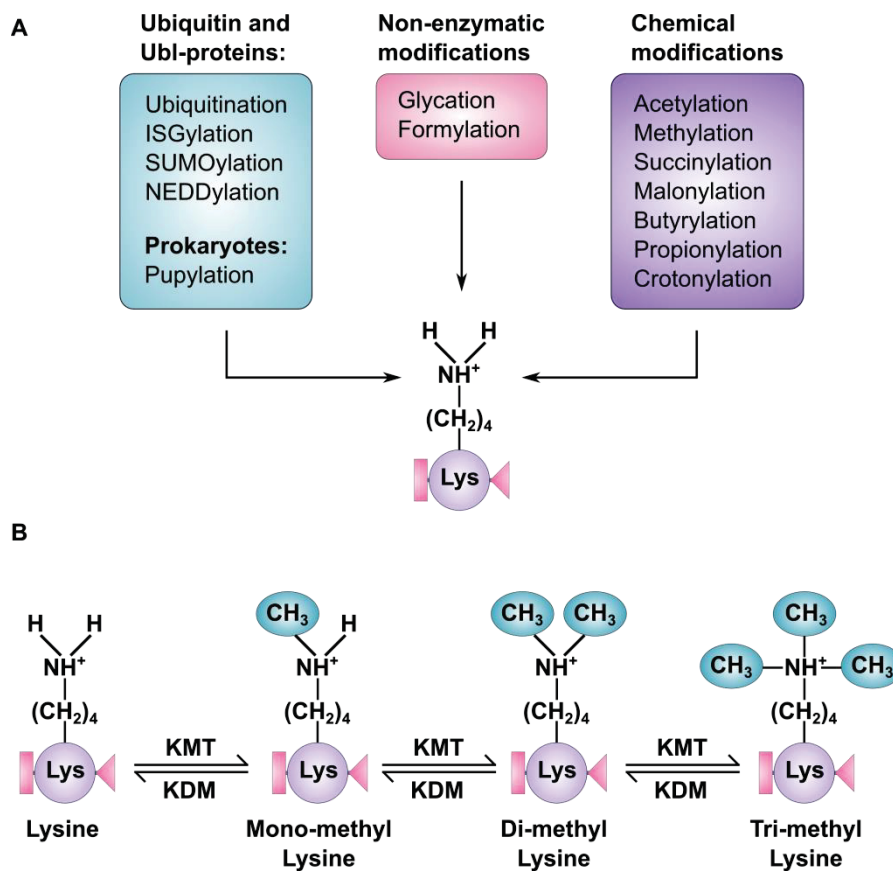


Figure 6: Posttranslational lysine modification

(A) Lysines possess a reactive ϵ -amine group, which is subject to multiple different types of post-translational modifications. These range from the covalent attachment of chemical functional groups and lipid moieties to small proteins such as ubiquitin and the ubiquitin-like proteins SUMO, NEDD8, ISG15 and PUP, the latter being the prokaryotic analogue expressed by actinobacteria (Liu et al., 2013). Non-enzymatic modifications include glycation and formylation. (B) Schematic representation of reversible lysine methylation. All KMTs identified to date use SAM as a co-factor to covalently attach up to three methyl-groups to the primary amine. These are readily removed by two different classes of lysine demethylases. SUMO = Small Ubiquitin-like Modifier, NEDD8 = neural-precursor-cell-

expressed developmentally down-regulated 8, ISG15 = Interferon-induced 15 kDa protein, PUP = Prokaryotic ubiquitin-like protein

Unlike other modifications such as acetylation, phosphorylation and ubiquitination, lysine methylation does not neutralize the positive charge of the primary amine, nor does it add a significant mass to the targeted residue (Lanouette et al., 2014; Leutz et al., 2011; West and Gozani, 2011). Rather, methylation acts in combination with other PTMs, promoting or inhibiting the modification of adjacent residues. For instance, methylation of K810 of the retinoblastoma protein (Rb) by the SET and MYND-domain containing protein 2 (SMYD2) promotes phosphorylation of serines S807 and S811 by CDK1 and CDK3, thereby inhibiting Rb functions (Cho et al., 2012). Furthermore, it has been proposed that methylation can enhance protein stability by preventing the addition of ubiquitin and thereby inhibit proteasomal degradation (Pang et al., 2010). However, whether this competition mechanism plays an important role *in vivo* is debatable as only a small fraction of lysines are methylated (Moore and Gozani, 2014). What is more, methylated lysines either block or generate new docking sites for protein-protein or protein-nucleic acid interactions (Clarke, 2013; Lanouette et al., 2014). For a long time, lysine methylation was thought to be restricted to histones, thereby influencing heterochromatin formation, X-chromosome inactivation and histone exchange and thus constituting epigenetic marks that mediate gene transcription. The discovery that methylation could be found on non-histone proteins has revived the interest in lysine methylation. It is now clear that methylated lysines are common on proteins with complex functions and thus important conveyors and regulators of many signal transduction pathways and other important cellular processes. Prime examples are the transcription factors p53 and NF κ B, which are differentially regulated via methylation (Levy et al., 2010; Marouco et al., 2013). Depending on the level of methylation and the presence or absence of adjacent PTMs, methylated lysines provide specific “instructions” which are recognized and executed by different downstream signal pathways components (Liu et al., 2013; Moore and Gozani, 2014). Given the versatility of this modification, it is not surprising that viruses have evolved strategies to usurp lysine methylation and the associated KMT-machinery. For instance, transcriptional activity of the human immunodeficiency virus (HIV) Tat protein is tightly controlled by sequential monomethylation and demethylation by SET7/8 and LSD1, respectively, as well as di- and trimethylation by SETDB1 (Pagans et al., 2010; Sakane et al., 2011; Van Duyne et al., 2008). A second, very powerful strategy employed by viruses is molecular mimicry. The non-structural protein NS1 from Influenza A virus subtype H3N2 contains a histone H3 tail-like sequence to sequester the transcriptional elongation complex PAF1C and inhibit the expression of viral genes (Marazzi et al., 2012).

To date, the majority of confirmed KMTs belong to the superfamily of SET-domain containing

proteins, which share a common catalytic SET-domain (Dillon et al., 2005; Helin and Dhanak, 2013). This is an evolutionary conserved, 130-140 amino-acid long motif, named after the drosophila proteins SU(var), Enhancer of Zeste and Trithorax in which it was first described (Tschiersch et al., 1994). Based on additional structural features, SET-domain proteins are further divided into the seven subfamilies: Enhancer of Zeste (EZ), retinoblastoma-interacting zinc-finger (RIZ) proteins, SET1, SET2, SET- and MYND-domain containing (SMYD) proteins, suppressor of variegation SUV3/9, SUV4-20 and the two orphans SET7/9 and SET8 (Dillon et al., 2005).

1.6 The SET- and MYND domain containing lysine methyltransferase SMYD3

1.6.1 Structural features

SMYD3 is one of five members of the SMYD subfamily of KMTs (Brown et al., 2006). It consists of two lobes, which are connected via a short flexible linker (Sirinupong et al., 2010; Xu et al., 2011). The N-terminal lobe is made up of the catalytic SET-domain, which, unlike conventional SET-proteins, is split by a Myeloid-Nervy-DEAF-1 (MYND) – type zinc finger (**Fig. 7A**) (Hamamoto et al., 2004). The SET-domain folds into a substrate-binding groove at the bottom of which the target lysine is inserted into a deep crevice where methylation takes place (**Fig. 7B and C**) (Sirinupong et al., 2010; Xu et al., 2011). The MYND-domain is a DNA- as well as protein-binding module with a preference for proline-rich sequences (Ansieau and Leutz, 2002). In addition, SMYD3 possesses DNA-binding activity. Although direct evidence is missing, it has been proposed to be mediated by its MYND-domain (Hamamoto et al., 2004; Xu et al., 2011). The C-terminal lobe has been proposed to undergo a hinge-like motion, partially blocking or exposing the substrate-binding site, thus acting as a regulator of catalytic activity (**Fig. 6B and C**) (Sirinupong et al., 2010; Xu et al., 2011).

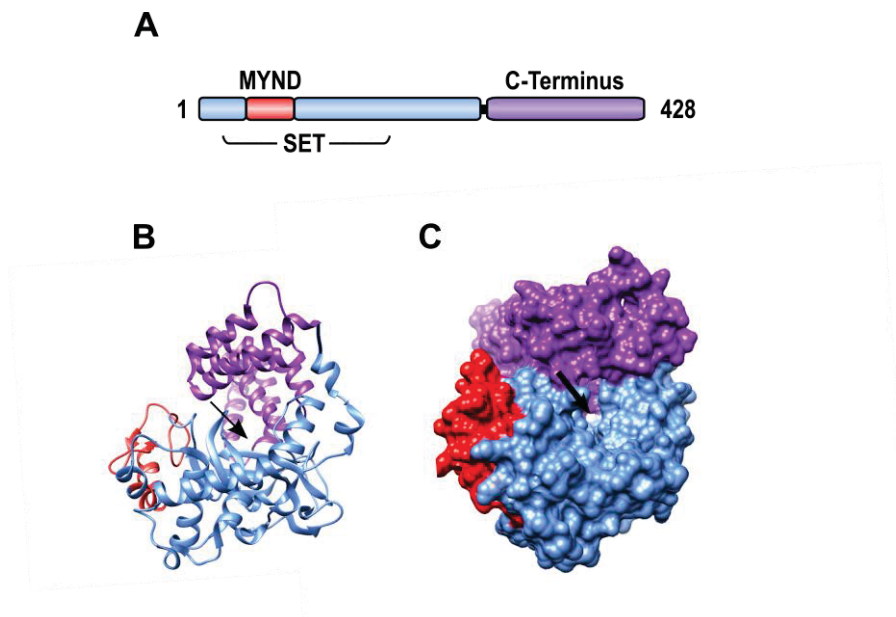


Figure 7: SMYD3 structure.

A) Schematic domain layout of SMYD3. SMYD3 consists of 428 amino acids and is composed of a catalytic SET domain (blue) split by a MYND-domain (red), a protein and DNA-binding module. The C-terminal domain (purple) is connected to the remainder of the protein via short linker sequence and has been proposed to act as “lid” for the substrate-binding cleft, thus regulating the catalytic activity of SMYD3. B) Ribbon-diagram and C) surface representation of SMYD3 in the “closed” conformation. Domains are colored as in (A). The substrate-binding groove is indicated with a black arrow. Of note, the MYND domain (red) protrudes away from the substrate-binding site, suggesting that is not required for substrate binding. Crystal structures in B and C were obtained from the protein databank (PDB entry: 3PDN) and modified using UCSF Chimera package (Pettersen et al., 2004)

1.6.2 Functional features

SMYD3 is abundantly expressed in skeletal muscle, brain, kidney, thymus and ovaries, but low levels are present in most organs (Brown et al., 2006; Hamamoto et al., 2004; Uhlen et al., 2010). In addition, it is highly up-regulated in numerous cancers, including breast, colon, prostate and liver cancer, where it is involved in the regulation of genes driving cell proliferation, migration and invasion (Cock-Rada et al., 2012; Hamamoto et al., 2004; 2006; Liu et al., 2012; Van Aller et al., 2012). Consequently, SMYD3 knockdown induces cell cycle arrest followed by apoptosis in numerous cancer cell lines, including Huh7 cells (Hamamoto et al., 2004; Van Aller et al., 2012). SMYD3 was initially reported to target histone 3 lysine 4 (H3K4), H4K5 and H4K20 *in vitro*, but it remains controversial whether it also methylates all three residues *in vivo* (Foreman et al., 2011; Hamamoto et al., 2004; Mazur et al., 2014; Van Aller et al., 2012). Given its potential role as a chromatin-modifying enzyme, SMYD3 was proposed to operate as a transcriptional regulator, either by directly binding to DNA and methylating the respective histone residues, or by acting in a complex with other transcription

factors (Foreman et al., 2011; Hamamoto et al., 2006; Liu et al., 2012; Luo et al., 2014; Mori et al., 2008). Besides histones, SMYD3 also targets cytoplasmic proteins. These include the Vascular Endothelial Growth Factor Receptor 1 (VEGFR1) and the Mitogen-Activated Protein Kinase Kinase 2 (MAP3K2). In both cases, methylation activates their kinase activity, potentiating downstream oncogenic signaling pathways (Kunizaki et al., 2007; Moore and Gozani, 2014). Depending on its subcellular localization, SMYD3 appears to possess two different functions, one controlling signaling pathways in the cytoplasm, the other as transcriptional regulator in the nucleus. This is in line with the observation that SMYD3 is predominantly cytoplasmic but can translocate to the nucleus (Hamamoto et al., 2006; Mazur et al., 2014). However, the molecular mechanisms underlying SMYD3 substrate specificity, activity and subcellular localization are unknown. Similarly, apart from its involvement in cancer, nothing is known about the physiological role of SMYD3. Some have reported involvement in embryonic development, spermatogenesis and muscle atrophy. However, this is questioned by the fact that SMYD3 knockout mice appear to be without phenotype (Fujii et al., 2011; Mazur et al., 2014; Proserpio et al., 2013; Zhou et al., 2005).

2. AIMS

The HCV non-structural protein NS5A plays several essential, yet still enigmatic roles in the HCV viral life cycle and disease pathogenesis. The methyltransferase SMYD3 was identified as a high-confidence interactor of NS5A as part of a large-scale proteomic screen performed in-house prior to this thesis (Pichlmair et al., 2012). Numerous studies have focused on NS5A phosphorylation and differential protein interactions in order to elucidate the mechanisms regulating NS5A's pleiotropic nature. On the other hand, the role of lysine methylation in NS5A functions has not been investigated. In this thesis, I aimed to confirm and further characterize the interaction of SMYD3 and NS5A. Furthermore, I tried to understand the functional role of SMYD3 in the context of HCV viral infection, using well-established *in vitro* models. Making use of already existing mass spectral data, I also tried to explore whether NS5A was subject to post-translational methylation. Overall, the goal of my thesis was to provide a better insight into the complex regulatory mechanisms underlying NS5A function and thus an improved understanding of the HCV life cycle.

3. RESULTS

3.1 Prologue manuscript: The lysine methyltransferase SMYD3 interacts with hepatitis C virus NS5A and is a negative regulator of viral particle production.

Being obligate intracellular parasites, co-opting host proteins and cellular pathways by viral proteins is a pivotal prerequisite to ensure a successful viral life cycle. To obtain a global perspective of virus-host interactions and common viral perturbation strategies, Dr. A. Pichlmair performed a large-scale proteomic screen to map novel virus – host interactions (Pichlmair et al., 2012). Based on its known ability to interfere with multiple host pathways, the HCV non-structural protein NS5A was included in the screen. Amongst the highest scoring putative binding proteins was the methyltransferase SMYD3. This finding was further verified when we performed an additional analysis of the same samples on a more sensitive mass spectrometer (MS) which has since become available.

In the following article “The lysine methyltransferase SMYD3 interacts with hepatitis C virus NS5A and is a negative regulator of viral particle production” published in *Virology* in August 2014, I describe the confirmation and functional validation of this interaction. I verified the interaction by transient overexpression in HEK 293T cells as well as at the endogenous level and in the context of viral infection. In addition, I mapped the binding sites to lie within DIII of NS5A and the MYND-domain of SMYD3. RNAi-mediated knockdown of SMYD3 is toxic to Huh7 cells. To avoid false results due to siRNA-induced cytotoxicity, I compared the effect of overexpressed wild type to catalytic-dead SMYD3 on subgenomic replicons as well as HCVcc. Interestingly, overexpressing wild type SMYD3 lead to reduction in infectious particle production, suggesting SMYD3 is a negative regulator of infectious particle assembly. Taken together, I confirmed that SMYD3 is an NS5A interactor and that SMYD3 is a negative regulator of HCV assembly.

HCV is a biosafety level 3 (BSL3) pathogen and thus requires a containment level 3 (L3) laboratory. To meet the respective safety requirements, I performed the functional validation in the laboratory of Prof. Ralf Bartenschlager at the University of Heidelberg. I performed the CRAPome analysis and planned and conducted all experiments, including confirmation of the interaction, mapping of the binding sites and the functional validation using subgenomic and infectious *in vitro* models of HCV. Tandem affinity purification of NS5A and subsequent MS and bioinformatics analyses were performed by colleagues as published in Pichlmair et al. I wrote the manuscript under the guidance of Prof. Giulio Superti-Furga and Prof. Ralf Bartenschlager. The article was published under a *Creative*

Commons license, meaning the copyright remains with the author and no permission from Elsevier is required.

3.1.1 The lysine methyltransferase SMYD3 interacts with hepatitis C virus NS5A and is a negative regulator of viral particle production.

Eberle Carol-Ann, Zayas Margarita, Stukalov Alexey, Pichlmair Andreas, Alvisi Gualtiero, Müller André C., Bennett Keiryn L., Bartenschlager Ralf, Superti-Furga Giulio.



ELSEVIER

Contents lists available at ScienceDirect

Virology

journal homepage: www.elsevier.com/locate/yviro

Brief Communication

The lysine methyltransferase SMYD3 interacts with hepatitis C virus NS5A and is a negative regulator of viral particle production



Carol-Ann Eberle^a, Margarita Zayas^b, Alexey Stukalov^a, Andreas Pichlmair^{a,c},
Gualtiero Alvisi^{b,d}, André C. Müller^a, Keiryn L. Bennett^a, Ralf Bartenschlager^{b,*},
Giulio Superti-Furga^{a,**}

^a CeMM Research Center for Molecular Medicine of the Austrian Academy of Sciences, Lazarettgasse 14, AKH BT 25.3, 1090 Vienna, Austria

^b Department of Infectious Diseases, Molecular Virology, Heidelberg University, Im Neuenheimer Feld 345, 69120 Heidelberg, Germany

^c Max-Planck Institute of Biochemistry, Am Klopferspitz 18, 82152 Martinsried, Germany

^d Department of Molecular Medicine, Via Gabelli 63, 35121 Padua, Italy

ARTICLE INFO

Article history:

Received 4 February 2014

Returned to author for revisions

28 February 2014

Accepted 14 May 2014

Available online 14 June 2014

Keywords:

SMYD3

NS5A

HCV

TAP-MS

Virus particle assembly

ABSTRACT

Hepatitis C virus (HCV) is a considerable global health and economic burden. The HCV nonstructural protein (NS) 5A is essential for the viral life cycle. The ability of NS5A to interact with different host and viral proteins allow it to manipulate cellular pathways and regulate viral processes, including RNA replication and virus particle assembly. As part of a proteomic screen, we identified several NS5A-binding proteins, including the lysine methyltransferase SET and MYND domain containing protein 3 (SMYD3). We confirmed the interaction in the context of viral replication by co-immunoprecipitation and co-localization studies. Mutational analyses revealed that the MYND-domain of SMYD3 and domain III of NS5A are required for the interaction. Overexpression of SMYD3 resulted in decreased intracellular and extracellular virus titers, whilst viral RNA replication remained unchanged, suggesting that SMYD3 negatively affects HCV particle production in a NS5A-dependent manner.

© 2014 The Authors. Published by Elsevier Inc. This is an open access article under the CC BY-NC-ND license (<http://creativecommons.org/licenses/by-nc-nd/3.0/>).

Introduction

Hepatitis C virus (HCV) is a positive-sense, single-stranded RNA virus and among the leading causes of chronic hepatitis, a condition often complicated by liver cirrhosis, steatosis and cancer. With an estimated ~170 million people persistently infected worldwide, HCV constitutes a major global health and economic burden (Davis et al., 2011; Mohd Hanafiah et al., 2013). The viral genome consists of a single-strand RNA molecule of ~9.6-kb, encoding only a single polyprotein, which is processed into the three structural proteins core, E1, E2, and the seven non-structural (NS) proteins, p7, NS2, NS3, NS4A, NS4B, NS5A and NS5B (reviewed in (Bartenschlager et al., 2011)). NS5A is a multifunctional, RNA-binding phosphoprotein with key functions in HCV replication and assembly. In addition, NS5A manipulates various cellular pathways to generate an intracellular environment favoring viral replication (Cordek et al., 2011).

The protein is composed of three domains (DI, DII and DIII) that are connected by trypsin-sensitive low complexity sequences (LCSI and II) and contains an N-terminal amphipathic α -helix which tethers NS5A to intracellular membranes (Brass et al., 2002; Penin et al., 2004; Reiss et al., 2011; Tellinghuisen et al., 2004). DI and DII are required for genome replication, whereas DIII is essential for the generation of infectious virus particles (Appel et al., 2008; Masaki et al., 2008; Tellinghuisen et al., 2008b). Thus far, no enzymatic activity has been ascribed to NS5A and although it has been subject to intensive research, the molecular events required for the various effects of NS5A are far from being fully understood. Nevertheless, differential interactions with host as well as viral proteins seem to form the basis of NS5A function (Cordek et al., 2011).

As part of a large-scale proteomic survey of virus–host protein interactions, we identified several cellular binding partners of NS5A (genotype 1b) using a tandem-affinity purification (TAP) mass spectrometry (MS) approach (Pichlmair et al., 2012). Included among the highest ranking proteins was the SET and MYND domain containing protein 3 (SMYD3). SMYD3 is a lysine methyltransferase (KMT) which catalyzes di- and trimethylation of histones H3 and H4, implicating it in transcriptional regulation (Cock-Rada et al., 2012; Foreman et al., 2011; Hamamoto et al.,

* Corresponding author. Tel.: +49 (0)6221 56 4569.

** Corresponding author. Tel.: +43 1 40160 70 001.

E-mail addresses: Ralf.Bartenschlager@med.uni-heidelberg.de (R. Bartenschlager), gsuperti@cemm.oew.ac.at (G. Superti-Furga).

2004). In addition, SMYD3 has also been shown to methylate the vascular endothelial growth factor receptor 1 (VEGFR1) and enhance its kinase activity (Kunizaki et al., 2007). However, there are no reports regarding a role of SMYD3 in the HCV life cycle.

Results and discussion

To follow up and expand on the initial NS5A screen results (Pichlmair et al., 2012), the original samples were re-analyzed on a hybrid linear trap quadrupole (LTQ) Orbitrap Velos. We identified a total of 274 proteins, compared to the 50 detected in the first analysis. A caveat of improved sensitivity is the higher detection rate of non-specific binding proteins. In order to filter false-positive interactors more efficiently, we included additional negative controls available from the recently published CRAPome repository (www.crapome.org) in our analysis. All identified protein interactions were scored using spectral counts to calculate both the SAINT probability and fold change (FC_B) score (Choi et al., 2011; Mellacheruvu et al., 2013). A SAINT probability ≥ 0.9 and an FC_B score ≥ 4 was used as threshold to enrich for high confidence interactors, leaving a total of 24 proteins (Fig. 1A), 50% of which overlapped with our previously published data set (supplemental table 1). In addition, 15 from the 24 were either already validated as NS5A-binding partners or have been confirmed in a study published during the preparation of this manuscript by Germain et al., using a similar experimental approach (supplemental table 1) (Germain et al., 2014).

In addition to the previously characterized NS5A-binding proteins Ubiquitin Specific Peptidase 19 (USP19) and Amphiphysin II (BIN1), one of the highest ranking proteins was the KMT SMYD3 (Masumi et al., 2005; Pichlmair et al., 2012; Zech et al., 2003). This finding is consistent with two previous studies, that further corroborated our results (de Chassey et al., 2008; Germain et al., 2014). Since none of these studies had confirmed the SMYD3–NS5A interaction, we verified it by employing Myc-tagged NS5A and HA-tagged SMYD3 that were co-expressed in HEK 293T cells and subjected to co-immunoprecipitation (co-IP) assays. As shown

in Fig. 1B, SMYD3 co-purified with immunoprecipitated NS5A and vice versa when the reciprocal co-IP was performed. The catalytic activity of SMYD3 was not relevant for the association, since NS5A interacted just as strongly with a point mutant of SMYD3 (Y239F) previously described to be catalytically inactive (Foreman et al., 2011; Xu et al., 2011). Finally, we confirmed the interaction of endogenous SMYD3 with TAP-tagged NS5A expressed in doxycycline-regulated HEK Flp-In cells (Fig. 1D) (Pichlmair et al., 2012).

To further characterize the interaction, we aimed to map the region in SMYD3 bound by NS5A. SMYD3 is a two-lobed protein: the N-terminal region harbors the catalytic SET-domain, which is split by a MYND-domain, a zinc-finger motif mediating protein–protein and protein–DNA interactions (Hamamoto et al., 2004). The C-terminal lobe consists of three tetratricopeptide repeat motifs and is proposed to have a regulatory role in SMYD3 activity by blocking the substrate binding site. Based on the crystal structure of SMYD3, internal deletion mutants were cloned. These lacked surface exposed areas or regions lining the catalytic site (Fig. 2A) (Foreman et al., 2011; Sirinupong et al., 2010; Xu et al., 2011). Although none of the mutants resulted in a complete loss of NS5A-binding, the deletion of the MYND-domain (mutant SΔ2) severely impaired the interaction. The mutant SΔ3 lacking the adjacent residues 88–124 also exhibited reduced binding to NS5A, suggesting that the MYND-domain is either improperly folded in this mutant, or that the binding region extends into the SET-domain (Figs. 2B and C). In addition SMYD3 SΔ2 failed to colocalize with Myc-NS5A when co-transfected in HeLa cells (Supplemental Fig. 1).

Next, we investigated which region of NS5A interacted with SMYD3. Of note, attempts to co-precipitate SMYD3 with immunopurified NS5A using a monoclonal mouse anti-NS5A antibody (9E10) failed, suggesting antibody binding may overlap with the SMYD3 binding site (data not shown). Since the antibody detects an epitope in DIII, we generated NS5A mutants lacking parts of the C-terminal portion of the protein (Fig. 2D). As shown in Fig. 2E and F, deleting residues encompassing DII had no effect on the interaction with SMYD3, whereas the absence of residues

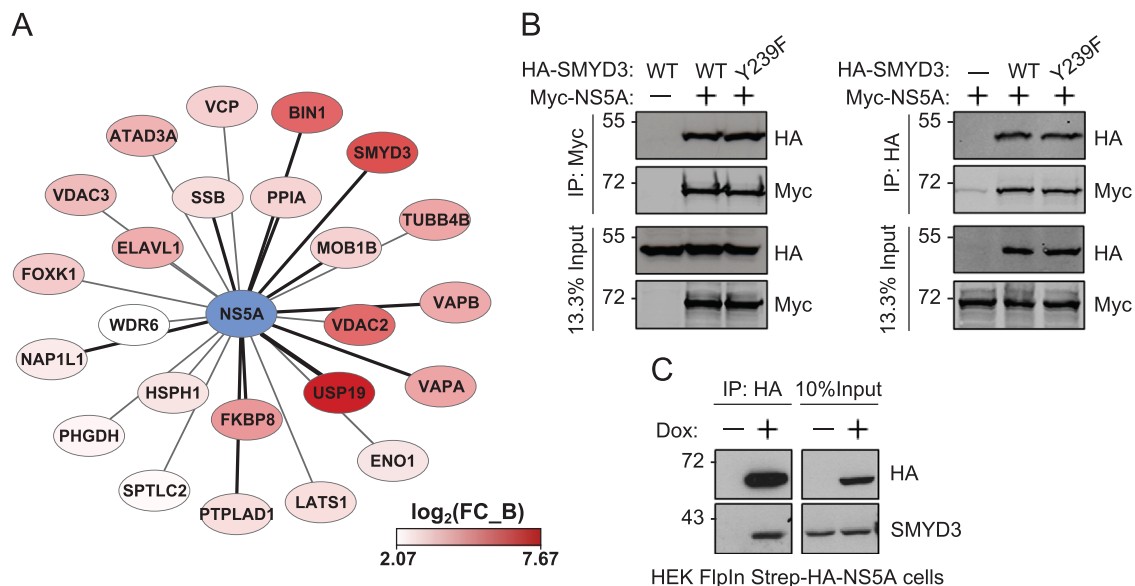


Fig. 1. Identification and confirmation of SMYD3 as interactor of NS5A. (A) Schematic representation of NS5A-binding proteins identified by TAP-MS with an FC_B score ≥ 4 . Node color gradient corresponds to increasing \log_2 FC_B scores. Known interactions are depicted by black edges, novel interactions by gray edges. NS5A is highlighted in blue. Two biological replicates were analyzed as technical duplicates. (B) Interaction of overexpressed SMYD3 and NS5A. Myc-NS5A, HA-SMYD3 or catalytic inactive SMYD3 (Y239F) were transiently expressed in HEK 293T cells. 48 h posttransfection, protein complexes were immunoprecipitated and analyzed by Western blot. Representative blots of 3 independent experiments are shown. (C) Interaction of endogenous SMYD3 with TAP-tagged NS5A. Expression of NS5A in HEK FlpIn Strep-HA-NS5A cells was induced by addition of 1 μ g/ml doxycycline. After 48 h, NS5A was immunoprecipitated and samples analyzed by Western blot.

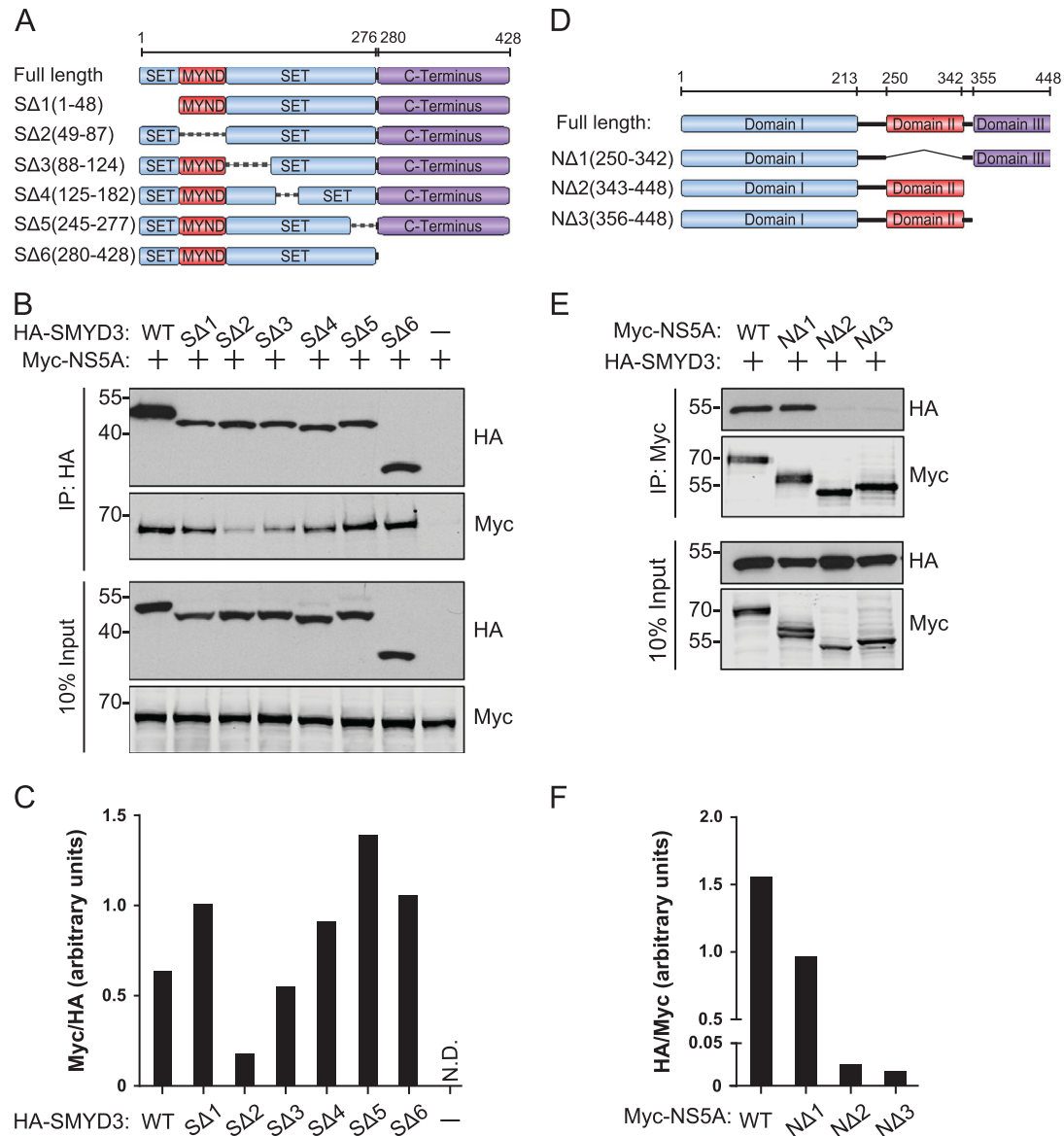


Fig. 2. Mapping the binding sites of SMYD3 and NS5A. (A) Schematic representation of full-length SMYD3 and respective deletion mutants. The N-terminal lobe contains the catalytic SET-domain (blue), which is split by the zinc-finger MYND-domain (red). The second lobe consists of regulatory C-terminal domain (purple). Residues spanning the individual domains are indicated. (B) Association of Myc-tagged NS5A with HA-tagged SMYD3 deletion mutants. The indicated plasmids were co-expressed in HEK 293T cells and co-immunoprecipitation experiments were performed as in Fig. 1B. (C) Ratio of co-purified NS5A with the respective SMYD3 mutants. Bars represent the ratio of quantified band signals of the Western blots shown above. (D) Schematic representation of full-length NS5A and respective deletion mutants. NS5A consists of 3 domains (blue, red and purple, respectively) connected by two low-complexity sequences (black). Residues spanning the individual domains are indicated. (E) Association of HA-tagged SMYD3 with Myc-tagged NS5A deletion mutants. The indicated plasmids were co-expressed in HEK 293T cells and co-immunoprecipitation experiments were performed as in (B). (F) Ratio of co-purified SMYD3 with the respective NS5A mutants. Bars represent the ratio of quantified band signals of the Western blots shown above. (B and E) Representative blots of at least 2 similar experiments are shown.

343–448, which correspond to LCSII and DIII, abolished SMYD3 binding. The LCSII contains numerous prolines, a common recognition motif of MYND-domains (Ansieau and Leutz, 2002). To distinguish if either LCSII or DIII were responsible for the interaction, we included an additional mutant lacking only DIII. The presence, however, of the polyproline motif in LCSII did not restore SMYD3 binding, meaning that the association is mediated by DIII. Taken together, our results confirm SMYD3 as specific binding partner of NS5A and identify the SMYD3 MYND-domain and DIII of NS5A as regions mediating the interaction.

To validate these results in a more authentic system we evaluated if SMYD3 also interacted with NS5A in the context of an active viral replicase. To this end, we generated Huh7.5 cells stably expressing HA-tagged SMYD3 (Huh7.5/HA-SMYD3). Previous reports have shown that adding an N-terminal tag to SMYD3

does not interfere with its catalytic activity, nor does it seem to alter its subcellular localization (Fig. 3E) (Foreman et al., 2011; Hamamoto et al., 2004; Kunizaki et al., 2007). Huh7.5/HA-SMYD3 cells were then electroporated with RNA encoding the genotype 2a subgenomic JFH1 replicon, or the full-length genome of the chimeric strain termed Jc1, which produces high amounts of infectious particles in culture (Pietschmann et al., 2006). In both cases, NS5A co-precipitated with HA-SMYD3 (Fig. 3A and C). NS5A exists in a basal and a hyperphosphorylated state. Based on apparent molecular weight, these are commonly referred to as p56 and p58, respectively (Tanji et al., 1995). Interestingly, we found the p58 form preferentially co-precipitated with SMYD3 (Fig. 3B and D).

In addition, we used immunofluorescence to examine the localization of SMYD3 with subgenomic replicon-derived NS5A

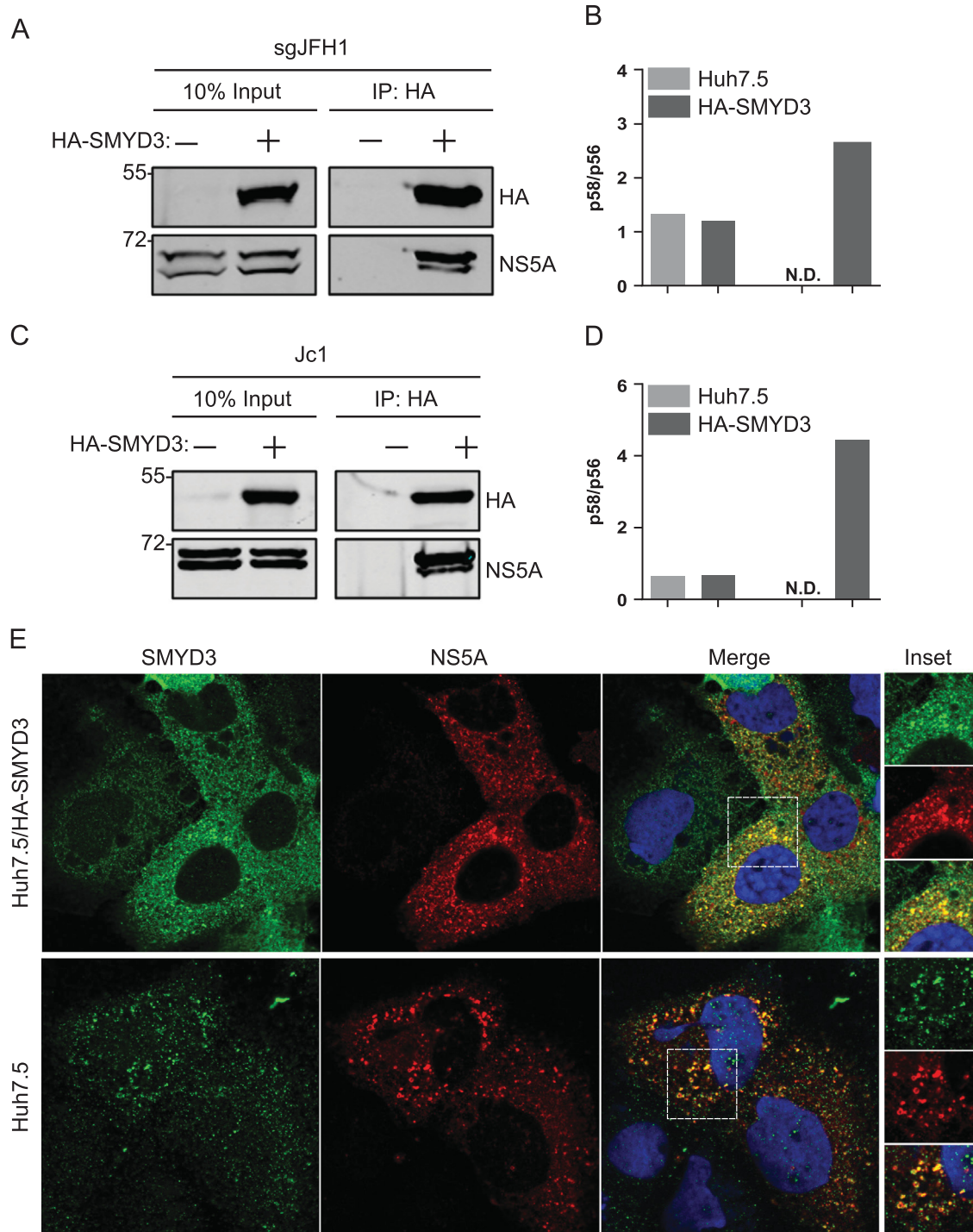


Fig. 3. Interaction of SMYD3 with NS5A in the context of viral replication. (A and C) Huh7.5/HA-SMYD3 cells were electroporated with RNA encoding the JFH1 subgenomic replicon (sgJFH1) or full-length Jc1. 72 h post electroporation, HA-SMYD3 was immunoprecipitated and analyzed by Western blot using anti-HA and anti-NS5A antibodies. (B and D) Enrichment of hyperphosphorylated NS5A (p58) in SMYD3 pull-downs. Western blot bands shown in (A) and (C) corresponding to the p56 and p58 phosphoforms of NS5A were quantified and the p58/p56 ratio calculated. (E) Co-localization of overexpressed HA-SMYD3 (top panel) or endogenous SMYD3 with subgenomic JFH1 NS5A. Huh7.5 cells were electroporated as described above. After 48 h, cells were fixed and proteins stained using SMYD3 (green) and NS5A (red) antibodies. Nuclei were counterstained with DAPI. Images were analyzed by confocal microscopy. Co-localization was quantified using ImageJ and the WCIF 'Intensity Correlation Analysis' plugin (upper panel: $R_r=0.746$; $R=0.903$; lower panel: $R_r=0.620$; $R=0.781$).

in Huh7.5 cells. In accordance with previous studies, NS5A localized to cytoplasmic, most often perinuclear foci (Fig. 3E insets) (Gosert et al., 2003). In some instances, NS5A staining appeared as ring-like structures, probably corresponding to lipid droplets decorated with this protein (Appel et al., 2008). As shown in Fig. 3E, NS5A clearly co-localized with HA-tagged overexpressed as

well as endogenous SMYD3. The latter is of particular importance, as attempts to detect an interaction between NS5A and endogenous SMYD3 were not successful, due to the lack of a suitable anti-SMYD3 antibody to immunoprecipitate the endogenous protein (data not shown). Collectively, our data reveal that SMYD3 and NS5A also interact and co-localize with each other in the context

of active viral replication. Furthermore, the fact that SMYD3 associates also with genotype 2a NS5A indicates that the interaction is not genotype-specific.

SMYD3 is upregulated in various types of cancer, in particular colon, breast, prostate and liver carcinomas, where it exhibits potent growth promoting effects. Interestingly, RNAi-mediated knockdown of SMYD3 has been shown to result in cell cycle arrest and apoptosis of different cancer cell lines, including the human hepatoma cell line Huh7, from which Huh7.5 and Huh7-Lunet cells used in this study are derived (Blight et al., 2002; Chen et al., 2007; Friebe et al., 2005; Hamamoto et al., 2004; Ren et al., 2010). In order to investigate if SMYD3 had a role in the HCV life cycle, but at the same time avoid off-target effects due to RNAi-induced cytotoxicity associated with SMYD3 knockdown, we generated a Huh7-Lunet-derived cell pool stably overexpressing wildtype SMYD3 (Lunet/S3) or the catalytically inactive point mutant SMYD3 Y239F (Lunet/YF) (Fig. 4A) that was still capable of interacting with NS5A (Fig. 1B).

First, we analyzed whether SMYD3 had an effect on viral RNA replication kinetics. To this end, stable Huh7-Lunet/S3 or Lunet/YF cells were electroporated with subgenomic JFH-1 reporter replicon RNA and viral replication was quantified by measuring Firefly luciferase activity in cell lysates harvested at several time points after transfection. As shown in Fig. 4B, luciferase activities were similar

for each cell line, excluding a role of SMYD3 in viral replication. Similar results were obtained for the full-length, infectious *Renilla luciferase* reporter virus JcR2A (Fig. 4C) (Reiss et al., 2011). Next, we assessed if SMYD3 influenced infectious virion production in the form of infectious particles release relative to viral replication (Infectivity/replication). For this purpose we infected naïve Huh7.5 cells with supernatants harvested from JcR2A-transfected Lunet/S3, Lunet/YF or Lunet/GFP cells and quantified *Renilla* activity 48 h post infection. Interestingly, relative infectivity of virus particles released from Lunet/S3 cells was more than 3-fold lower as compared to GFP-control cells. This effect appeared to be specific as it was not observed in cells overexpressing catalytic inactive SMYD3 (Fig. 4D). To distinguish if this defect occurred at the level of virus particle assembly or release, we determined relative infectivity in cell culture supernatants and corresponding cell lysates that were prepared by repeated cycles of freezing and thawing (extra- and intracellular infectivity, respectively). Naïve Huh7.5 cells were inoculated with the respective fractions and luciferase activity was determined 48 h later. As shown in Fig. 4E, cells overexpressing wildtype SMYD3 exhibited a reduction of relative intra- as well as extracellular infectivity amounts (5-fold and 2-fold, respectively), whereas titers of Lunet/YF cells were similar to Lunet-GFP cells, arguing that SMYD3 impaired infectious particle assembly.

To corroborate this observation, we repeated this experiment by using a reporter-free virus genome and more direct assays. The

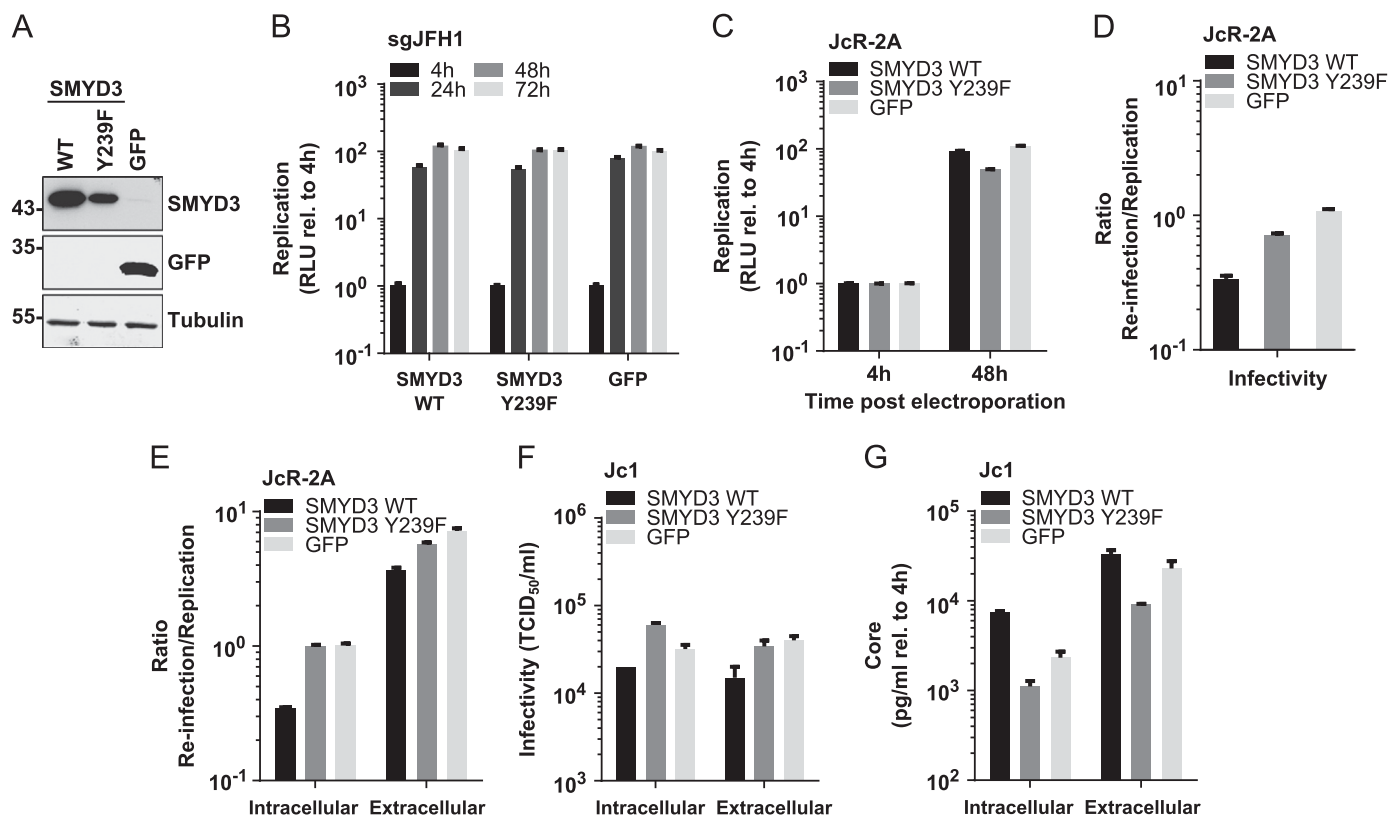


Fig. 4. SMYD3 is a negative regulator of HCV infectious particle assembly. (A) Western blot analysis of Huh7-Lunet cells stably expressing wildtype (WT) SMYD3, catalytic inactive (Y239F) SMYD3 or GFP. (B) Effect of SMYD3 overexpression on HCV RNA replication kinetics. Indicated cell lines were electroporated with RNA encoding the subgenomic JFH1 luciferase reporter replicon. Viral replication was measured at the indicated time points by luciferase assay. Luciferase activity is expressed in relative light units (RLU) normalized to the 4 h value to account for different transfection efficiencies. (C) Effect of SMYD3 overexpression on replication of the full-length infectious *Renilla* reporter virus JcR-2A. Indicated cell lines were electroporated with JcR-2A RNA and harvested after 4 and 48 h. Viral replication was quantified as mentioned above. (D) Effect of SMYD3 overexpression on JcR-2A relative infectivity. Supernatants from (C) were harvested at the indicated time points and used to inoculate naïve Huh7.5 cells in duplicate. 48 h post infection, *Renilla* activity in reinfected cells was measured as in (B). Viral infectivity is expressed as ratio of re-infection over replication. (E) JcR-2A intra- and extracellular infectivity. Cells pellets and supernatants of cells transfected with JcR-2A RNA were subjected to 3 freeze-thaw cycles 48 h postelectroporation. Viral infectivity in the respective fractions was determined as mentioned above. (F) Effect of SMYD3 overexpression on intra- and extracellular virus titers of the non-reporter virus Jc1. The different Huh7-Lunet cell lines were transfected with Jc1 RNA. 48 h postelectroporation, cell pellets and supernatants were treated by freezing and thawing as described above. Viral infectivity was determined by limiting dilution assay and data are represented as TCID₅₀/ml. (G) Intra- and extracellular amounts of HCV core protein. Core levels in cell lysates and corresponding supernatants were determined by core-specific ELISA 4 and 48 h postelectroporation of Jc1 RNA. Concentrations of core are depicted as pg/ml normalized to intracellular core levels 4 h post electroporation to account for different transfection efficiencies. Bars represent mean values and standard error of the means from 3 (JcR-2A) or 2 (sgJFH1 and Jc1) independent experiments.

individual cell lines were electroporated with RNA encoding the chimeric virus Jc1 and after 48 h intra- and extracellular virus titers were quantified by limiting dilution assay (TCID₅₀/ml) (Fig. 4F). In addition, we determined concentrations of HCV core protein in cell lysates and supernatants by core ELISA (Fig. 4F). In accordance with our previous results, virus titers were 4 times lower in Lunet/S3 cells, whereas overexpressing catalytically inactive SMYD3 resulted in titers similar to GFP control cells (Fig. 4F). Interestingly, the reduction in virus titers coincided with an overall intracellular accumulation of core protein (Fig. 4G), with levels detected in Lunet/S3 cells on average three times higher compared to GFP control cells.

To exclude the possibility that SMYD3 overexpression influenced the cellular secretory capacity in general, we transfected the different Huh7-Lunet cell lines with a plasmid encoding the naturally secreted *Gaussia luciferase* (G-luc) and monitored G-luc activity in the supernatants over time. Protein secretion was almost identical among the different cell lines, indicating that the reduction of virus titers in response to SMYD3 overexpression was specific for HCV assembly and not the consequence of impaired protein secretion (supplemental Fig. 2). Taken together, our data suggest that SMYD3 negatively regulates virus particle production by interfering with the assembly process of infectious virions, which is reflected in form of reduced virus titers and an overall accumulation of intracellular core protein.

As mentioned in the introduction, NS5A is a multitasking protein, coordinating various stages of the viral life cycle, as well as interfering with many different host cellular pathways. It is believed, that different NS5A interactions with viral and cellular proteins, presumably regulated by the NS5A phosphorylation state, determine its functional state (Cordek et al., 2011; Huang et al., 2007). As shown here and in earlier studies, one of these interaction partners is SMYD3. To date, very little is known about its physiological role. Given that lysine methylation is increasingly recognized as an important post-translational modification regulating protein function and fine-tuning many essential signaling pathways, one might speculate that SMYD3 is a component of one or more cellular processes that are involved in virus production (Erce et al., 2012). Alternatively, SMYD3 might be involved in the modification and impairment of other HCV proteins required for assembly. Binding to SMYD3 would therefore allow NS5A to counteract SMYD3 function and ensure productive virion assembly. This hypothesis is supported by the fact that NS5A interacted with SMYD3 through DIII, the domain essential for virus formation (Appel et al., 2008, 2005; Hughes et al., 2009; Tellinghuisen et al., 2008a).

Conclusion

In summary, we report the identification of the lysine methyltransferase SMYD3 as a binding partner of HCV NS5A. Using cell lines overexpressing wildtype or non-functional SMYD3, we identified SMYD3 as potential negative regulator of HCV infectious particle assembly. Further studies, in particular regarding the cellular function and targets of SMYD3, may aid to gain more mechanistic insight into SMYD3-mediated assembly inhibition and help to decipher the still only partially understood HCV assembly process.

Materials and methods

Liquid chromatography mass spectrometry and data validation

TAP-MS analyses of NS5A-associated protein complexes has been performed as previously described (Pichlmair et al., 2012). The same samples were re-analyzed by liquid chromatography mass spectrometry (LCMS) on a hybrid linear trap quadrupole

(LTQ) Orbitrap Velos (ThermoFisher Scientific) coupled to an Agilent 1200 series HPLC (Agilent technologies) as previously described (Huber et al., 2014). The list of all identified proteins was uploaded to the 'Contaminant Repository for Affinity Purification-Mass spectrometry data (CRAPome) repository' (www.crapome.org) and filtered against a set of 17 negative control samples. Negative control samples were chosen according to the following criteria: cell line (HEK 293), epitope tag (Strep-HA), subcellular fraction (total cell lysate), instrument type (LTQ Orbitrap Velos). Spectral count data was used to calculate the 'Significance Analysis of Interactome' (SAINT) probability (low mode=0, min fold=1, Normalize=1) and a fold change score (FC_B; default settings) (Choi et al., 2011; Mellacheruvu et al., 2013). Both scoring tools are available on the repository website. Proteins were first filtered based on a SAINT probability ≥ 0.9 , followed by a second filter corresponding to a FC_B score ≥ 4 . The NS5A interactome was visualized using cytoscape (www.cytoscape.org).

Cell lines and cell culture

All cell lines were maintained in Dulbecco's Modified Eagle Medium (Gibco) supplemented with 10% FCS (Invitrogen), 2 mM Glutamine and antibiotics (100 U/ml penicillin and 100 mg/ml streptomycin). HEK FlpIn Strep-HA-NS5A cells have been described previously (Pichlmair et al., 2012). The human hepatoma cell line Huh7.5 was purchased from Apath LLC (St. Louis, MO). Huh7-Lunet cells have been described previously (Friebe et al., 2005; Koutsoudakis et al., 2006). Cells stably expressing SMYD3, SMYD3 Y239F, GFP or HA-SMYD3 were generated by lentiviral transduction and selected and maintained in DMEM containing 5 μ g/ml of puromycin.

Plasmid constructs

Expression vectors encoding full-length or truncated proteins were generated by Gateway[®] recombination reactions (Invitrogen) as described previously (Pichlmair et al., 2012). Expression vectors used in this study were: pcDNA-N-2HA-TEV-GW and pCS2-N-6xMyc-GW for transient expression in HEK 293T cells and pWPI-GW and pWPI-N-HA-GW for the generation of lentiviral particles. Internal and point mutations were introduced by site-directed mutagenesis (Agilent Technologies) of the respective pDONR201 vectors according to the manufacturer's instructions. All primer sequences used in this study are available upon request.

Plasmids pFK_i389LucNS3-3'JFH_ δ g (sgJFH1), pFK-J6/Core-846/JFH1_wt_ δ g (Jc1) and pFK_i389-JcR2a_ δ g_JC1 (JcR2a) encoding the JFH1 subgenomic reporter replicon, the full-length chimeric genome Jc1 and the Jc-1 derived reporter virus JcR-2A, respectively, have been described recently (Kaul et al., 2007; Pietschmann et al., 2006; Reiss et al., 2011).

Lentiviral gene transduction

Huh7-Lunet and Huh7.5 cells stably expressing SMYD3, SMYD3 Y239F, GFP or HA-SMYD3, respectively, were generated by lentiviral transduction. For lentivirus production, HEK 293T were seeded in 6-well plates and co-transfected with the respective lentiviral vector pWPI (1 μ g), the packaging vector pCMVR8.91 (750 ng) and the envelope vector pMD.G (250 ng) using Lipofectamine2000 (Invitrogen) as recommended by the manufacturer. Target cells were seeded in a 6-well plate and infected with filtered viral supernatants harvested after 48 h. Transduced cells were selected by addition of 5 μ g/ml puromycin 24 h post infection. SMYD3 WT, SMYD3 Y239F or GFP expression was analyzed by Western blot using rabbit anti-SMYD3 (Abcam, 1:2000) or mouse anti-GFP (Roche, 1:5000) antibodies.

Co-Immunoprecipitations

HEK 293T cells were co-transfected with the indicated plasmids using Polyfect (QIAGEN) according to the manufacturer's protocol. The amount of DNA per plasmid was adjusted to achieve equal expression. Total levels of transfected DNA were kept constant by the addition of empty vector. For co-precipitation of endogenous SMYD3 with TAP-tagged NS5A: HEK FlpIn cells inducibly expressing NS5A fused to a tandem Strep-tag II-hemagglutinin (Strep-HA or TAP-tag) were cultured in the presence of 1 µg/ml doxycycline. 48 h post transfection or doxycycline induction, cells were lysed in IP-buffer (50 mM Tris/HCl pH 8.0, 150 mM NaCl, 1%NP40, 5 mM EDTA, 5 mM EGTA, protease inhibitor cocktail (Roche), 50 mM NaF and 1 mM Na₃VO₄) and cleared by centrifugation. 1.5 or 2 mg of total protein was incubated with anti-HA, or anti-Myc agarose beads (SIGMA) for 1.5 h at 4 °C. Beads were washed 3 × with IP-buffer and then eluted in 5% (v/v) SDS/PBS. Immunoprecipitates were analyzed by Western blot using the tag-specific directly conjugated antibodies rabbit anti-Myc IRDye™800 (Rockland) and mouse anti HA7-HRP (SIGMA) as indicated. Endogenous SMYD3 in HEK FlpIn cells was detected using rabbit anti-SMYD3 as mentioned above. NS5A expressed in the context of the subgenomic or full-length replicons was detected using the monoclonal mouse anti-NS5A 9E10 (1:10,000; kind gift from Prof. Charles Rice; Rockefeller University, New York). Bands were quantified using the ImageJ software (Schneider et al., 2012).

Confocal microscopy

Huh7.5 wildtype or Huh7.5/HA-SMYD3 cells electroporated with subgenomic JFH1 replicon transcripts were grown on coverslips for 72 h. Cells were rinsed with PBS, fixed with 4% paraformaldehyde for 15 min, and then permeabilized with 0.1% Triton X-100 for 15 min. After rinsing with PBS, cells were blocked with 5% goat serum (GS) for 1 h. Cells were stained with rabbit anti-SMYD3 (1:300; Abcam) and mouse anti-NS5A (1:1000; 9E10) diluted in 5% GS for 1 h. After four washes with PBS, slips were incubated in the dark with Alexa Fluor 488 anti-rabbit and 568 anti-mouse secondary antibodies (both 1:1000 in 5%GS; Molecular Probes) for 1 h. Nuclei were counterstained with DAPI. Cover slips were mounted on glass slides using ProLong Gold Antifade reagent (Invitrogen). Images were acquired using a Zeiss LSM 700 confocal laser scanning microscope. Co-localization of fluorescence signals was evaluated quantitatively for Pearson's correlation coefficient (R_p) and Manders coefficient (R) by using the 'Image J' software and the 'Intensity Correlation Analysis' plugin.

RNA in vitro transcription and electroporation

in vitro transcription of *Mlu*I-linearized plasmids was performed as described previously (Krieger et al., 2001). Briefly, 5–10 µg of linearized plasmids were in vitro transcribed in an overnight reaction using T7 RNA polymerase and terminated by the addition of DNase. RNA was extracted with acidic phenol and chloroform, precipitated in isopropanol and the pellet dissolved in H₂O. RNA integrity was assessed by agarose gel electrophoresis.

For electroporation of in vitro transcribed RNA, 1×10^7 cells/ml of Huh7-Lunet cells were suspended in cytomix supplemented with 2 mM ATP, pH 7.6 and 5 mM glutathione (van den Hoff et al., 1990). 200 µl of cell suspension were mixed with 5 µg of RNA, transferred to an electroporation cuvette (gap width of 0.2 cm) and electroporated using the BioRad Gene Pulser System at 975 µF and 166 V. Cells were immediately transferred to 13 ml of fresh medium and seeded as described below. For co-precipitation experiments, 1.5×10^7 cells/ml of Huh7.5 or Huh7.5/HA-SMYD3 cells were suspended in cytomix as above. 400 µl of cell

suspension was mixed with 7.5 µg of RNA and electroporated in cuvettes with a 0.4 gap width at 975 µF and 270 V. Cells were then resuspended in 20 ml DMEM, transferred to 15 cm² dishes and incubated for 72 h.

Replication and infectivity assays

Quantification of Firefly or Renilla luciferase activity as readout for sgJFH1 and JcR2A replication, respectively, was performed as described previously (Reiss et al., 2011). Briefly, cells were lysed in 300 µl (6-well plate) of lysis buffer at the indicated time points post electroporation. Luminescence in 20 µl of lysate was quantified in technical duplicates for 10 s in a luminometer (Lumat LB9507; Berthold, Freiburg, Germany). Relative light units (RLUs) were normalized to the respective 4 h value to account for differences in transfection efficiency.

To measure JcR-2A infectivity, supernatants were collected 48 h post electroporation and used to inoculate naïve Huh7.5 cells seeded in 24-well plates the day before (5×10^4 ml⁻¹). Renilla activity was measured 48 h post reinfection as described above. Jc1 infectivity was determined by limiting dilution assay on Huh7.5 cells (Lindenbach et al., 2005). Positive cells were stained with a mouse monoclonal NS3 (2E3) antibody and HRP-conjugated anti-mouse polyclonal antibody (Sigma) (Backes et al., 2010). To measure intra- and extracellular infectivity, electroporated (Jc1 or JcR-2A) cells were seeded on 10 cm² dishes. After 48 h, cells were harvested and subjected to multiple freeze-thaw cycles as described previously (Gastaminza et al., 2006). Viral titers of the respective fractions were determined as described above.

Core ELISA

To quantify HCV core protein amounts, transfected cells were seeded into 6-well plates (2 ml/well). After 48 h, cell culture supernatants were filtered through 45 µm filters and diluted 1:2 with PBS supplemented with 1% Triton X-100. To determine intracellular core amounts, cell monolayers were washed twice with PBS and lysed by addition of 0.5 ml PBS containing 0.5% Triton X-100 and 1 mM PMSF, 0.1 µg/ml Aprotinin and 4 µg/ml Leupeptin. Lysates were cleared by centrifugation at 10,000 RPM for 10 min at 4 °C. HCV core protein was quantified in the Central Laboratory of the University Hospital Heidelberg (Analysezentrum, Heidelberg, Germany). If required, samples were diluted with PBS containing 0.5% Triton X-100.

Acknowledgments

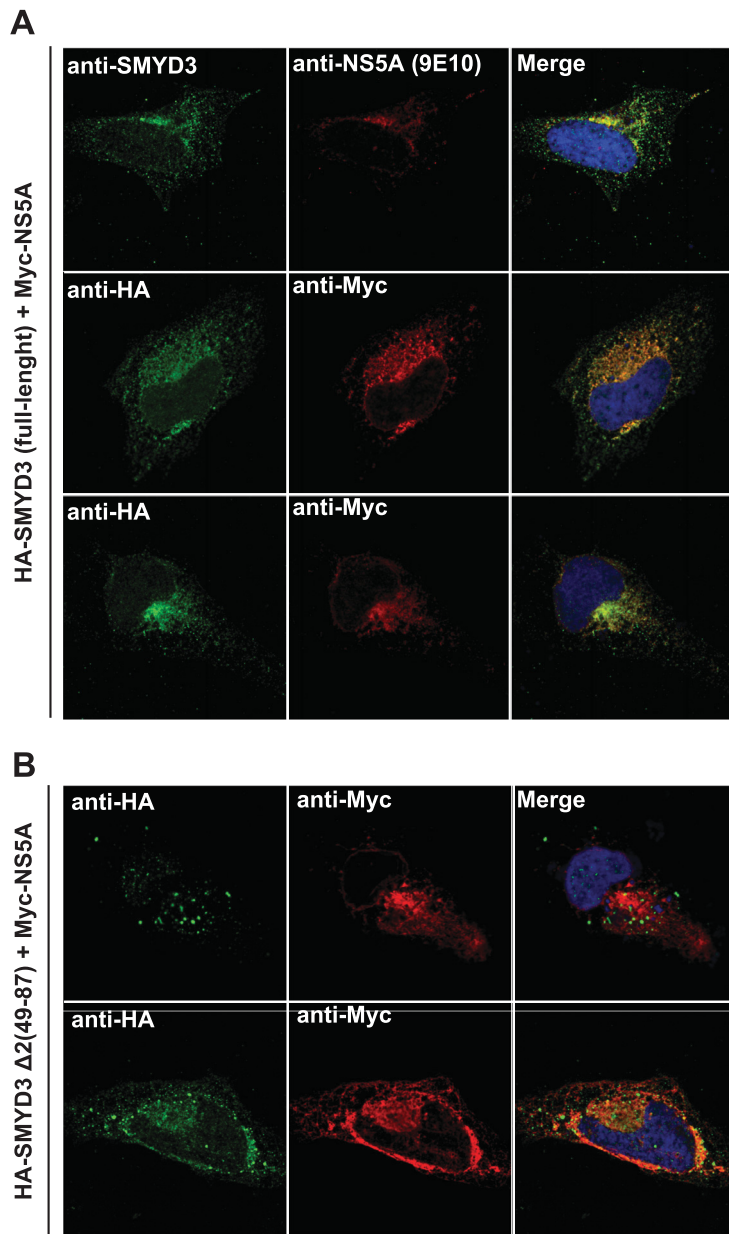
The work of C.A.E was supported by the Austrian Science Fund (FWF W1205-B09, CCHD PhD program). Work of R.B. is supported by the Deutsche Forschungsgemeinschaft (Transregional Collaborative Research Project TR83, TP13 and Collaborative Research Project 638, TP A5). We thank Prof. Charles M. Rice for the kind gift of the monoclonal mouse anti-NS5A antibody (Rockefeller University, New York); Roberto Giambruno, Marielle Klein, Berend Snijder and Richard Kumaran Kandasamy for critical comments on the manuscript.

Appendix A. Supporting information

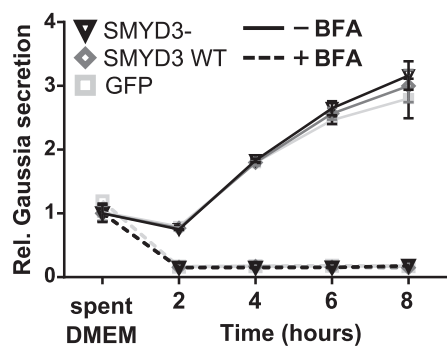
Supplementary data associated with this article can be found in the online version at <http://dx.doi.org/10.1016/j.virol.2014.05.016>.

References

- Ansieau, S., Leutz, A., 2002. The conserved Mynd domain of BS69 binds cellular and oncoviral proteins through a common PXLXP motif. *J. Biol. Chem.* 277, 4906–4910.
- Appel, N., Pietschmann, T., Bartenschlager, R., 2005. Mutational analysis of hepatitis C virus nonstructural protein 5A: potential role of differential phosphorylation in RNA replication and identification of a genetically flexible domain. *J. Virol.* 79, 3187–3194.
- Appel, N., Zayas, M., Miller, S., Krijnse-Locker, J., Schaller, T., Friebe, P., Kallis, S., Engel, U., Bartenschlager, R., 2008. Essential role of domain III of nonstructural protein 5A for hepatitis C virus infectious particle assembly. *PLoS Pathog.* 4, e1000035.
- Backes, P., Quinkert, D., Reiss, S., Binder, M., Zayas, M., Rescher, U., Gerke, V., Bartenschlager, R., Lohmann, V., 2010. Role of annexin A2 in the production of infectious hepatitis C virus particles. *J. Virol.* 84, 5775–5789.
- Bartenschlager, R., Penin, F., Lohmann, V., André, P., 2011. Assembly of infectious hepatitis C virus particles. *Trends Microbiol.* 19, 95–103.
- Blight, K.J., McKeating, J.A., Rice, C.M., 2002. Highly permissive cell lines for subgenomic and genomic hepatitis C virus RNA replication. *J. Virol.* 76, 13001–13014.
- Brass, V., Bieck, E., Montserret, R., Wolk, B., Hellings, J.A., Blum, H.E., Penin, F., Moradpour, D., 2002. An amino-terminal amphipathic alpha-helix mediates membrane association of the hepatitis C virus nonstructural protein 5A. *J. Biol. Chem.* 277, 8130–8139.
- Chen, L.-B., Xu, J.-Y., Yang, Z., Wang, G.-B., 2007. Silencing SMYD3 in hepatoma demethylates RIZ1 promoter induces apoptosis and inhibits cell proliferation and migration. *World J. Gastroenterol.* 13, 5718–5724.
- Choi, H., Larsen, B., Lin, Z.-Y., Breitkreutz, A., Mellacheruvu, D., Fermin, D., Qin, Z.S., Tyers, M., Gingras, A.-C., Nesvizhskii, A.I., 2011. SAINT: probabilistic scoring of affinity purification-mass spectrometry data. *Nat. Methods* 8, 70–73.
- Cock-Rada, A.M., Medjkane, S., Janski, N., Yousfi, N., Perichon, M., Chaussepied, M., Chluba, J., Langsley, G., Weitzman, J.B., 2012. SMYD3 promotes cancer invasion by epigenetic upregulation of the metalloproteinase MMP-9. *Cancer Res.* 72, 810–820.
- Cordek, D.G., Bechtel, J.T., Maynard, A.T., Kazmierski, W.M., Cameron, C.E., 2011. Targeting the NS5A protein of HCV: an emerging option. *Drugs Future* 36, 691–711.
- Davis, K.L., Mitra, D., Medjedovic, J., Beam, C., Rustgi, V., 2011. Direct economic burden of chronic hepatitis C virus in a United States managed care population. *J. Clin. Gastroenterol.* 45, e17–24.
- de Chassey, B., Navratil, V., Taffereau, L., Hiet, M.S., Aublin-Gex, A., Agaugué, S., Meiffren, G., Pradezynski, F., Faria, B.F., Chantier, T., Le Breton, M., Pellet, J., Davoust, N., Mangeot, P.E., Chaboud, A., Penin, F., Jacob, Y., Vidalain, P.O., Vidal, M., André, P., Rabourdin-Combe, C., Lotteau, V., 2008. Hepatitis C virus infection protein network. *Mol. Syst. Biol.* 4.
- Erce, M.A., Pang, C.N.I., Hart-Smith, G., Wilkins, M.R., 2012. The methylproteome and the intracellular methylation network. *Proteomics* 12, 564–586.
- Foreman, K.W., Brown, M., Park, F., Emtage, S., Harriss, J., Das, C., Zhu, L., Crew, A., Arnold, L., Shaaban, S., Tucker, P., 2011. Structural and functional profiling of the human histone methyltransferase SMYD3. *PLoS ONE* 6, e22290.
- Friebe, P., Boudet, J., Simorre, J.P., 2005. Kissing-loop interaction in the 3' end of the hepatitis C virus genome essential for RNA replication. *J. Virol.* 79, 380–392.
- Gastaminza, P., Kapadia, S.B., Chisari, F.V., 2006. Differential biophysical properties of infectious intracellular and secreted hepatitis C virus particles. *J. Virol.* 80, 11074–11081.
- Germain, M.A., Chatel-Chaix, L., Gagne, B., Bonneil, E., Thibault, P., Pradezynski, F., de Chassey, B., Meyniel-Shicklin, L., Lotteau, V., Baril, M., Lamarre, D., 2014. Elucidating novel hepatitis C virus/host interactions using combined mass spectrometry and functional genomics approaches. *Mol. Cell. Proteomics* 13, 184–203.
- Gosert, R., Egger, D., Lohmann, V., Bartenschlager, R., Blum, H.E., Bienz, K., Moradpour, D., 2003. Identification of the hepatitis C virus RNA replication complex in Huh-7 cells harboring subgenomic replicons. *J. Virol.* 77, 5487–5492.
- Hamamoto, R., Furukawa, Y., Morita, M., Iimura, Y., Silva, F.P., Li, M., Yagyu, R., Nakamura, Y., 2004. SMYD3 encodes a histone methyltransferase involved in the proliferation of cancer cells. *Nat. Cell Biol.* 6, 731–740.
- Huang, Y., Staschke, K., De Francesco, R., Tan, S.-L., 2007. Phosphorylation of hepatitis C virus NS5A nonstructural protein: a new paradigm for phosphorylation-dependent viral RNA replication? *Virology* 364, 1–9.
- Huber, M.L., Sacco, R., Parapatics, K., Skucha, A., Khamina, K., Müller, A.C., Rudashevskaya, E.L., Bennett, K.L., 2014. abFASP-MS: affinity-based filter-aided sample preparation mass spectrometry for quantitative analysis of chemically labeled protein complexes. *J. Proteome Res.* 13, 1147–1155.
- Hughes, M., Griffin, S., Harris, M., 2009. Domain III of NS5A contributes to both RNA replication and assembly of hepatitis C virus particles. *J. Gen. Virol.* 90, 1329–1334.
- Kaul, A., Woerz, I., Meuleman, P., Leroux-Roels, G., Bartenschlager, R., 2007. Cell culture adaptation of hepatitis C virus and in vivo viability of an adapted variant. *J. Virol.* 81, 13168–13179.
- Koutsoudakis, G., Herrmann, E., Kallis, S., Bartenschlager, R., Pietschmann, T., 2006. The level of CD81 cell surface expression is a key determinant for productive entry of hepatitis C virus into host cells. *J. Virol.* 81, 588–598.
- Krieger, N., Lohmann, V., Bartenschlager, R., 2001. Enhancement of hepatitis C virus RNA replication by cell culture-adaptive mutations. *J. Virol.* 75, 4614–4624.
- Kunizaki, M., Hamamoto, R., Silva, F.P., Yamaguchi, K., Nagayasu, T., Shibuya, M., Nakamura, Y., Furukawa, Y., 2007. The lysine 831 of vascular endothelial growth factor receptor 1 is a novel target of methylation by SMYD3. *Cancer Res.* 67, 10759–10765.
- Lindenbach, B.D., Evans, M.J., Syder, A.J., Wolk, B., 2005. Complete replication of hepatitis C virus in cell culture. *Science* 280, 747–749.
- Masaki, T., Suzuki, R., Murakami, K., Aizaki, H., Ishii, K., Murayama, A., Date, T., Matsuura, Y., Miyamura, T., Wakita, T., Suzuki, T., 2008. Interaction of hepatitis C virus nonstructural protein 5A with core protein is critical for the production of infectious virus particles. *J. Virol.* 82, 7964–7976.
- Masumi, A., Aizaki, H., Suzuki, T., DuHadaway, J.B., Prendergast, G.C., Komuro, K., Fukazawa, H., 2005. Reduction of hepatitis C virus NS5A phosphorylation through its interaction with amphiphysin II. *Biochem. Biophys. Res. Commun.* 336, 572–578.
- Mellacheruvu, D., Wright, Z., Couzens, A.L., Lambert, J.-P., St-Denis, N.A., Li, T., Miteva, Y.V., Hauri, S., Sardi, M.E., Low, T.Y., Halim, V.A., Bagshaw, R.D., Hubner, N.C., al-Hakim, A., Bouchard, A., Faubert, D., Fermin, D., Dunham, W.H., Goudreau, M., Lin, Z.-Y., Badillo, B.G., Pawson, T., Durocher, D., Coulombe, B., Aebersold, R., Superti-Furga, G., Colinge, J., Heck, A.J.R., Choi, H., Gstaiger, M., Mohammed, S., Cristea, I.M., Bennett, K.L., Washburn, M.P., Raught, B., Ewing, R. M., Gingras, A.-C., Nesvizhskii, A.I., 2013. The CRAPOME: A contaminant repository for affinity purification mass spectrometry data. *Nat. Methods* 10, 730–736.
- Mohd Hanafiah, K., Groeger, J., Flaxman, A.D., Wiersma, S.T., 2013. Global epidemiology of hepatitis C virus infection: new estimates of age-specific antibody to HCV seroprevalence. *Hepatology* 57, 1333–1342.
- Penin, F., Brass, V., Appel, N., Ramboarina, S., Montserret, R., Ficheux, D., Blum, H.E., Bartenschlager, R., Moradpour, D., 2004. Structure and function of the membrane anchor domain of hepatitis C virus nonstructural protein 5A. *J. Biol. Chem.* 279, 40835–40843.
- Pichlmair, A., Kandasamy, K., Alvisi, G., Mulhern, O., Sacco, R., Habjan, M., Binder, M., Stefanovic, A., Eberle, C.-A., Goncalves, A., Bürckstümmer, T., Müller, A.C., Fauster, A., Holze, C., Lindsten, K., Goodbourn, S., Kochs, G., Weber, F., Bartenschlager, R., Bowie, A.G., Bennett, K.L., Colinge, J., Superti-Furga, G., 2012. Inhibitome. *Nature* 487, 486–490.
- Pietschmann, T., Kaul, A., Koutsoudakis, G., Shavinskaya, A., Kallis, S., Steinmann, E., Abid, K., Negro, F., Dreux, M., Cosset, F.-L., Bartenschlager, R., 2006. Construction and characterization of infectious intragenotypic and intergenotypic hepatitis C virus chimeras. *Proc. Natl. Acad. Sci. USA* 103, 7408–7413.
- Reiss, S., Rebhan, I., Backes, P., Romero-Brey, I., Erfle, H., Matula, P., Kaderali, L., Poenisch, M., Blankenburg, H., Hiet, M.-S., Longrich, T., Diehl, S., Ramirez, F., Balla, T., Rohr, K., Kaul, A., Bühler, S., Pepperkok, R., Lengauer, T., Albrecht, M., Eils, R., Schirmacher, P., Lohmann, V., Bartenschlager, R., 2011. Recruitment and activation of a lipid kinase by hepatitis C Virus NS5A is essential for integrity of the membranous replication compartment. *Cell Host Microbe* 9, 32–45.
- Ren, T.-N., Wang, J.-S., He, Y.-M., Xu, C.-L., Wang, S.-Z., Xi, T., 2010. Effects of SMYD3 over-expression on cell cycle acceleration and cell proliferation in MDA-MB-231 human breast cancer cells. *Med. Oncol.* 2012.
- Schneider, C.A., Rasband, W.S., Eliceiri, K.W., 2012. NIH Image to ImageJ: 25 years of image analysis. *Nat. Methods* 9, 671–675.
- Sirinupong, N., Brunzelle, J., Doko, E., Yang, Z., 2010. Structural insights into the autoinhibition and posttranslational activation of histone methyltransferase SmyD3. *J. Mol. Biol.* 1–11.
- Tanji, Y., Kaneko, T., Satoh, S., Shimotohno, K., 1995. Phosphorylation of hepatitis C virus-encoded nonstructural protein NS5A. *J. Virol.* 69, 3980–3986.
- Tellinghuisen, T.L., Foss, K.L., Treadaway, J., 2008a. Regulation of hepatitis C virus production via phosphorylation of the NS5A protein. *PLoS Pathog.* 4, e1000032.
- Tellinghuisen, T.L., Foss, K.L., Treadaway, J.C., Rice, C.M., 2008b. Identification of residues required for RNA replication in domains II and III of the hepatitis C virus NS5A protein. *J. Virol.* 82, 1073–1083.
- Tellinghuisen, T.L., Marcotrigiano, J., Gorbalenya, A.E., Rice, C.M., 2004. The NS5A protein of hepatitis C virus is a zinc metalloprotein. *J. Biol. Chem.* 279, 48576–48587.
- van den Hoff, M.J., Labryère, W.T., Moorman, A.F., Lamers, W.H., 1990. The osmolarity of the electroporation medium affects the transient expression of genes. *Nucl. Acids Res.* 18, 6464.
- Xu, S., Wu, J., Sun, B., Zhong, C., Ding, J., 2011. Structural and biochemical studies of human lysine methyltransferase Smyd3 reveal the important functional roles of its post-SET and TPR domains and the regulation of its activity by DNA binding. *Nucl. Acids Res.* 39, 4438–4449.
- Zech, B., Kurtenbach, A., Krieger, N., Strand, D., Blencke, S., Morbitzer, M., Salassidis, K., Cotten, M., Wissing, J., Obert, S., Bartenschlager, R., Herget, T., Daub, H., 2003. Identification and characterization of amphiphysin II as a novel cellular interaction partner of the hepatitis C virus NS5A protein. *J. Gen. Virol.* 84, 555–560.



Supplemental Figure 1



Supplemental Figure 2

Supplemental table 1: List of identified proteins with a SAINT score ≥ 0.9

Uniprot Accession	Gene name	Full name	Sum Spectral Counts	SAINT probability	FC_B score	log2 (FC_B)	Identified in original screen	Pubmed ID
O94966	USP19	Ubiquitin carboxyl-terminal hydrolase 19	548	1	203.76	7.67 x	18985028; 24169621	
Q9H7B4	SMYD3	SET and MYND domain-containing protein 3	158	1	59.57	5.90 x	18985028; 24169621	
O00499	BIN1	Myc box-dependent-interacting protein 1	123	1	42.43	5.41 x	12604805; 16139795; 16530520; 18985028; 24169621	
P45880	VDAC2	Voltage-dependent anion-selective channel protein 2	107	1	40.58	5.34	24169621;	
Q14318	FKBP8	Peptidyl-prolyl cis-trans isomerase FKBP8	52	1	20.27	4.34 x	16844119; 17024179; 24169621;	
Q9P0L0	VAPA	Vesicle-associated membrane protein-associated protein A	43	1	16.87	4.08 x	10544080; 18985028; 24169621	
P68371	TUBB4B	Tubulin beta-4B chain	41	1	16.15	4.01 x		
O95292	VAPB	Vesicle-associated membrane protein-associated protein B/C	39	1	15.24	3.93	16227268; 18985028; 24169621	
Q15717	ELAVL1	ELAV-like protein 1	47	1	14.58	3.87 x		
Q9NV17	ATAD3A	ATPase family AAA domain-containing protein 3A	83	1	13.42	3.75		
Q9Y277	VDAC3	Voltage-dependent anion-selective channel protein 3	29	1	11.4	3.51	24169621;	
P85037	FOXK1	Forkhead box protein K1	23	1	9.38	3.23		
P55072	VCP	Transitional endoplasmic reticulum ATPase	21	1	8.58	3.10	24169621;	
Q7L9L4	MOB1B	MOB kinase activator 1B	23	1	8.48	3.08 x	18985028; 24169621	
P62937	PPIA	Peptidyl-prolyl cis-trans isomerase A	26	1	8.15	3.03 x	19297321;	

P05455	SSB	Lupus La protein Very-long-chain (3R)-3- hydroxyacyl-[acyl-carrier protein] dehydratase 3	30	1	7.07	2.82 x	18985028;
Q9P035	PTPLAD1	Serine/threonine-protein kinase LATS1	16	1	6.78	2.76	18160438; 24169621
O95835	LATS1	Heat shock protein 105 kDa	16	1	6.77	2.76	
Q92598	HSPH1	Alpha-enolase	51	1	6.22	2.64	
P06733	ENO1	Nucleosome assembly protein 1-like 1	73	1	6.2	2.63 x	
P55209	NAP1L1	D-3-phosphoglycerate dehydrogenase	32	1	5.81	2.54 x	18985028; 24169621
O43175	PHGDH	Serine palmitoyltransferase 2	13	0.98	5.01	2.32	24169621;
O15270	SPTLC2	WD repeat-containing protein 6	11	0.985	4.61	2.20	
Q9NNW5	WDR6	Pyruvate kinase isozymes M1/M2	12	0.91	4.22	2.08	
P14618	PKM	Proactivator polypeptide	12	0.95	3.92	1.97	
P07602	PSAP	Triosephosphate isomerase	21	0.95	3.76	1.91	
P60174	TP11	Threonylcarbamoyladenine tRNA methyltransferase	19	0.965	3.59	1.84 x	
Q5VV42	CDKAL1	Prothymosin alpha	9	0.96	3.58	1.84	
P06454	PTMA	Stathmin	18	0.965	3.51	1.81	
P16949	STMN1	Nuclear migration protein	18	0.975	3.5	1.81	
Q9Y266	NUDC	nudC	7	0.9	3.47	1.79	
P12277	CKB	Creatine kinase B-type	14	1	3.41	1.77	
Q9GZT9	EGLN1	Egl nine homolog 1	8	0.945	3.36	1.75	
P80723	BASP1	Brain acid soluble protein 1	28	0.995	3.26	1.70 x	
P32119	PRDX2	Peroxiredoxin-2	15	0.975	3.2	1.68	
P63244	GNB2L1	Guanine nucleotide-binding protein subunit beta-2-like 1	9	0.995	3.15	1.66	
Q99729	HNRNPAB	Heterogeneous nuclear ribonucleoprotein A/B	21	1	3.13	1.65	

P61604	HSPE1	10 kDa heat shock protein Programmed cell death	14	0.96	3.13	1.65 x
O14737	PDCD5	protein 5	5	0.92	3.11	1.64
O95757	HSPA4L	Heat shock 70 kDa protein 4L	23	0.99	3	1.58
P27797	CALR	Calreticulin	12	0.955	2.92	1.55
P21796	VDAC1	Voltage-dependent anion- selective channel protein 1	12	0.965	2.92	1.55
O15173	PGRMC2	Membrane-associated progesterone receptor component 2	6	0.95	2.84	1.51
P29966	MARCKS	Myristoylated alanine-rich C- kinase substrate	10	0.92	2.7	1.43 x
P00441	SOD1	Superoxide dismutase [Cu-Zn]	10	0.975	2.7	1.43
P61586	RHOA	Transforming protein RhoA	10	0.97	2.68	1.42
P37802	TAGLN2	Transgelin-2	12	0.995	2.65	1.41
P30044	PRDX5	Peroxiredoxin-5	9	0.96	2.57	1.36
P50502	ST13	Hsc70-interacting protein	9	0.925	2.57	1.36
P31942	HNRNPH3	Heterogeneous nuclear ribonucleoprotein H3	22	1	2.54	1.34
Q9UNF1	MAGED2	Melanoma-associated antigen D2	10	0.965	2.52	1.33
P40926	MDH2	Malate dehydrogenase	9	0.905	2.52	1.33
P34932	HSPA4	Heat shock 70 kDa protein 4	44	1	2.42	1.28
P22626	HNRNPA2B1	Heterogeneous nuclear ribonucleoproteins A2/B1	35	1	2.33	1.22
Q9Y230	RUVBL2	RuvB-like 2	10	0.96	2.32	1.21
P51572	BCAP31	B-cell receptor-associated protein 31	7	0.9	2.31	1.21
Q9H910	HN1L	Hematological and neurological expressed 1-like protein	7	0.925	2.31	1.21
O75347	TBCA	Tubulin-specific chaperone A	7	0.93	2.31	1.21

P78527	PRKDC	DNA-dependent protein kinase catalytic subunit	105	0.995	2.26	1.18
Q15843	NEDD8	NEDD8	6	0.905	2.24	1.16
P23528	CFL1	Cofilin-1	6	0.93	2.18	1.12
Q99733	NAP1L4	Nucleosome assembly protein 1-like 4	13	1	2.15	1.10
P51149	RAB7A	Ras-related protein Rab-7a	6	0.91	2.14	1.10
P62826	RAN	GTP-binding nuclear protein Ran	5	0.92	2.03	1.02
Q9Y2B0	CNPY2	Protein canopy homolog 2	5	0.925	2.02	1.01
Q99497	PARK7	Protein DJ-1	18	0.98	2.02	1.01
P62745	RHOB	Rho-related GTP-binding protein RhoB	5	0.9	2.02	1.01
P35637	FUS	RNA-binding protein FUS	26	1	1.82	0.86
P62258	YWHAE	14-3-3 protein epsilon	25	1	1.71	0.77
P07195	LDHB	L-lactate dehydrogenase B chain	6	0.99	1.64	0.71
Q06830	PRDX1	Peroxisome-dependent thioredoxin-dependent peroxide reductase	32	1	1.51	0.59 x
P30048	PRDX3	Small nuclear ribonucleoprotein E	10	0.97	1.51	0.59
P62304	SNRPE	Vimentin	4	0.925	1.49	0.58
P08670	VIM	RNA-binding protein EWS	32	0.915	1.46	0.55
Q01844	EWSR1	Plasminogen activator inhibitor 1 RNA-binding protein	17	0.975	1.43	0.52
Q8NC51	SERBP1	Tumor protein D54	15	0.985	1.38	0.46
O43399	TPD52L2	14-3-3 protein beta/alpha	2	0.985	1.35	0.43
P31946	YWHAB	ATP synthase subunit delta	6	0.97	1.35	0.43
P30049	ATP5D	Interferon-induced protein with tetratricopeptide repeats 5	5	0.92	1.34	0.42
Q13325	IFIT5	14-3-3 protein zeta/delta	5	0.98	1.3	0.38
P63104	YWHAZ		7	0.965	1.2	0.26

P53007	SLC25A1	Tricarboxylate transport protein	5	0.9	1.19	0.25
P10809	HSPD1	60 kDa heat shock protein	32	1	1.02	0.03 x
Q3ZCQ8	TIMM50	Mitochondrial import inner membrane translocase subunit TIM50	15	0.905	0.65	-0.62
Q01105	SET	Protein SET	15	0.915	0.59	-0.76

3.2 Prologue: Generating a SMYD3-binding mutant virus and identification of NS5A post-translational methylation sites

To better understand the functional outcome of the interaction of SMYD3 and NS5A, I mapped the binding site of SMYD3 on NS5A to the two conserved prolines P417 and P418 that are located in DIII. In addition, I generated a respective mutant virus to test if this would reproduce the phenotype observed with overexpressed SMYD3. And indeed, the mutant virus produced less infectious virus compared to wild type.

As part of a side project I also investigated the possibility that post-translational lysine methylation might be involved in coordinating NS5A function. The role of the different states of NS5A phosphorylation and their respective roles in regulating NS5A function have been studied extensively. However, the possibility that post-translational lysine methylation might also be involved in coordinating NS5A has not been addressed. In recent years, MS has emerged as the method of choice to identify methylated lysines. Compared to conventional methods, such as Edman degradation, radioactive isotope-labeling assays and the use of methyllysine-directed antibodies, MS is highly sensitive and reproducible and most importantly, capable of determining the site and methylation state of the modified residue (Lanouette et al., 2014).

By re-analysing already existing NS5A mass spectral data I identified lysine K240 as putative methylation site. K240 is located within a proposed K/R-S/T/A-K consensus methylation motif and with the exception of a few genotype 2 strains, it is highly conserved across all genotypes. Substituting the lysine by arginine or alanine in the subgenomic genotype 1b replicon Con1/ET (sgCon1/ET) enhanced replication, while the opposite was observed when arginine in the genotype 2a replicon JFH-1 was replaced by lysine or alanine. This suggested K240 might be involved in viral replication, highlighting the complex, genotype-dependent mechanisms mediating NS5A function. In addition, the alanine mutant resulted in an upward band shift in both genotypes, suggesting an effect on an adjacent PTM.

This work was performed under the supervision of Giulio Superti-Furga. Mass spectral data to identify putative lysine methylation sites was performed by Dr. Florian Breitwieser. I conducted the subsequent validation and sequence analyses. Furthermore, I generated all mutants and carried out the functional validation. Experiments using HCVcc were performed in Heidelberg. Attempts to verify methylation in *in vitro* assays were not successful, due to difficulties in generating recombinant proteins.

To find out if one of these motifs was required for the SMYD3-NS5A interaction, I replaced either P417/P418 or P423/P426 with alanine and co-expressed each mutant with SMYD3 in HEK 293T cells. As shown in (Fig. 9), mutating P417A/P418A completely abolished the interaction, while no loss in binding was observed for the P423A/P426A mutants, suggesting that SMYD3 indeed interacted with NS5A through P417 and P418.

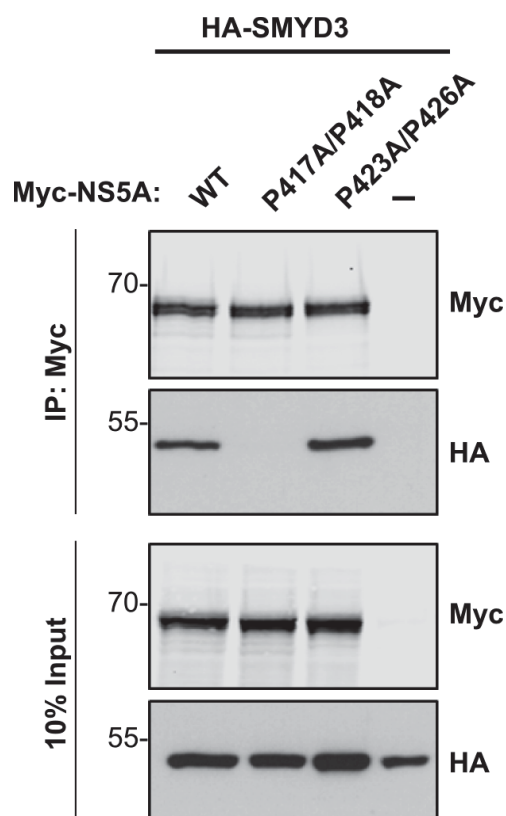


Figure 9: SMYD3 interacts with NS5A through prolines P417 and P418.

HEK 293T cells were co-transfected with HA-SMYD3 and wild type or mutant Myc-NS5A. SMYD3 co-transfected with pCDNA served as negative control. 36h post transfection, cells were lysed in IP-buffer and subjected to immunoprecipitation using anti-Myc beads. Eluates and the respective lysates were analysed by western blot. The figure shown here is representative of two independent experiments.

3.2.2 Effect of P417/P418 on the viral life cycle

Numerous studies have used mutational analysis of conserved residues and other important regions to study NS5A function (Appel et al., 2005; Fridell et al., 2013; Tellinghuisen et al., 2008b). Although

conserved prolines in NS5A have been addressed as well, nothing has been reported on P417/P418 (Ansari and Striker, 2012; Hughes et al., 2009).

To further dissect how SMYD3 affected the HCV life cycle, I introduced the P417A/P418A double mutation into the JcR-2A reporter genome (JcR-2A/PA). *In vitro* transcribed RNA was electroporated into Huh7-Lunet cells and replication and infectious particle production monitored by R-Luc assay. Contrary to previous reports, which show that DIII is dispensable for viral replication, JcR-2A/PA replicated less efficiently than the wild type virus (Appel et al., 2008; Tellinghuisen et al., 2008b), but this was largely overcome after 72h (**Fig. 10B**). To investigate the impact of P417/P418 on particle production, I measured R-Luc activity in Huh7.5 cells re-infected with supernatants harvested at the respective time points. Infectivity is commonly represented as relative light units (RLU) measured in the lysates of re-infected cells (Schmitt m). As shown in figure 9C, viral titers appear to be reduced compared to the wild type virus (4.4-fold at 72h). It is common practice to measure luciferase activity four hours post electroporation (hpe) to account for differences in electroporation efficiency. At this time point, luciferase activity is solely dependent on electroporation and/or translation efficiency of the transfected RNA. All values subsequent values are then represented relative to the four hour value (Lohmann, 2009). It is important to note that RNA input levels at four hours post electroporation (hpe) were already reduced compared to the wild type virus (**Fig. 10A**), suggesting defects in initial HCV polyprotein translation. In this setting, the lower RNA input could lead to the false assumption that particle production was impaired. Taking this into account, I determined relative infectivity as the ratio of infectious particles release to replication to better compare wild type and mutant JcR-2A. Indeed, there was no difference in relative particle release between both strains 24 and 48h after electroporation (**Fig. 10D**). Interestingly, infectivity of JcR-2A/PA dropped 2.5-fold after 72h although replication levels were almost identical to the wild type virus (**Fig. 10B and D**)

In summary, SMYD3 binds to two highly conserved prolines, P417 and P418, in DIII of NS5A. Replacing the respective prolines with alanines resulted in a slightly delayed replication kinetic, while infectious particle assembly was initially comparable to wild type levels but impaired at later time points.

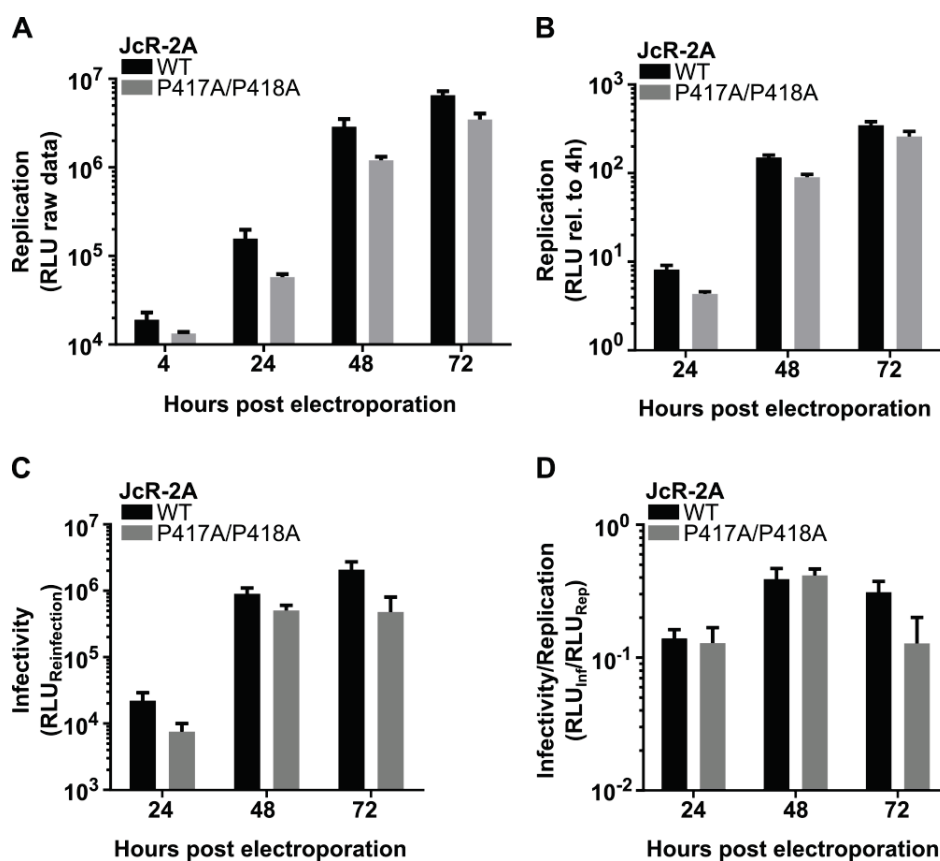


Figure 10: Effect of NS5A P417A/P418A on the viral life cycle.

(A + B) Replication of JcR-2A/PA compared to the wild type virus. Huh7-Lunet cells were electroporated with the respective RNA transcripts and R-Luc activity in the lysates was measured at the indicated time points. (A) Raw values and (B) values relative to the 4h input to normalize for different electroporation efficiencies. (C + D) Infectious particle release from JcR-2A/PA and wild type virus. (C) Supernatants from A were harvested at the indicated time points and used to inoculate naïve Huh7.5 cells. R-Luc activity in the lysates was determined 72h post infection Infectivity. (D) Infectivity normalized to replication to calculate relative infectious particle release. Data bars represent the mean value +S.E.M. of two independent experiments measured in duplicate.

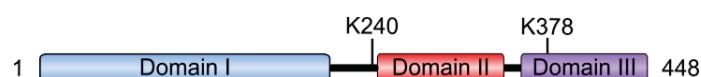
3.2.3 Proteomic approach to Identify putative methylation sites in NS5A

To investigate if NS5A contained any methylation sites, I decided to examine the already available mass spectral data from tandem-affinity purified NS5A (Eberle et al., 2014; Pichlmair et al., 2012). To increase the probability of identifying high-confidence methylation sites, data that originated from both analyses (LTQ Orbitrap XL and LTQ Orbitrap Velos mass spectrometer) was searched for peptides exhibiting the characteristic 14, 28 and 42 Da mass shift corresponding to the three different methylation states (Jung et al., 2008). Given that arginine mono- and dimethylation induces the same shift as the respective lysine methylation, arginine methylated peptides were also detected by our approach. Interestingly, numerous peptides appeared to be methylated. To increase the stringency of the analysis, I only took into account hits that were present in all samples, leaving a total of 10 different putative methylation sites (**Table 1**). Overall, two putative lysine methylation sites were identified (Fig. III.X1): K240, which is located in the flexible linker region LCS I connecting domains DI and DII and K378 in the N-terminal part of DIII (**Fig. 11**). Moreover, both lysines are located in regions closely resembling two putative methylation motifs S/T **K** X and X **K** S that were proposed by Kunizaki et al (Kunizaki et al., 2007).

Table 1: List of peptides harboring putative lysine or arginine methylation sites

Peptide	Site	#Peptides		%Methylated
		#Total	#Methylated	
Lysine:				
GSPPSLASSSASQLSAPSLK(2me)	K240	51	10	19.6
TVVLTESTVSSALAEATK(2me)	K378	71	9	12.7
Arginine:				
LPGVPPFFSCQR(2me)	R41	53	3	5.7
TTGPCTPSPAPNYSR(2me)	R108	38	5	13.2
VAAEYVEITR(2me)	R123	121	18	14.9
CPCQVPAPEFFTELDGVR(2me)	R157	61	8	13.1
ATCTTHHDSPDADLIEANLLWR(me)	R262	42	3	7.1
VVILDSFDPLR(2me)	R288	42	5	11.9
AEEDEREVSVAEILR(2me)	R304	34	5	14.7
EVSVAEILR(2me)		64	13	20.3
SPDYVPPAVHGCPLPPTTGPIPPPR(2me)	R356	34	3	8.8

List of methylated peptides present in all samples. Shown are the identified peptides, the site and the relative abundance of methylated over the total number of peptides. **2me**: di-methylated

**Figure 11: NS5A possesses two putative lysine methylation sites.**

Schematic of NS5A showing the localization of the two identified putative methylation sites K240 and K378.

To further investigate the putative lysine methylation sites, I first analyzed the level of conservation of each lysine residue using the NS5A reference sequence alignment mentioned in chapter III.2.1. K240 was highly conserved across the different HCV genotypes. In rare cases it was replaced by the chemically similar arginine, which is reflected by the high conservation and quality scores (**Fig 12A**), arguing that this lysine might be functionally important. One exception was genotype 2, including the JFH-1 strain, where arginine was more prevalent. In addition, the genotype 4a isolate ED43 possessed a glutamine at this

position, while all other genotype 4 strains expressed a lysine. K378 on the other hand is considerably less well conserved (Jalview conservation score = 4), and frequently replaced by arginine, threonine, alanine, and in some case, glutamine. In addition, directly adjacent amino acids also exhibited a large degree of chemical and structural variation, which might have a profound effect on the recognition by putative methyltransferases and other binding proteins (**Fig. 12B**). In addition, two studies performing a systematic analysis of domain DIII show that deleting regions containing K378 does not have a profound effect on replication and virion formation. For these reasons, subsequent experiments were focused on K240. In conclusion, by analyzing NS5A mass spectra, I identified K240 as putative methylation site. What is more, K240 is highly conserved among all HCV genotypes and is located within a proposed methylation consensus motif.

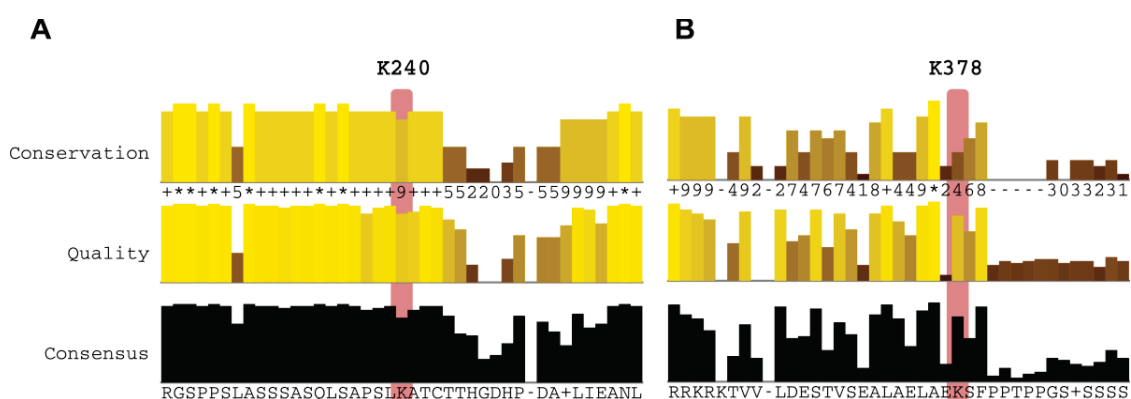


Figure 12: Conservation of K240 and K378.

117 reference sequences covering all genotypes were obtained and aligned using the Los Alamos HCV sequence database. Results were uploaded to Jalview and the degree of conservation and consensus sequence calculated. For NS5A protein sequence alignment of regions surrounding (A) K240 and (B) K378. Residues are colored based on the percentage of conservation (as calculated by JalView).

3.2.4 Functional validation of K240

Given the evidence supporting K240 as potential methylation site, I next investigated its role in the HCV life cycle, first focusing on replication. To this end, I generated subgenomic genotype 1b reporter replicons (sgCon1/ET) in which the lysine was replaced by either alanine or arginine and assessed their replication efficiency by luciferase reporter assay. Arginine was included, because it is chemically similar lysine but cannot be methylated by KMTs. Taking into account that the majority of genotype 2a strains, including JFH-1, express arginine at this site, I included subgenomic sgJFH1 reporter replicons containing R240K and R240A point mutations in the analysis.

In vitro transcribed wild type or mutant replicon RNA was electroporated into Huh7-Lunet cells and replication efficiency was measured after 4, 24, 48, 72 and 96 hpe by luciferase reporter assay (**Fig. 13A**).

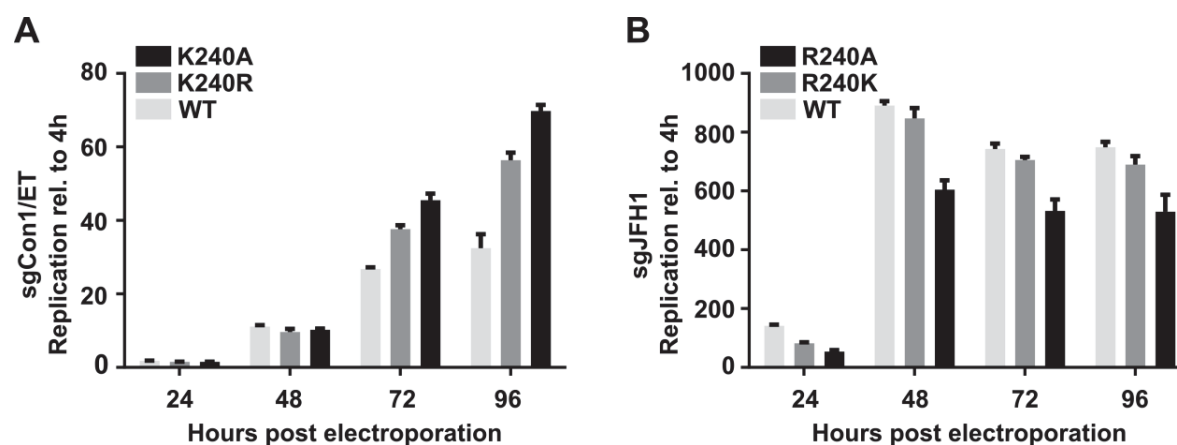


Figure 13: Effect of K240, R240 and A240 on viral replication.

In vitro transcripts of (A) sgCon1/ET or (B) sgJFH1 replicons bearing the indicated mutations were electroporated into Huh7-Lunet cells. F-luc luciferase activity in the lysates was determined at the indicated time points. Relative light units (RLUs) were normalized to the 4h values to account for differences in electroporation efficiency. Bars and error bars depict the mean \pm standard errors of the mean (SEM) of two (sgCon1/ET) or three (sgJFH1) independent experiments, each measured in biological and technical duplicates.

Up to 48h post electroporation, I observed no difference among the different sgCon1/ET constructs. However, replication efficiencies of both mutants was increased at later time points, with the K240A mutants displaying a two-fold difference compared to the the wild type construct at 72 and 96hpe (**Fig. 13A**). Interestingly, the opposite was true for the sgJFH1 replicon. While the R240K mutant replicated almost as efficiently as the wild type construct, the R240A replicon barely reached 70% of wild type levels (**Fig. 13B**).

Immunoblot analysis of NS5A from the same lysates revealed that the results from the transient reporter replication assay could partially be translated to the protein level. For sgCon1/ET, NS5A protein levels clearly reflected the replication capacity of the respective construct, with levels being highest for the K240A mutant (**Fig. 14A+B**). Unexpectedly, I observed an additional band for NS5A K240A, which resembled the p58 hyperphosphorylated form of NS5A (**Fig. 14A** and **Fig. 14C** for comparison). The case was not as clear cut for sgJFH1. As for sgCon1/ET, protein levels for R240A were lowest, thus correlating with the poor replication of this mutant. However, the R240K mutant displayed higher NS5A protein levels, despite the similar replication capacity compared to wild type. Interestingly, the R240A mutant also exhibited an upward band shift, resulting in the disappearance of NS5A p56 (**Fig. 14B+D**).

In summary, my data suggest that K240 and R240 are involved in viral replication, but that this role differs amongst genotypes. What is more, replacing residue 240 by alanine induced a band shift in both genotypes which suggests that this mutant alters the levels of NS5A phosphorylation.

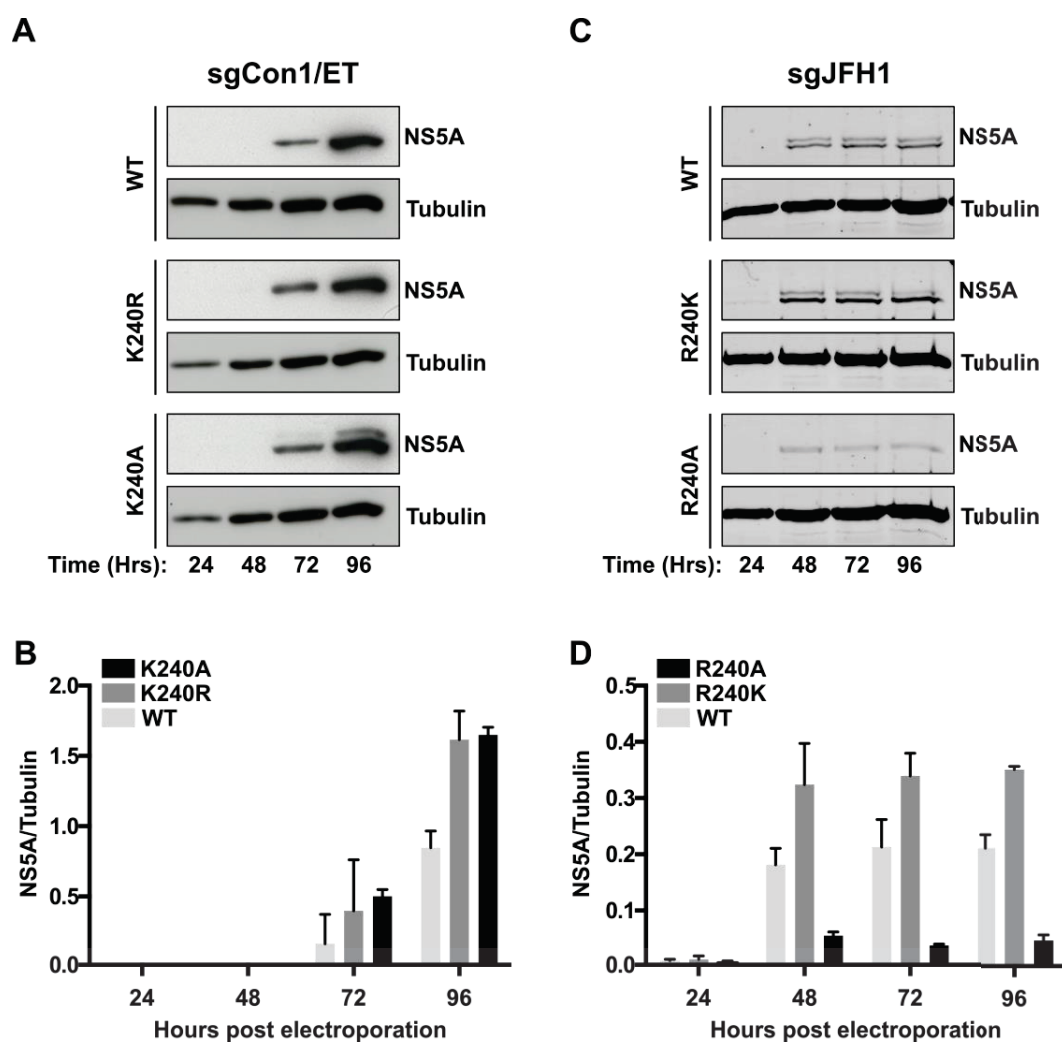


Figure 14: Protein levels of wild type and mutant NS5A.

Lysates from fig. 12 were subjected to SDS-PAGE and NS5A from sgCon1/ET (A) and sgJFH1 (C) detected by western blot. One representative blot of two independent experiments is shown. (C and D) Band intensities were quantified with ImageJ. Bars and error bars depict the mean \pm SEM from two independent blots. To account for variation in protein content and blot-to-blot variability, values were normalized to the respective tubulin band. Differences in picture quality are due to the fact that (A) was developed in Heidelberg using enhanced chemiluminescences (ECL) and (B) in Vienna on an Odyssey LiCor imager

4. CONCLUDING DISCUSSION

Even 25 years after its discovery, HCV remains a global health and economic burden and, until recently, available treatment options were only of limited efficacy. However, recent progress in the understanding of the HCV life cycle has led to the development of several direct-acting antiviral agents, including a set of promising agents targeting NS5A. Despite these promising advances, the emergence of resistant strains and intergenotypic differences pose ongoing challenges. As a consequence, continuing the investigation into HCV biology and pathology remains a must. As discussed in the following part, I investigate the interaction of the methyltransferase SMYD3 with NS5A. Functional validation using different *in vitro* models for HCV, suggested that SMYD3 is as a novel negative regulator of HCV infectious particle assembly. As part of an attempt to identify post-translational methylation sites in NS5A, I discovered K240 as being important in regulation of viral replication in a genotype-dependent manner.

4.1 Identification of NS5A-binding proteins using a proteomic approach

Viruses heavily depend upon the host cell machinery for completion of their viral life cycle. As a consequence, viruses have evolved numerous strategies to bind to and co-opt host proteins for their own benefit (Vidalain and Tangy, 2010). Investigating virus-host protein interactions is thus essential for a better understanding of the viral lifecycles and the mechanisms underlying pathogenesis as well as the identification of novel treatment targets. (Pichlmair et al., 2012). Comparing data obtained from the same sample but from two different mass spectrometers, I analyzed the NS5A-host interactome. Overall, I observed a remarkable overlap between the two runs, as well as with previous proteome-wide studies on HCV-host protein interactions (de Chasseay et al., 2008; Germain et al., 2013). Amongst these are also already known HCV factors, for instance BIN1, which interferes with NS5A hyperphosphorylation (Masumi et al., 2005). Another important host factor is cyclophilin A (PPIA), which induces structural changes in NS5A and is involved in viral replication (see described below). Although this level of compliance argues for our approach, it also suggests that at least in HEK 293-derived cells, the NS5A interactome is close to being complete (Germain et al., 2013). However, it is important to note that HEK 293 cells are not liver cells, hence potential hepatocyte-specific interactions might be missed. In addition, active replication and the presence of other HCV proteins may also have an impact on virus – host

protein interactions by influencing the subcellular localization and PTM status of NS5A. This is exemplified by phosphatidylinositol 4-kinase PI4KIII α . NS5A binds and activates PI4KIII α resulting in increased levels of PI4P, which contributes towards membranous web formation and integrity of viral replication complexes (Reiss et al., 2011). Despite being expressed in HEK 293 cells, we did not detect PI4KIII α in our pull-downs, most likely because of the absence of virus-induced membranous webs and replication complexes. Another issue that I faced during the analyses, was the high sensitivity of the next generation mass spectrometer. Overall, it detected almost six times as much as the original machine (274 vs. 50, respectively). Although improved sensitivity allows for the identification of low-abundance interactors, it also increases the number of rare non-specific binding proteins, highlighting the need for more stringent filtering methods (Mellacheruvu et al., 2013). Taken together, the overlap with the original analysis and previous independent studies confirm the validity, robustness and reproducibility of our approach. However, stringent filters are required to reduce the number of false positives.

4.2 SMYD3 interacts with NS5A and negatively regulates HCV virion assembly

Amongst the highest-scoring NS5A-binding proteins in both analyses was the methyltransferase SMYD3. Indeed, SMYD3 interacted with NS5A in transiently transfected HEK 293T cells as well as in the context of active viral replication. I performed various structural and functional studies to elucidate the role of SMYD3 in the HCV life cycle. Overall, my results point towards a role of SMYD3 as a negative regulator of infectious virion assembly: Firstly, overexpressing wild type SMYD3 inhibited virion assembly, while viral replication was not affected. Secondly, intracellular infectivity, i.e. the amount of infectious virus prior to secretion, was already reduced, thus ruling out the possibility that SMYD3 interfered with the secretion process. Thirdly, SMYD3 binds to two prolines, P417 and P418 in domain DIII of NS5A, a region essential for infectious particle production (Appel et al., 2008). A mutant virus (JcR2A/PA), lacking the SMYD3 binding prolines, released fewer infectious particles compared to the wild type virus. Finally, SMYD3 preferentially interacted with hyperphosphorylated NS5A, which has been associated with infectious particle assembly (Tellinghuisen et al., 2008a). In the following part I will discuss each point in more detail.

4.2.1 SMYD3 overexpression inhibits infectious particle assembly

I investigated the effect of SMYD3 on the various stages of the viral life cycle using cell lines stably overexpressing wild type SMYD3 or a catalytically inactive point mutant. Overexpressed wild type SMYD3 clearly led to a reduction of viral titers, while viral replication was not affected. Moreover, I observed a reduction in intracellular infectivity, i.e. the amount of infectious virus present prior to secretion. Core levels on the other hand accumulated in the cells, which suggested that SMYD3 interfered with the assembly process, rather than maturation and release. This is further supported by the fact that SMYD3 did not alter secretion of Gaussia luciferase into the cell supernatants, which ruled out a SMYD3-induced defect in the secretory pathway. Although my results are clear and robust, it would be necessary to validate them in a different system. As mentioned in the introduction, SMYD3 knockdown is toxic for Huh7 cells. Although I did attempt loss-of-protein assays, results were very inconsistent and non-reproducible (data not shown). An alternative approach might thus include the use of cell lines expressing inducible SMYD3-targeting short-hairpin RNAs (shRNA), allowing reversible and adjustable SMYD3 knockdown.

Lastly, SMYD3 preferentially interacted with hyperphosphorylated NS5A, which has been associated with infectious particle assembly (Tellinghuisen et al., 2008b). Basal phosphorylated NS5A also co-precipitated with SMYD3. However, whether p56 NS5A bound directly to SMYD3, or if it co-purified as part of an NS5A dimer, remains to be determined (Tellinghuisen et al., 2005). Additional experiments such as phosphatase assays and NS5A point mutants are necessary to further verify this observation.

4.2.2 Infectious particle assembly is impaired in a SMYD3-binding mutant virus

Mutational analysis identified the MYND-domain of SMYD3 and prolines P417 and P418 in NS5A as the respective binding sites for their interaction. The SMYD3 MYND-domain is located opposite from the catalytic SET-domain, thus excluding the possibility of NS5A being a novel SMYD3 substrate (Foreman et al., 2011; Sirinupong et al., 2010; Xu et al., 2011). Interestingly, prolines P417 and P418 are located in domain D III of NS5A. D III is essential for infectious particle assembly, further supporting a role for SMYD3 in this process. To gain a better understanding of how SMYD3 might impact the HCV life cycle, I monitored replication and particle formation of HCVcc lacking both prolines. Surprisingly, exchanging P417 and P418 with alanines resulted in delayed viral replication kinetics. However, 72hpe, replication was comparable to wild type levels. Since overexpressing SMYD3 per se had no effect on replication, other factors must be responsible for this observation. Prolines possess a distinctive cyclic backbone and have a profound impact on protein conformation. Thus, replacing both prolines with alanine could

greatly influence NS5A structure and hence function. Another possibility would be the perturbation of other NS5A-host interactions. NS5A binds to the peptidyl-prolyl isomerases (PPIase) PPIA and PPIB (also known as cyclophilins CYP A and CYP B), which catalyze the cis-trans isomerization of peptidyl-proline bonds and are important for HCV replication. Several prolines in NS5A, including P418, have been identified as PPIA substrates (Hanouille et al., 2009a; Verdegem et al., 2011). Hence, diminished binding of PPIAs might also explain the reduced replication. Interestingly, the ratio of infectious particle release relative to replication was initially comparable to the wild type virus, but dropped at later time points. Given that the concurrent RNA replication levels were the same for both viruses, suggested that these residues are indeed important for assembly. However, as already mentioned above, proline mutants can have profound effects on the respective protein. Although it is tempting to believe that a lack of SMYD3 binding is responsible for the drop in infectivity, additional experiments are required to further characterize this observation. For instance, to avoid possible structural changes imposed by the proline double mutant, it should be tested if mutating adjacent amino acids could also disrupt the interaction and result in a similar phenotype.

Taken together, I could show that SMYD3 negatively influences infectious particle production, while replication is not affected. Likewise, a virus lacking the SMYD3-binding site is capable of replicating, but assembly is impaired at later time points. How SMYD3 might influence virion formation, I can only speculate since too little is known about the biological function of SMYD3. Based on my results, one might hypothesize that SMYD3 is involved in a cellular pathway that negatively affects the assembly process. For instance, SMYD3 has recently been found to methylate and activate MAP3K2. MAP3K2 is a MAP-kinase involved in the regulation of NF κ B and Jun N-terminal kinase (JNK) signaling pathways in response to inflammatory cytokines, growth factors and environmental stress (Wagner and Nebreda, 2009; Zhao and Lee, 1999). Given that NS5A binds to the MYND domain, it might sequester SMYD3 and prevent it from binding its target protein. Alternatively, NS5A might induce structural changes, which affect SMYD3 substrate specificity. Moreover, performing a BLAST search of the proline motif in NS5A identified heatshock protein 90 (HSP90) as a top hit. HSP90 interacts with SMYD3 and potentiates its catalytic activity, raising the possibility that NS5A might mimic HSP90 (Hamamoto et al., 2004). Quantitative proteomics to monitor HCV-induced changes in the SMYD3 interactome might shed more light on the mechanisms involved. Although technically challenging, it would also be interesting to investigate the effect of NS5A on SMYD3 catalytic activity. Last but not least, one should also consider the effects of SMYD3 on the host. Alterations in SMYD3 function could contribute to HCV-induced liver

pathology, but also to the various HCV-induced extrahepatic manifestations, including cryoglobulinaemia, non-Hodgkin B-cell lymphoma, insulin resistance and type 2 diabetes, polyarthritis and several neuropathological changes (Negro, 2013). Current HCV models are based on cancer cell lines and are only of limited suitability for studying HCV pathology. However, advances in generating human iPSC-derived hepatocyte-like cells, 3D liver organoids and better *in vivo* mouse models will allow the study of HCV in more complex, physiologically-relevant systems (Lu et al., 2012; Schwartz et al., 2012; Tawar et al., 2014). Although SMYD3 might not seem a suitable target for anti-HCV therapy, future research focused on the mechanisms underlying its inhibitory action could help shed light on the as yet enigmatic process of virion assembly and HCV-induced liver pathology.

4.3 Identification of K240 as a putative NS5A post-translational methylation site

Methylation of lysine residues has emerged as versatile post-translational modification regulating numerous complex proteins and signaling pathways. Hence it is not surprising that viruses have evolved many different strategies to usurp lysine methylation and the associated KMT-machinery. Owing to the multifunctionality of NS5A and the versatility of methyllysines, I sought to investigate if NS5A possessed post-translational lysine methylation sites, which might be involved in regulating NS5A function. Using a MS-based approach I identified K240 as a putative methylation site. The residue is located in a proposed K/R-S/T/A-K consensus methylation motif and with the exception of genotype 2, it is highly conserved across all genotypes. Interestingly, introducing point mutations at this position enhanced replication of a genotype 1b replicon. The opposite was observed for genotype 2a, suggesting that K/R240 influence replication in a genotype-dependent manner. Considering the high degree of conservation of this area, it is likely that mechanisms *in trans* are responsible for the genotype-specific effects. For one, the region spanning K/R240 directly interacts with viral RNA (Hwang et al., 2010). Hence, differences in the HCV genome sequence, and RNA secondary structures that change the affinity of NS5A for RNA, might provide a possible explanation for genotypic differences. Alternatively, changes in host- and intraviral-protein interactions might be responsible (Dimitrova et al., 2003; Hagen et al., 2014).

What is more, both, the K240A and the R240A mutants exhibited an upward band shift closely resembling hyperphosphorylated NS5A. Indeed, K/R240 is located closely to a highly phosphorylated serine cluster (Appel et al., 2005). Other PTMs capable of inducing such a prominent band shift involve the attachment of ubiquitin and ubiquitin-like proteins. However, there are only few other conserved lysines within NS5A, the closest being K278. Although phosphorylation is the most likely PTM, this should

be confirmed either by treating purified NS5A with phosphatase or by radioisotope-labeling. As mentioned in the introduction, a common drawback of genotype 1 cell-culture adapted HCV strains is their lack of infectivity. More precisely, the degree of NS5A hyperphosphorylation is inversely correlated with infectious particle release (Pietschmann et al., 2009). Given that mutating K240A enhanced replication, it would be intriguing to speculate that this mutant might restore infectivity while maintaining high levels of replication. Additional support for this hypothesis is provided by the fact that JFH-1, one of the few strains which lack the lysine at this position, is the only isolate to date to produce high levels of infectious particles *in vitro*.

Although I could clearly show that K240 played a role in replication, it is not clear whether NS5A is methylated *in vivo* and whether this modification regulates its function. In fact, although both mass spectrometers detected the same peptides harboring putative dimethylated arginines and lysines, the identified methylation sites need to be treated with caution. As part of the sample preparation process, proteins are digested by trypsin, which cleaves C-terminally of lysine and arginine residues (Ong et al., 2004). Post-translational methylation of these residues hence reduces the efficiency of tryptic cleavage, resulting in missed cleavage events. All my identified residues are located at the C-terminus of the respective peptides, which would not be expected if these sites were methylated prior to the tryptic digest (Ong et al., 2004). Indeed, Jung et al reported the possibility of exogenous methylation reactions elicited by commonly used reagents such as methanol (Jung et al., 2008). To better distinguish these artifacts from true methylation events, “Stable Isotope Labeling by Amino Acids in Cell Culture”, or SILAC, could be used for future MS-based approaches. Cells are grown in the presence of heavy [¹³CD₃]methionine which is converted into [¹³CD₃]SAM, which is isotopically labeled on its sulfonium methyl group. Subsequent methylation reactions result in an 18 rather than a 14 kDa mass shift (Ong et al., 2004). Although MS-based methods for the detection of post-translation methylation have greatly improved in recent years, it remains essential to verify the identified sites by conventional *in vitro* methylation assays. However, these assays are challenging and in my experiments I was not successful in confirming NS5A methylation; the major issue being the generation of catalytically active, recombinant SMYD3.

In conclusion, I identified K/R240 as a residue important for viral replication. Since the observed effect was genotype-dependent, future experiments should aim at further investigating the role of this residue on the replication and more importantly, infectivity of other genotypes. In addition, characterizing the nature of the observed band shift might also provide better insight into the genotype-specific

mechanisms coordinating the multiple functions of NS5A. This could aid in the development of pan-HCV treatment options.

5. MATERIALS AND METHODS

5.1 Materials

5.1.1 Buffers and solutions

0,1%(v/v)Triton/PBS:	10µl Triton X-100 in 10ml PBS. Stored at RT.
0,1%(v/v)PBS-T:	5ml of Tween20 in 500ml 10XPBS and 4,5L H ₂ O. Stored at RT
4%(v/v) PFA:	10ml of 16% Paraformaldehyde (PFA) in 40ml PBS. Stored at 4°C.
5%(w/v)Milk/PBS-T:	5g non-fat milk powder in 100ml PBS-T. Stored at 4°C.
5%(v/v)Goat serum:	250µl of goat serum in 4,75ml PBS
5%(v/v)SDS/PBS:	5ml 10% SDS in 1ml 10X PBS and 4ml H ₂ O. Stored at RT. 5mg Coelenterazine in 11,6ml methanol. Stored at 80°C.
Coelenterazine:	Diluted 1:700 in luciferase assay buffer for use (without ATP and DTT). 120mM KCl, 0.15mM CaCl ₂ , 10mM potassium phosphate buffer (pH 7.6), 25mM HEPES (pH 7.6), 2mM EGTA, 5mM MgCl ₂ , pH adjusted to 7.6 using KOH. Freshly added prior to use: 2mM ATP and 5mM glutathione
Cytomix:	400mM HEPES (pH7.5), 60mM MgCl ₂ , 10mM spermidine, 200mM DTT
<i>In vitro</i> transcription buffer (5X):	50mM Tris/HCL (pH 8.0), 150mM NaCl, 1% NP-40, 5mM EDTA, 5mM EGTA, pH adjusted to 8.0 using HCl or KOH. 1 tablet of protease inhibitor cocktail was diluted in 50ml of IP buffer. Buffer was then aliquoted and stored at -20°C.
IP buffer:	

	Freshly added prior to lysis: 50mM NaF and 1mM Na ₃ VO ₄
4X Lämmli Buffer:	0.5M Tris/HCl (pH 6.8), 2.5% glycerol, 8%(w/v) SDS, small amount of bromophenol blue. 1ml aliquots stored at -20°C. Prior to use, 10%(v/v) of β-mercaptoethanol are added to each aliquot.
Luciferase assay buffer:	25mM Glycyl-glycine (pH 7.8), 15mM potassium phosphate buffer (pH 7.8), 15mM MgSO ₄ , 4mM EGTA. Freshly added prior to use: 2mM ATP and 1mM DTT.
Luciferase lysis buffer:	25mM Glycyl-glycine (pH 7.8), 15mM MgSO ₄ , 4mM EGTA, 0.1% Triton X-100. Stored at 4°C. Freshly added prior to lysis: 1mM DTT.
Luciferin solution:	1mM Luciferin in 25mM Glycyl-glycine (pH 7.8). Stored at -80°C. Diluted 1:5 in luciferase assay buffer for use.
5X SDS Running buffer:	250mM Tris, 1%(w/v) SDS, 1,9M Glycine
TAE Buffer:	2M Tris base, 2M glacial acetic acid, 50mM EDTA, adjust to pH 8.5
TCID ₅₀ detection substrate:	Carbazole: 0.4g Carbazole in 125nl NN-dimethylformamide. Stored at 4°C in the dark and no longer than 3 months. Acetate buffer: 0.5M sodium acetate and 0.5M acetic acid. Stored at 4°C.

5.1.2 Antibodies

Protein	Supplier	Dilution
Polyclonal rabbit anti-SMYD3	Abcam	1:1000
Monoclonal mouse anti-NS5A 9E10	Prof. Charles M. Rice	1:10 000

Polyclonal rabbit anti-HA	Santa Cruz	1:2000
Monoclonal mouse anti-GFP	Roche	1:5000
Anti- α Tubulin	Abcam	1:10 000
HRP-conjugated anti-HA7	SIGMA	1:10 000
HRP-conjugated anti-mouse IgG	Jackson ImmunoResarch	1:20 000
HRP-conjugated anti-rabbit IgG	Jackson ImmunoResarch	1:20 000
IRDye 800 [®] anti-Myc IgG	Rockland	1:10 000
Alexa Fluor [®] 680 anti-mouse IgG	Molecular Probes	1:10 000

All antibodies were diluted in 2.5%(w/v) non-fat milk/PBS-0.1%(v/v)Tween

5.1.3 Plasmids

Uniprot accessions of proteins in this thesis:

SMYD3 (Q9H7B4), NS5A - Con1 (Q9WMX2), NS5A - AP (D16435), NS5A - JFH1 (Q99IB8)

Gateway Entry vectors:

pDONR201
pDONR201-SMYD3
pDONR201-NS5A (Con1)
pDONR201-NS5A (AP)
pDONR201-eGFP

Gateway destination vectors:

pCS2-N-6xMyc-GW
pcDNA3.1-N-2HA-TEV-GW
pWPI-GW
pWPI-N-HA-GW

Expression plasmids

pCS2-N-6Myc-SMYD3
pCS2-N-6Myc-SMYD3 Y239F
pCS2-N-6Myc-Con1-NS5A
pCS2-N-6Myc-NS5A
pCS2-N-6xmyc-NS5A (Con1)
pCS2-N-6xmyc-NS5A-N Δ 1(250-342)(Con1)
pCS2-N-6xmyc-NS5A-N Δ 2(343-448)(Con1)

HCV constructs

pFK_i389-Luc-NS3-3'JFH_ δ g
pFK_i389-Luc-NS3-3'JFH_ δ g NS5A R240K
pFK_i389-Luc-NS3-3'JFH_ δ g NS5A R240A
pFK-J6/Core-846/JFH1_wt_ δ g
pFK_i389-JcR2a_ δ g_JC1
pFK_i389-JcR2a_ δ g_JC1 NS5A P417A/P418A
pFK-J6/Core-846/JFH1_wt_ δ g

pCS2-N-6xmyc-NS5A-NΔ3(356-448)(Con1)	pFK_i389-JcR2a_δg_JC1
pCS2-N-6xmyc-NS5A-P417A/P418A(Con1)	pFK_i389-JcR2a_δg_JC1 NS5A P417A/P418A
pCS2-N-6xmyc-NS5A-P423A/P426A(Con1)	
pcDNA-3.1-N-2xHA-TEV-SMYD3	Other plasmids
pcDNA-3.1-N-2xHA-TEV-SMYD3 Y239F	pMD.G: Lentiviral envelope vector
pcDNA-3.1-N-2xHA-TEV-SMYD3Δ1(1-48)	pCMVR8.91: Lentiviral packaging vector
pcDNA-3.1-N-2xHA-TEV-SMYD3Δ2(49-87)	pcDNA: Empty control vector
pcDNA-3.1-N-2xHA-TEV-SMYD3Δ3(88-124)	
pcDNA-3.1-N-2xHA-TEV-SMYD3Δ4(125-182)	
pcDNA-3.1-N-2xHA-TEV-SMYD3Δ5(254-277)	
pcDNA-3.1-N-2xHA-TEV-SMYD3Δ6(280-428)	
pWPI-SMYD3	
pWPI-SMYD3 Y239F	
pWPI-GFP	
pWPI-N-HA-SMYD3	

5.1.4 Primer sequences

Gateway primer

SMYD3	Sense	<u>ggggacaagtttgtacaataaaagcaggctccatggagccgc tgaaggtgga aaag</u>
	Antisense	<u>ggggaccactttgtacaagaaagctgggttaggatgctctgatgttgcgctcg</u>
NS5A Con1	Sense	<u>ggggacaagtttgtacaataaaagcaggcttatccggctcgtggctaagagat</u>
	Antisense	<u>ggggaccactttgtacaagaaagctgggttcagcagacgacgtcctcactag</u>
Δ2(343-448)	Antisense	<u>ggggaccactttgtacaagaaagctgggttacaccctgtaccactgga</u>
NS5A AP	Sense	<u>gggg aca agt ttg tac aaa aaa gca ggc tcctccggctcgtggctaagggatg</u>
	Antisense	<u>ggggaccactttgtacaagaaagctgggttcagcagacgatgtcgtcgccg</u>

Site-directed mutagenesis

SMYD3:

Y239F	Sense	gagaggagctcacatctgcttccctggatatgctgatgaccagt
	Antisense	actggtcatcagcatatccaggaagcagatggtgagctcctctc
SΔ1(1-48)	Sense	agcaggctccatgtgaccgctgcc
	Antisense	ggcagcggctgcacatggagcctgct
SΔ2(49-87)	Sense	ggagtcgtggcgtcgtcaaatgccttaaagctg
	Antisense	cagctttaaggcatttgacgacgccagactcc
SΔ3(88-124)	Sense	gaccacaagcgggaatgctcattttatgatctggag
	Antisense	ctccagatcataaaatgagcattcccgttggtgc
SΔ4(125-182)	Sense	cagaatcagagaagctttacttcacatctgtaatgcgga
	Antisense	tccgattacagatggtgaagtaaagcttctctgattctg
SΔ5(245-277)	Sense	tacctggatatgctgatgggtgatgagcaagtatgg
	Antisense	ccatacttgctcatcaccatcagcatatccaggta
SΔ6(280-428)	Sense	caaggatgctgatatgctaacttaaccagctttctgtacaa
	Antisense	ttgtacaagaaagctgggttaagttagcatatcagcatccttg
NS5A Con1		
K240R	Sense	ccttcttgagagcaacatgcactaccctg
	Antisense	gcatgttgactcaaggaaggcgagacag
K240A	Sense	ccttcttgaggccaacatgcactaccctg
	Antisense	gcatgttgccgaaggaaggcgagacag
P417A/P418A	Sense	tactcctcatggccgccttgaggggg
P417A/P418A	Antisense	ccccctcaaggcgccatggaggagta
P423A/P426A	Sense	gagggggaggcgggggatgccgatctca
P423A/P426A	Antisense	tgagatcggcatccccgcctccccctc
NΔ1(250-342)	Sense	gcaacatgcactaccattgccgctgcc
	Antisense	ggcaggcggcaatgggtagtgcatgttg
NΔ3(356-448)	Sense	ataccacctccacgggaggacgtcgtctgc
	Antisense	gcagacgacgtcctccgtggaggtggtat
NS5A JFH1		
R240K	Sense	gcaccgtcgtg aag gccacctgcaccacc
	Antisense	ggtgcaggtggc ctt cagcaggctgctga

R240A	Sense	gcaccgtcgctg aga gccacctgcaccacc
	Antisense	ggcgcaggtggc tct cagcgaggctgctga
P417A/P418A	Sense	gcctcctctatggccgccctcgaggggg
P417A/P418A	Antisense	ccccctcgagggcggccatagaggagc

siRNA

Hs_SMYD3_11	Qiagen	caagtatggaaggaagttaa
Hs_SMYD3_6	Qiagen	gacaaggatgctgatatgcta
Hs_SMYD2_3	Qiagen	aagatagaaatgaccggtaa
Hs_SMYD2_2	Qiagen	gaggtagtctgaatcttgaa
Allstar negative control	Qiagen	not disclosed
Non-targeting 1	Qiagen*	tggtttacatgtcgactaa

5.2 Methods

5.2.1 Cloning

Generation of expression plasmids

Expression vectors were generated using the Gateway® recombination technology (Invitrogen) as recommended by the manufacturer. Briefly, 150ng of pDONR plasmid were mixed with 150ng of respective destination vector and 2µl of LR recombinase. The total volume was brought up to 10µl with H₂O. After 2h or overnight incubation at room temperature (RT), 5µl were transformed into *E.Coli* DH5α by heatshock. Clones were verified by test-digest with BsrGI (NEB).

Mutagenesis

Deletion and point mutants of SMYD3 and NS5A were generated by site-directed mutagenesis using the respective pDONR-vector as template and PfuUltra High-Fidelity DNA Polymerase (Agilent). The reaction mixture contained 20ng DNA, 1X UltraPfu High-Fidelity Reaction Buffer AD, 0.3µM per primer, 200µM dNTPs, 5% DMSO and 2.5U of enzyme. Depending on the template and primer sequences, following cycling parameters were used:

	Step	°C	Time(s)	Cycles
1	Activation	95	60	1
2	Denaturing	95	10	18
3	Annealing	53-60	30	
4	Extension	72	1min/kb	
5	Final extension	72	240	1
6	Storage	8	∞	1

After PCR, template DNA was digested by adding 20U of DpnI (NEB) and incubating at 37°C for 1-2h. 10µl of mix were transformed into *E.Coli* DH5α by heat shock. Obtained clones were subjected to an analytical restriction digest and then sequence verified.

Point mutants of HCV constructs were generated by fusion PCR, using overlapping primers that carry the point mutation in the middle and flanking primers containing suitable restriction sites. In the first round,

two fragments were generated using the flanking and the mutagenesis primers. Fragments were gel-purified, mixed 1:1 (2 μ l each) and fused in a second PCR reaction containing only the flanking primers. PCR reactions contained 250ng template DNA in 1x PCR buffer, 200 μ M dNTPs, 0.1 μ M per primer and 1.25U of FidelityTM (Affymetrix). Depending on the template, following cycling parameters were used:

	Step	°C	Time(s)	Cycles
1	Activation	95	60	1
2	Denaturing	95	30	8 (PCR1)
3	Annealing	53	60	
4	Extension	68	1min/kb	14(PCR2)
5	Final extension	68	240	1
6	Storage	8	∞	1

The resulting fragments were cut with the respective restriction enzymes and ligated into the target plasmid.

Restriction and ligation

All restriction enzymes and calf intestinal phosphatase (CIP) and T4 ligases were from NEB and used according to the manufacturer's recommendations. For analytical digests, 0.5 – 1 μ g of DNA was digested in a volume of 20 μ l. Preparative digests for subsequent ligation reactions contained 3-5 μ g of DNA in a total volume of 100 μ l. Fragments were separated on 1% agarose gels. Reactions containing the plasmid backbone fragment were dephosphorylated with 10U CIP for 1h at 37°C.

For ligation, DNA fragments and dephosphorylated backbone fragments were mixed at a ratio of 3:1 in a 20 μ l reaction containing 800U of T4 ligase and 1X ligase buffer. Reactions were incubated at 16°C overnight and 5 μ l transformed into *E.Coli* DH5 α by heatshock. Colonies were first subjected to a test-digest and successful clones were sequence verified.

5.2.2 *In vitro* transcription

Linearization

10µg of pFK-based plasmid DNA were linearized in 200µl reactions with either MluI (sgJFH1, JcR-2A, Jc1) or by sequential digest with AgeI and ScaI (all Con1 constructs). Linearized DNA was column-purified (NucleoSpin® Gel and PCR Clean-up kit) and eluted in RNase free H₂O.

***In vitro* transcription**

All enzymes used for *in vitro* transcription were purchased from Promega. T7 RNA polymerase used in Heidelberg was home-made by the Bartenschlager laboratory. Linearized plasmids were *in vitro* transcribed 37°C overnight in a 200µl reaction containing 1X *in vitro* transcription buffer, 1.56 mM of each ribonucleoside, 200U of RNasin® and 160U T7 RNA polymerase. Transcription was terminated by the addition of 6U DNase (Promega) for 1h at 37°C. If the RNA was not purified immediately, the reaction was stored at -20°C.

Phenol-Chloroform extraction

Terminated transcription reactions were combined with 60µl 2M sodium acetate (pH4.5) and 340µl H₂O and then mixed with 400µl of water-saturated phenol by vigorous vortexing for 30s. The tubes were incubated on ice for 10min and then centrifuged (13 000 RPM, 4°C, 10 minutes). The aqueous phase (~550µl) was transferred to a fresh tube and mixed with an equal volume of chloroform. Tubes were vortexed and then centrifuged (13 000 RPM, RT, 5 minutes). To precipitate the RNA, the aqueous phase was transferred to a fresh tube containing 0.7 volumes isopropanol and pelleted by centrifugation (13 000 RPM, RT, 30 minutes). The pellet was washed once with 70% ethanol and dissolved in 50µl RNase free H₂O. After determining RNA integrity by agarose gel electrophoresis, RNA was aliquoted in 5 or 10µg aliquots and stored at -80°C.

5.2.3 Cell biology

Cell culture

HEK 293T and Hela cells were obtained from ATCC, HEK FlpIn™ 293 cells from Invitrogen and Huh7.5 cells from Apath LLC. Huh7-Lunet and Huh7-Lunet/T7 cells were a kind gift from Prof. Ralf Bartenschlager, University of Heidelberg. All cell lines were cultured in Dulbecco's modified Eagle medium (DMEM; Gibco or SIGMA) supplemented with 10% fetal calf serum (Gibco), 2mM Glutamine (SIGMA) and antibiotics (100U/ml penicillin and 100µg/ml streptomycin; GE Healthcare) at 37 °C in a humidified incubator with 5% CO₂. The concentrations of antibiotics used are listed below.

Concentration of antibiotics			
Cell line	Antibiotic	Concentration	Manufacturer
HEK FlpIN Strep-HA-NS5A	Hygromycin	50µg/ml	Invitrogen
Lentiviral-transduced cells	Puromycin	5µg/ml	SIGMA
Huh7-Lunet/T7	Blasticidin	10µg/ml	Invivogen

Cells were passaged 1:4 or 1:6 twice a week.

Transfection

Polyfect: HEK 293T cells were transfected using PolyFect (PF; QIAGEN) according to the manufacturer's instructions. Briefly, HEK 293T cells were seeded in 6-well dishes (1×10^6 /well) and incubated overnight. Prior to transfection, DMEM was replaced with 1.5ml fresh medium. DNA was diluted in 250 µl OptiMEM® (OM; Invitrogen), mixed with PF at a ratio of 10µl PF/1µg Plasmid DNA and incubated at room temperature (RT) for 15 minutes. After incubation, the DNA-PF solution was further diluted with 600µl of OM and then added drop-wise to the cells. Cells were incubated at 37° and harvested 36-48h post transfection.

Lipofectamine2000®: For the generation of lentiviral particles, HEK 293T cells were transfected using Lipofectamine2000® (L2000; Invitrogen) according to the manufacturer's protocol. Briefly, 5×10^6 cells were seeded in 10cm² dishes and incubated overnight. Prior to transfection, medium was replaced with 4.5ml antibiotic-free medium. 750µl OM were mixed with 30µl of L2000 and incubated at RT for 5 minutes. Meanwhile, 1.5µg of pMD2G, 4.5µg of pCMV-gag-pol and 4.5µg of pWPI vector were diluted in 750µl OM and incubated at RT for 5 minutes. DNA and L2000 solutions were mixed and complex formation allowed for 20 minutes at RT. Solutions were then added drop-wise to cells. Cells were incubated at 37°C and supernatants harvested after 48h by passing them through a 0.2 micron filter. 7ml were used to infect a 50% confluent T75 flask. 24h post transduction, cells were selected with the appropriate concentration of puromycin.

Transit®-LT1: Huh7-Lunet/T7 were transfected using Transit®-LT1 (Transit; Mirus Bio LLC) according to the manufacturer's recommendations. Briefly, Lunet-T7 cells were seeded in 6-well plates (2.5×10^5 /well) and incubated overnight. 2.5µg of DNA were diluted in 250µl OM. Transit was brought to RT, vortexed and 5µl added to the diluted DNA. DNA-Transit solutions were then incubated at RT for 20 minutes. After complex formation, transfection mixes were added drop-wise to the cells. Cell were incubated at 37°C and harvested after 24 – 36 hours.

Lentiviral gene transduction

Huh7-Lunet and Huh7.5 cells stably expressing HA-tagged or untagged SMYD3, SMYD3 Y239F or GFP were generated by lentiviral gene transduction. For small-scale virus production, low passage HEK 293T cells were seeded in a 6-well plate at 1×10^6 cells/well. The following day, cells were transfected with 250 ng of pMD2G, 750 ng of pCMV-gag-pol and 1 μ g of pWPI vector using PF as described above. After overnight incubation at 37°, medium was replaced with 2ml of fresh DMEM. Lentivirus-containing supernatants were collected after 48 and 72h, pooled and filtered through a 0.2 μ m filter. Supernatants were stored at 4°C until used. 24h prior to transduction, cells were seeded in 6-well plates so that cells would be 50% confluent at the time of infection. In the evening, cells were transduced with 3ml of lentiviral supernatants. In the morning, medium was exchanged with fresh DMEM. Following a 24-48h recovery time, cells were cultured in selection medium containing 5 μ g/ml Puromycin. For large-scale lentiviral particle production, low passage HEK 293T cells were transfected in the morning with lentiviral constructs and L2000 as described above. In the evening, transfection medium was replaced with fresh DMEM. After 24h and 48h, supernatants were harvested, filtered through a 0.45 μ m filter and stored at 4°C. Target cells were seeded T-75 flasks 24h prior to transduction. Depending on the cell lines, densities ranged from 1-3 $\times 10^6$ /flask. Cells were then transduced with 8ml of virus-containing supernatant. After overnight incubation, medium was replaced with 10ml fresh DMEM. Following a recovery time of 24h, positive cells were selected by adding medium containing 5 μ g/ml Puromycin (see 5.2.3).

Electroporation

In vitro transcribed HCV RNA was transfected by electroporation using a BioRad Gene Pulser II system. Huh7.5 or Huh7-Lunet cell suspensions were washed 1x in PBS and then resuspended in Cytomix at a concentration of 1,5 or 1×10^7 cells/ml, respectively. The different conditions used are listed below.

Electroporation conditions

Assay type	Cells (μ l)	RNA (μ g)	Cuvette	DMEM (ml)	Plate ml/well
Replication subgenomic replicons	100	2.5	0.2	6.5	24/0.5
Lifecycle/lifecycle kinetics JcR-2A	200	5	0.2	13	12/1.0
Intra/Extracellular infectivity	200	5	0.2	13	6/2

Immunoprecipitations	400	10	0.4	20	20cm ² /20
----------------------	-----	----	-----	----	-----------------------

Appropriate amounts of RNA were aliquoted in eppendorfs and stored on ice until use. Cells were mixed with pre-aliquoted RNA and immediately transferred to the cuvette (BioRad) and electroporated using the settings listed below.

BioRad Gene Pulser settings			
Cuvette (cm)	Volume (μl)	μFaraday (μF)	Volts (V)
0.2	100	500	166
0.2	200	975	166
0.4	400	975	270

After electroporation cells were immediately, yet carefully, transferred to falcons containing the respective amounts of fresh DMEM. After a short recovery time at RT, cells were plated according to need and incubated at 37°C. For safety reasons, cells electroporated with RNA encoding infectious HCV were transferred to the biosafety level 3 laboratory prior to plating.

5.2.4 SDS-PAGE and Western blot

Prior to Western Blot analysis, proteins in cell lysates or immunoprecipitation eluates were separated by SDS polyacrylamide gel electrophoresis (SDS-PAGE). Samples were mixed with 4X Lämmli buffer, boiled for 5 minutes and loaded onto 8% polyacrylamide gels. The gels were run at 100-120V (constant voltage) using the Mini-PROTEAN® Tetra Cell System from BioRad. Once the dye front had run off, the gels were stopped. Proteins were transferred to nitrocellulose (Whatman™ Protran™ Nitrocellulose Blotting membrane; Amersham) by wet blot (100V, 300mA, 60 minutes) in a Mini Trans-Blot® Cell system from BioRad. Complete transfer was checked by staining membranes with Ponceau S. Membranes were then blocked for 30 – 60 minutes in 5%(w/v) non-fat milk (BioRad) dissolved in PBS-T (containing 0.1%(v/v) Tween20). Blots were incubated overnight with primary antibodies diluted in 2.5% milk in PBS-T as indicated in 5.1.2. After 3 rounds of washing (10 minutes each) in PBS-T, blots were incubated with secondary antibodies for 45-60 minutes at RT. After 3 further rounds of washing, proteins were

visualized either by enhanced chemiluminescence (ECL; Amersham) or detected directly using a Li-Cor Infrared imager (Odyssey).

5.2.5 Virological methods

Luciferase reporter assays and infectivity assays

Transient replication of subgenomic or full-length reporter viruses was quantified by F-luc or R-luc reporter assay. Electroporated (replication) or infected (infectivity) cells were harvested after the indicated time points by washing the monolayers once with PBS and subsequent lysis in luciferase lysis buffer (100 μ l for 24-well plates and 150 μ l for 12-well plates).

F-luc assay: 30 μ l of lysate were first diluted in 360 μ l of luciferase assay buffer and then mixed with 200 μ l Luciferin solution. F-luc activity was measured for 20 seconds in a tube luminometer (Lumat, Berthold)

R-Luc assay: 20 μ l of lysate were mixed with R-Luc substrate solution and measured in a tube luminometer for 10 seconds.

In both assays, relative light units (RLUs) were normalized to the respective 4h value to account for differences in transfection efficiency.

To determine JcR-2A infectivity, supernatants from cells electroporated with JcR-2A RNA were harvested at the indicated time points. Naïve Huh7.5 cells seeded in 24-well plates (2.5x10⁴ cells/well). After 24h, the cells were inoculated in duplicate with the respective virus supernatants. After three hours, monolayers were washed 1x with PBS, lysed and R-luc activity determined as described above.

TCID₅₀

TCID₅₀ assays to determine viral titers of the non-reporter virus Jc1 were performed as described in Lindenbach et al, with slight modifications (Lindenbach et al., 2005). Huh7.5 cells were seeded in 96-well plates in a total volume of 100 μ l (1x10⁴ cells/well). After 24h, cells were infected with a 2-fold dilution series of virus supernatants, using a starting dilution of 1:400. 72h post infection, medium was aspirated and cells fixed in ice-cold methanol (30 minutes at -20°C). Monolayers were then washed 2x with PBS. To detect HCV positive cells, monolayers were stained with a mouse monoclonal NS3 (2E3) antibody diluted 1:100 in PBS (1-2h, RT). After three washes with PBS, primary antibodies were detected using a HRP-conjugated anti-mouse polyclonal antibody diluted 1:200 in PBS. Following three further washes, positive cells were visualized by adding home-made TCID50 detection substrate.

Quantification of HCV Core protein

HCV Core protein was quantified by ELISA in the Central Laboratory of the University Hospital Heidelberg (Analysezentrum, Heidelberg, Germany). Cells electroporated with HCV RNA were seeded in 6-well plates (2 ml/well). 48hpe, supernatants were filtered through 45µm filters and diluted 1:2 with PBS containing 1%(v/v)Triton X-100. For quantifying intracellular amounts of Core, cell monolayers were washed twice with PBS and lysed in 0.5 ml of PBS supplemented with 0.5%(v/v) Triton X-100 and 1 mM PMSF, 0.1 mg/ml Aprotinin and 4 mg/ml Leupeptin. Lysates were cleared by centrifugation (10 000 RPM, 10 min, 4°C). If required, samples were diluted in PBS/0.5%(v/v) Triton X-100.

Determination of intra- and extracellular infectivity

To measure intra- and extracellular infectivity, electroporated cells were seeded on 10cm² dishes. After 48 hours, filtered supernatants and cell pellets were subjected to three freeze-thaw cycles. Following the last thawing step, both fractions were centrifuged (13 000 RPM, 4°C, 5 minutes). The cleared supernatants were transferred to fresh eppendorfs and the respective titers determined as described above.

6. BIBLIOGRAPHY

Agnello, V., Abel, G., Elfahal, M., Knight, G.B., and Zhang, Q.X. (1999). Hepatitis C virus and other flaviviridae viruses enter cells via low density lipoprotein receptor. *Proc. Natl. Acad. Sci. U.S.a.* *96*, 12766–12771.

Aizaki, H., Morikawa, K., Fukasawa, M., Hara, H., Inoue, Y., Tani, H., Saito, K., Nishijima, M., Hanada, K., Matsuura, Y., et al. (2008). Critical role of virion-associated cholesterol and sphingolipid in hepatitis C virus infection. *Journal of Virology* *82*, 5715–5724.

Alter, H.J., and Klein, H.G. (2008). The hazards of blood transfusion in historical perspective. *Blood* *112*, 2617–2626.

Ansari, I.-U.H., and Striker, R. (2012). Subtype specific differences in NS5A domain II reveals involvement of proline at position 310 in cyclosporine susceptibility of hepatitis C virus. *Viruses* *4*, 3303–3315.

Ansieau, S., and Leutz, A. (2002). The conserved Mynd domain of BS69 binds cellular and oncoviral proteins through a common PXLXP motif. *J Biol Chem* *277*, 4906–4910.

Appel, N., Pietschmann, T., and Bartenschlager, R. (2005). Mutational Analysis of Hepatitis C Virus Nonstructural Protein 5A: Potential Role of Differential Phosphorylation in RNA Replication and Identification of a Genetically Flexible Domain. *Journal of Virology* *79*, 3187–3194.

Appel, N., Zayas, M., Miller, S., Krijnse-Locker, J., Schaller, T., Friebe, P., Kallis, S., Engel, U., and Bartenschlager, R. (2008). Essential role of domain III of nonstructural protein 5A for hepatitis C virus infectious particle assembly. *PLoS Pathogens* *4*, e1000035.

Asabe, S.I., Tanji, Y., Satoh, S., Kaneko, T., Kimura, K., and Shimotohno, K. (1997). The N-terminal region of hepatitis C virus-encoded NS5A is important for NS4A-dependent phosphorylation. *Journal of Virology* *71*, 790–796.

Bartenschlager, R., Lohmann, V., and Penin, F. (2013). The molecular and structural basis of advanced antiviral therapy for hepatitis C virus infection. *Nat Rev Micro* *11*, 482–496.

Bartenschlager, R., Penin, F., Lohmann, V., and André, P. (2011). Assembly of infectious hepatitis C virus particles. *Trends in Microbiology* *19*, 95–103.

Barth, H., Schafer, C., Adah, M.I., Zhang, F., Linhardt, R.J., Toyoda, H., Kinoshita-Toyoda, A., Toida, T., Van Kuppevelt, T.H., Depla, E., et al. (2003). Cellular binding of hepatitis C virus envelope glycoprotein E2 requires cell surface heparan sulfate. *J Biol Chem* *278*, 41003–41012.

Betts, M., and Russell, R.B. (2003). Amino Acid Properties and Consequences of Substitutions. In *Bioinformatics for Geneticists*, M.R. Barnes, and I.C. Gray, eds. (Chichester, UK: John Wiley & Sons, Ltd.), pp. 289–316.

Blanchard, E., Belouzard, S., Goueslain, L., Wakita, T., Dubuisson, J., Wychowski, C., and Rouillé, Y. (2006). Hepatitis C virus entry depends on clathrin-mediated endocytosis. *Journal of Virology* *80*, 6964–6972.

- Blight, K.J., McKeating, J.A., and Rice, C.M. (2002). Highly permissive cell lines for subgenomic and genomic hepatitis C virus RNA replication. *Journal of Virology* 76, 13001–13014.
- Brass, V., Bieck, E., Montserret, R., Wölk, B., Hellings, J.A., Blum, H.E., Penin, F., and Moradpour, D. (2002). An amino-terminal amphipathic alpha-helix mediates membrane association of the hepatitis C virus nonstructural protein 5A. *J Biol Chem* 277, 8130–8139.
- Brown, M., Sims, R., III, Gottlieb, P., and Tucker, P. (2006). Identification and characterization of Smyd2: a split SET/MYND domain-containing histone H3 lysine 36-specific methyltransferase that interacts with the Sin3 histone deacetylase complex. *Mol Cancer* 5, 1–11.
- Chang, K.-S., Jiang, J., Cai, Z., and Luo, G. (2007). Human apolipoprotein e is required for infectivity and production of hepatitis C virus in cell culture. *Journal of Virology* 81, 13783–13793.
- Chen, Y.-C., Su, W.-C., Huang, J.-Y., Chao, T.-C., Jeng, K.-S., Machida, K., and Lai, M.M.C. (2010). Polo-like kinase 1 is involved in hepatitis C virus replication by hyperphosphorylating NS5A. *Journal of Virology* 84, 7983–7993.
- Cho, H.-S., Hayami, S., Toyokawa, G., Maejima, K., Yamane, Y., Suzuki, T., Dohmae, N., Kogure, M., Kang, D., Neal, D.E., et al. (2012). RB1 methylation by SMYD2 enhances cell cycle progression through an increase of RB1 phosphorylation. *Neo* 14, 476–486.
- Clarke, S.G. (2013). Protein methylation at the surface and buried deep: thinking outside the histone box. *Trends in Biochemical Sciences* 38, 243–252.
- Cock-Rada, A.M., Medjkane, S., Janski, N., Yousfi, N., Perichon, M., Chaussepied, M., Chluba, J., Langsley, G., and Weitzman, J.B. (2012). SMYD3 promotes cancer invasion by epigenetic upregulation of the metalloproteinase MMP-9. *Cancer Research* 72, 810–820.
- Conrad, K.D., Giering, F., Erfurth, C., Neumann, A., Fehr, C., Meister, G., and Niepmann, M. (2013). MicroRNA-122 dependent binding of Ago2 protein to hepatitis C virus RNA is associated with enhanced RNA stability and translation stimulation. *PLoS ONE* 8, e56272.
- Cox, E. (2011a). INCIVEK™ NDA no. 201917 Approval Letter, accessed 30/09/2014 (Silver Spring : U.S. Food and Drug Administration).
- Cox, E. (2011b). Victrelis™ NDA no. 202258 Approval Letter , accessed 30/09/2014 (Silver Spring : U.S. Food and Drug Administration).
- Date, T., Kato, T., Miyamoto, M., Zhao, Z., Yasui, K., Mizokami, M., and Wakita, T. (2004). Genotype 2a hepatitis C virus subgenomic replicon can replicate in HepG2 and IMY-N9 cells. *J Biol Chem* 279, 22371–22376.
- de Chasse, B., Navratil, V., Tafforeau, L., Hiet, M.S., Aublin-Gex, A., Agaagué, S., Meiffren, G., Pradezynski, F., Faria, B.F., Chantier, T., et al. (2008). Hepatitis C virus infection protein network. *Molecular Systems Biology* 4.
- Dillon, S.C., Zhang, X., Trievel, R.C., and Cheng, X. (2005). The SET-domain protein superfamily: protein lysine methyltransferases. *Genome Biol* 6, 227.

- Dimitrova, M., Imbert, I., Kieny, M.P., and Schuster, C. (2003). Protein-protein interactions between hepatitis C virus nonstructural proteins. *Journal of Virology* 77, 5401–5414.
- Dubuisson, J., Hsu, H.H., Cheung, R.C., Greenberg, H.B., Russell, D.G., and Rice, C.M. (1994). Formation and intracellular localization of hepatitis C virus envelope glycoprotein complexes expressed by recombinant vaccinia and Sindbis viruses. *Journal of Virology* 68, 6147–6160.
- Eberle, C.-A., Zayas, M., Stukalov, A., Pichlmair, A., Alvisi, G., Müller, A.C., Bennett, K.L., Bartenschlager, R., and Superti-Furga, G. (2014). The lysine methyltransferase SMYD3 interacts with hepatitis C virus NS5A and is a negative regulator of viral particle production. *Virology* 462-463, 34–41.
- Egger, D., Wölk, B., Gosert, R., Bianchi, L., Blum, H.E., Moradpour, D., and Bienz, K. (2002). Expression of hepatitis C virus proteins induces distinct membrane alterations including a candidate viral replication complex. *Journal of Virology* 76, 5974–5984.
- Evans, M.J., Hahn, von, T., Tscherne, D.M., Syder, A.J., Panis, M., Wölk, B., Hatzioannou, T., McKeating, J.A., Bieniasz, P.D., and Rice, C.M. (2007). Claudin-1 is a hepatitis C virus co-receptor required for a late step in entry. *Nature* 446, 801–805.
- Foreman, K.W., Brown, M., Park, F., Emtage, S., Harriss, J., Das, C., Zhu, L., Crew, A., Arnold, L., Shaaban, S., et al. (2011). Structural and Functional Profiling of the Human Histone Methyltransferase SMYD3. *PLoS ONE* 6, e22290.
- Fridell, R.A., Valera, L., Qiu, D., Kirk, M.J., Wang, C., and Gao, M. (2013). Intragenic complementation of hepatitis C virus NS5A RNA replication-defective alleles. *Journal of Virology* 87, 2320–2329.
- Friebe, P., Boudet, J., Simorre, J.-P., and Bartenschlager, R. (2005). Kissing-loop interaction in the 3' end of the hepatitis C virus genome essential for RNA replication. *Journal of Virology* 79, 380–392.
- Fujii, T., Tsunesumi, S.-I., Yamaguchi, K., Watanabe, S., and Furukawa, Y. (2011). Smyd3 is required for the development of cardiac and skeletal muscle in zebrafish. *PLoS ONE* 6, e23491.
- Gale, M., Blakely, C.M., Kwieciszewski, B., Tan, S.L., Dossett, M., Tang, N.M., Korth, M.J., Polyak, S.J., Gretch, D.R., and Katze, M.G. (1998). Control of PKR protein kinase by hepatitis C virus nonstructural 5A protein: molecular mechanisms of kinase regulation. *Molecular and Cellular Biology* 18, 5208–5218.
- Gao, M., Nettles, R.E., Belema, M., Snyder, L.B., Nguyen, V.N., Fridell, R.A., Serrano-Wu, M.H., Langley, D.R., Sun, J.-H., O'Boyle, D.R., II, et al. (2010). Chemical genetics strategy identifies an HCV NS5A inhibitor with a potent clinical effect. *Nature* 465, 96–100.
- Gastaminza, P., Cheng, G., Wieland, S., Zhong, J., Liao, W., and Chisari, F.V. (2008). Cellular determinants of hepatitis C virus assembly, maturation, degradation, and secretion. *Journal of Virology* 82, 2120–2129.
- Germain, M.A., Chatel-Chaix, L., Gagne, B., Bonneil, E., Thibault, P., Pradezynski, F., de Chasse, B., Meyniel-Shicklin, L., Lotteau, V., Baril, M., et al. (2013). Elucidating Novel Hepatitis C Virus/Host Interactions Using Combined Mass Spectrometry and Functional Genomics Approaches. *Molecular & Cellular Proteomics* 1–61.
- Gower, E., Estes, C., Blach, S., Razavi-Shearer, K., and Razavi, H. (2014). Global epidemiology and

genotype distribution of the hepatitis C virus infection. *Journal of Hepatology* *61*, S45–S57.

Grakoui, A., McCourt, D.W., Wychowski, C., Feinstone, S.M., and Rice, C.M. (1993). A second hepatitis C virus-encoded proteinase. *Proc. Natl. Acad. Sci. U.S.A.* *90*, 10583–10587.

Hagen, N., Bayer, K., Rösch, K., and Schindler, M. (2014). The intraviral protein interaction network of hepatitis C virus. *Molecular & Cellular Proteomics* *13*, 1676–1689.

Hajarizadeh, B., Grebely, J., and Dore, G.J. (2013). nrgastro.2013.107. *Nature Publishing Group* *10*, 553–562.

Hamamoto, R., Furukawa, Y., Morita, M., Iimura, Y., Silva, F.P., Li, M., Yagyu, R., and Nakamura, Y. (2004). SMYD3 encodes a histone methyltransferase involved in the proliferation of cancer cells. *Nat Cell Biol* *6*, 731–740.

Hamamoto, R., Silva, F.P., Tsuge, M., Nishidate, T., Katagiri, T., Nakamura, Y., and Furukawa, Y. (2006). Enhanced SMYD3 expression is essential for the growth of breast cancer cells. *Cancer Science* *97*, 113–118.

Hanouille, X., Badillo, A., Wieruszkeski, J.M., Verdegem, D., Landrieu, I., Bartenschlager, R., Penin, F., and Lippens, G. (2009a). Hepatitis C Virus NS5A Protein Is a Substrate for the Peptidyl-prolyl cis/trans Isomerase Activity of Cyclophilins A and B. *Journal of Biological Chemistry* *284*, 13589–13601.

Hanouille, X., Verdegem, D., Badillo, A., Wieruszkeski, J.-M., Penin, F., and Lippens, G. (2009b). Domain 3 of non-structural protein 5A from hepatitis C virus is natively unfolded. *Biochemical and Biophysical Research Communications* *381*, 634–638.

Helin, K., and Dhanak, D. (2013). Chromatin proteins and modifications as drug targets. *Nature* *502*, 480–488.

Hill, A., and Cooke, G. (2014). *Medicine*. Hepatitis C can be cured globally, but at what cost? *Science* *345*, 141–142.

Houghton, M. (1996). Hepatitis C viruses. In *Fields Virology*, P.M. Holey, B.N. Fields, and K.D. M, eds. (Philadelphia: Lippincott Williams & Wilkins), pp. 1035–1058.

Huang, H., Sun, F., Owen, D.M., Li, W., Chen, Y., Gale, M., and Ye, J. (2007a). Hepatitis C virus production by human hepatocytes dependent on assembly and secretion of very low-density lipoproteins. *Proc. Natl. Acad. Sci. U.S.A.* *104*, 5848–5853.

Huang, Y., Staschke, K., De Francesco, R., and Tan, S.-L. (2007b). Phosphorylation of hepatitis C virus NS5A nonstructural protein: A new paradigm for phosphorylation-dependent viral RNA replication? *Virology* *364*, 1–9.

Hughes, M., Gretton, S., Shelton, H., Brown, D.D., McCormick, C.J., Angus, A.G.N., Patel, A.H., Griffin, S., and Harris, M. (2009). A conserved proline between domains II and III of hepatitis C virus NS5A influences both RNA replication and virus assembly. *Journal of Virology* *83*, 10788–10796.

Hwang, J., Huang, L., Cordek, D.G., Vaughan, R., Reynolds, S.L., Kihara, G., Raney, K.D., Kao, C.C., and

- Cameron, C.E. (2010). Hepatitis C Virus Nonstructural Protein 5A: Biochemical Characterization of a Novel Structural Class of RNA-Binding Proteins. *Journal of Virology* *84*, 12480–12491.
- Jones, C.T., Murray, C.L., Eastman, D.K., Tassello, J., and Rice, C.M. (2007). Hepatitis C virus p7 and NS2 proteins are essential for production of infectious virus. *Journal of Virology* *81*, 8374–8383.
- Jones, D.M., Patel, A.H., Targett-Adams, P., and McLauchlan, J. (2009). The hepatitis C virus NS4B protein can trans-complement viral RNA replication and modulates production of infectious virus. *Journal of Virology* *83*, 2163–2177.
- Jung, S.Y., Li, Y., Wang, Y., Chen, Y., Zhao, Y., and Qin, J. (2008). Complications in the Assignment of 14 and 28 Da Mass Shift Detected by Mass Spectrometry as in Vivo Methylation from Endogenous Proteins. *Anal. Chem.* *80*, 1721–1729.
- Kaneko, T., Tanji, Y., Satoh, S., Hijikata, M., Asabe, S., Kimura, K., and Shimotohno, K. (1994). Production of two phosphoproteins from the NS5A region of the hepatitis C viral genome. *Biochemical and Biophysical Research Communications* *205*, 320–326.
- Kato, T., Date, T., Miyamoto, M., Furusaka, A., Tokushige, K., Mizokami, M., and Wakita, T. (2003). Efficient replication of the genotype 2a hepatitis C virus subgenomic replicon. *Yeast* *125*, 1808–1817.
- Kato, T., Date, T., Miyamoto, M., Zhao, Z., Mizokami, M., and Wakita, T. (2005). Nonhepatic cell lines HeLa and 293 support efficient replication of the hepatitis C virus genotype 2a subgenomic replicon. *Journal of Virology* *79*, 592–596.
- Kim, Y.K., Kim, C.S., Lee, S.H., and Jang, S.K. (2002). Domains I and II in the 5' nontranslated region of the HCV genome are required for RNA replication. *Biochemical and Biophysical Research Communications* *290*, 105–112.
- Koch, J.O., and Bartenschlager, R. (1999). Modulation of hepatitis C virus NS5A hyperphosphorylation by nonstructural proteins NS3, NS4A, and NS4B. *Journal of Virology* *73*, 7138–7146.
- Kosol, S., Contreras-Martos, S., Cedeño, C., and Tompa, P. (2013). Structural characterization of intrinsically disordered proteins by NMR spectroscopy. *Molecules* *18*, 10802–10828.
- Koutsoudakis, G., Herrmann, E., Kallis, S., Bartenschlager, R., and Pietschmann, T. (2006). The level of CD81 cell surface expression is a key determinant for productive entry of hepatitis C virus into host cells. *Journal of Virology* *81*, 588–598.
- Krieger, N., Lohmann, V., and Bartenschlager, R. (2001a). Enhancement of hepatitis C virus RNA replication by cell culture-adaptive mutations. *Journal of Virology* *75*, 4614–4624.
- Krieger, N., Lohmann, V., and Bartenschlager, R. (2001b). Viral and cellular determinants of hepatitis C virus RNA replication in cell culture. *Journal of Virology* *75*, 4614–4624.
- Kuiken, C., Yusim, K., Boykin, L., and Richardson, R. (2005). The Los Alamos hepatitis C sequence database. *Bioinformatics* *21*, 379–384.
- Kumthip, K., Chusri, P., Jilg, N., Zhao, L., Fusco, D.N., Zhao, H., Goto, K., Cheng, D., Schaefer, E.A., Zhang,

- L., et al. (2012). Hepatitis C Virus NS5A Disrupts STAT1 Phosphorylation and Suppresses Type I Interferon Signaling. *Journal of Virology* *86*, 8581–8591.
- Kunizaki, M., Hamamoto, R., Silva, F.P., Yamaguchi, K., Nagayasu, T., Shibuya, M., Nakamura, Y., and Furukawa, Y. (2007). The Lysine 831 of Vascular Endothelial Growth Factor Receptor 1 Is a Novel Target of Methylation by SMYD3. *Cancer Research* *67*, 10759–10765.
- Lanouette, S., Mongeon, V., Figeys, D., and Couture, J.-F. (2014). The functional diversity of protein lysine methylation. *Molecular Systems Biology* *10*, 724.
- Leutz, A., Pless, O., Lappe, M., Dittmar, G., and Kowenz-Leutz, E. (2011). Crosstalk between phosphorylation and multi-site arginine/lysine methylation in C/EBPs. *Transcription* *2*, 3–8.
- Levy, D., Kuo, A.J., Chang, Y., Schaefer, U., Kitson, C., Cheung, P., Espejo, A., Zee, B.M., Liu, C.L., Tangsombatvisit, S., et al. (2010). Lysine methylation of the NF- κ B subunit RelA by SETD6 couples activity of the histone methyltransferase GLP at chromatin to tonic repression of NF- κ B signaling. *Nature Publishing Group* *12*, 29–36.
- Liang, Y., Kang, C.B., and Yoon, H.S. (2006). Molecular and structural characterization of the domain 2 of hepatitis C virus non-structural protein 5A. *Mol Cells* *22*, 13–20.
- Lindenbach, B.D., Evans, M.J., Syder, A.J., and Wölk, B. (2005). Complete replication of hepatitis C virus in cell culture. *Science*.
- Lindenbach, B.D., and Rice, C.M. (2013). The ins and outs of hepatitis C virus entry and assembly. *Nat Rev Micro* *11*, 688–700.
- Lindenbach, B.D., Meuleman, P., Ploss, A., Vanwolleghem, T., Syder, A.J., McKeating, J.A., Lanford, R.E., Feinstone, S.M., Major, M.E., Leroux-Roels, G., et al. (2006). Cell culture-grown hepatitis C virus is infectious in vivo and can be recultured in vitro. *Proc. Natl. Acad. Sci. U.S.a.* *103*, 3805–3809.
- Liu, C., Xu, D., Han, H., Fan, Y., Schain, F., Xu, Z., Claesson, H.-E., Björkholm, M., and Sjöberg, J. (2012). Transcriptional Regulation of 15-Lipoxygenase Expression by Histone H3 Lysine 4 Methylation/Demethylation. *PLoS ONE* *7*, e52703.
- Liu, Q., Bhat, R.A., Prince, A.M., and Zhang, P. (1999). The hepatitis C virus NS2 protein generated by NS2-3 autocleavage is required for NS5A phosphorylation. *Biochemical and Biophysical Research Communications* *254*, 572–577.
- Liu, Z., Wang, Y., Gao, T., Pan, Z., Cheng, H., Yang, Q., Cheng, Z., Guo, A., Ren, J., and Xue, Y. (2013). CPLM: a database of protein lysine modifications. *Nucleic Acids Research* *42*, D531–D536.
- Lohmann, V. (1999). Replication of Subgenomic Hepatitis C Virus RNAs in a Hepatoma Cell Line. *Science* *285*, 110–113.
- Lohmann, V., and Bartenschlager, R. (2013). Hepatitis C Virus Replicons Volume 3 and 4. *Ygast* *144*, 13–15.
- Lohmann, V., Hoffmann, S., Herian, U., Penin, F., and Bartenschlager, R. (2003). *Viral and Cellular*

- Determinants of Hepatitis C Virus RNA Replication in Cell Culture. *Journal of Virology* 77, 3007–3019.
- Lohmann, V. (2009). HCV Replicons: Overview and Basic Protocols. In *Hepatitis C: Methods and Protocols*, H. Tang, ed. (Humana Press, a part of Springer Science+Business Media).
- Lohmann, V. (2013). Hepatitis C virus RNA replication. *Curr. Top. Microbiol. Immunol.* 369, 167–198.
- Lu, Y., Zhang, G., Shen, C., Uygun, K., Yarmush, M.L., and Meng, Q. (2012). A novel 3D liver organoid system for elucidation of hepatic glucose metabolism. *Biotechnol. Bioeng.* 109, 595–604.
- Luo, X.-G., Zhang, C.-L., Zhao, W.-W., Liu, Z.-P., Liu, L., Mu, A., Guo, S., Wang, N., Zhou, H., and Zhang, T.-C. (2014). Histone methyltransferase SMYD3 promotes MRTF-A-mediated transactivation of MYL9 and migration of MCF-7 breast cancer cells. *Cancer Letters* 344, 129–137.
- Lupberger, J., Zeisel, M.B., Xiao, F., Thumann, C., Fofana, I., Zona, L., Davis, C., Mee, C.J., Turek, M., Gorke, S., et al. (2011). EGFR and EphA2 are host factors for hepatitis C virus entry and possible targets for antiviral therapy. *Nature Medicine* 17, 589–595.
- Marazzi, I., Ho, J.S.Y., Kim, J., Manicassamy, B., Dewell, S., Albrecht, R.A., Seibert, C.W., Schaefer, U., Jeffrey, K.L., Prinjha, R.K., et al. (2012). nature10892. *Nature* 483, 428–433.
- Marouco, D., Garabadgiu, A.V., Melino, G., and Barlev, N.A. (2013). Lysine-specific modifications of p53: a matter of life and death? *Oncotarget* 4, 1556–1571.
- Masaki, T., Suzuki, R., Murakami, K., Aizaki, H., Ishii, K., Murayama, A., Date, T., Matsuura, Y., Miyamura, T., Wakita, T., et al. (2008). Interaction of Hepatitis C Virus Nonstructural Protein 5A with Core Protein Is Critical for the Production of Infectious Virus Particles. *Journal of Virology* 82, 7964–7976.
- Masumi, A., Aizaki, H., Suzuki, T., DuHadaway, J.B., Prendergast, G.C., Komuro, K., and Fukazawa, H. (2005). Reduction of hepatitis C virus NS5A phosphorylation through its interaction with amphiphysin II. *Biochemical and Biophysical Research Communications* 336, 572–578.
- Mazur, P.K., Reynoird, N., Khatri, P., Jansen, P.W.T.C., Wilkinson, A.W., Liu, S., Barbash, O., Van Aller, G.S., Huddleston, M., Dhanak, D., et al. (2014). nature13320. *Nature* 510, 283–287.
- Mellacheruvu, D., Wright, Z., Couzens, A.L., Lambert, J.-P., St-Denis, N.A., Li, T., Miteva, Y.V., Hauri, S., Sardi, M.E., Low, T.Y., et al. (2013). the CRaPome: a contaminant repository for affinity purification–mass spectrometry data. *Nature Methods* 1–11.
- Merz, A., Long, G., Hiet, M.-S., Brügger, B., Chlanda, P., André, P., Wieland, F., Krijnse-Locker, J., and Bartenschlager, R. (2011). Biochemical and morphological properties of hepatitis C virus particles and determination of their lipidome. *Journal of Biological Chemistry* 286, 3018–3032.
- Meylan, E., Curran, J., Hofmann, K., Moradpour, D., Binder, M., Bartenschlager, R., and Tschopp, J. (2005). Cardif is an adaptor protein in the RIG-I antiviral pathway and is targeted by hepatitis C virus. *Nat Cell Biol* 437, 1167–1172.
- Miyanari, Y., Atsuzawa, K., Usuda, N., Watashi, K., Hishiki, T., Zayas, M., Bartenschlager, R., Wakita, T., Hijikata, M., and Shimotohno, K. (2007a). The lipid droplet is an important organelle for hepatitis C virus

production. *Nat Cell Biol* 9, 1089–1097.

Miyanari, Y., Atsuzawa, K., Usuda, N., Watashi, K., Hishiki, T., Zayas, M., Bartenschlager, R., Wakita, T., Hijikata, M., and Shimotohno, K. (2007b). The lipid droplet is an important organelle for hepatitis C virus production. *Nat Cell Biol* 9, 1089–1097.

Moore, K.E., and Gozani, O. (2014). An unexpected journey: Lysine methylation across the proteome. *BBA - Gene Regulatory Mechanisms* 1–9.

Moradpour, D., Penin, F., and Rice, C.M. (2007). Replication of hepatitis C virus. *Nat Rev Micro* 5, 453–463.

Mori, M., Yoneda-Kato, N., Yoshida, A., and Kato, J.-Y. (2008). Stable form of JAB1 enhances proliferation and maintenance of hematopoietic progenitors. *J Biol Chem* 283, 29011–29021.

Neddermann, P., Clementi, A., and De Francesco, R. (1999). Hyperphosphorylation of the hepatitis C virus NS5A protein requires an active NS3 protease, NS4A, NS4B, and NS5A encoded on the same polyprotein. *Journal of Virology* 73, 9984–9991.

Negro, F. (2013). negro2013. *Nature Publishing Group* 11, 77–78.

Neumann, A.U., Lam, N.P., Dahari, H., Gretch, D.R., Wiley, T.E., Layden, T.J., and Perelson, A.S. (1998). Hepatitis C viral dynamics in vivo and the antiviral efficacy of interferon-alpha therapy. *Science* 282, 103–107.

Ong, S.-E., Mittler, G., and Mann, M. (2004). Identifying and quantifying in vivo methylation sites by heavy methyl SILAC. *Nature Methods* 1, 119–126.

Pagans, S., Kauder, S.E., Kaehlcke, K., Sakane, N., Schroeder, S., Dormeyer, W., Triebel, R.C., Verdin, E., Schnolzer, M., and Ott, M. (2010). The Cellular Lysine Methyltransferase Set7/9-KMT7 Binds HIV-1 TAR RNA, Monomethylates the Viral Transactivator Tat, and Enhances HIV Transcription. *Cell Host and Microbe* 7, 234–244.

Pang, C., Gasteiger, E., and Wilkins, M.R. (2010). Identification of arginine- and lysine-methylation in the proteome of *Saccharomyces cerevisiae* and its functional implications. *BMC Genomics* 11, 92.

Penin, F., Brass, V., Appel, N., Ramboarina, S., Montserret, R., Ficheux, D., Blum, H.E., Bartenschlager, R., and Moradpour, D. (2004). Structure and function of the membrane anchor domain of hepatitis C virus nonstructural protein 5A. *J Biol Chem* 279, 40835–40843.

Pettersen, E.F., Goddard, T.D., Huang, C.C., Couch, G.S., Greenblatt, D.M., Meng, E.C., and Ferrin, T.E. (2004). UCSF Chimera--a visualization system for exploratory research and analysis. *J Comput Chem* 25, 1605–1612.

Pichlmair, A., Kandasamy, K., Alvisi, G., Mulhern, O., Sacco, R., Habjan, M., Binder, M., Stefanovic, A., Eberle, C.-A., Goncalves, A., et al. (2012). inhibitome. *Nature* 487, 486–490.

Pietschmann, T., Kaul, A., Koutsoudakis, G., Shavinskaya, A., Kallis, S., Steinmann, E., Abid, K., Negro, F., Dreux, M., Cosset, F.-L., et al. (2006). Construction and characterization of infectious intragenotypic and

intergenotypic hepatitis C virus chimeras. *Proc. Natl. Acad. Sci. U.S.A.* *103*, 7408–7413.

Pietschmann, T., Zayas, M., Meuleman, P., Long, G., Appel, N., Koutsoudakis, G., Kallis, S., Leroux-Roels, G., Lohmann, V., and Bartenschlager, R. (2009). Production of Infectious Genotype 1b Virus Particles in Cell Culture and Impairment by Replication Enhancing Mutations. *PLoS Pathogens* *5*, e1000475.

Pileri, P., Uematsu, Y., Campagnoli, S., Galli, G., Falugi, F., Petracca, R., Weiner, A.J., Houghton, M., Rosa, D., Grandi, G., et al. (1998). Binding of hepatitis C virus to CD81. *Science* *282*, 938–941.

Ploss, A., Evans, M.J., Gaysinskaya, V.A., Panis, M., You, H., de Jong, Y.P., and Rice, C.M. (2009). Human occludin is a hepatitis C virus entry factor required for infection of mouse cells. *Nature* *457*, 882–886.

Proserpio, V., Fittipaldi, R., Ryall, J.G., Sartorelli, V., and Caretti, G. (2013). The methyltransferase SMYD3 mediates the recruitment of transcriptional cofactors at the myostatin and c-Met genes and regulates skeletal muscle atrophy. *Genes & Development* *27*, 1299–1312.

Quinkert, D., Bartenschlager, R., and Lohmann, V. (2005). Quantitative Analysis of the Hepatitis C Virus Replication Complex. *Journal of Virology* *79*, 13594–13605.

Quintavalle, M., Sambucini, S., Summa, V., Orsatti, L., Talamo, F., De Francesco, R., and Neddermann, P. (2007). Hepatitis C virus NS5A is a direct substrate of casein kinase I-alpha, a cellular kinase identified by inhibitor affinity chromatography using specific NS5A hyperphosphorylation inhibitors. *J Biol Chem* *282*, 5536–5544.

Reardon, S. (2014). United States to approve potent oral drugs for hepatitis C
. *Nature News*.

Reed, K.E., Xu, J., and Rice, C.M. (1997). Phosphorylation of the hepatitis C virus NS5A protein in vitro and in vivo: properties of the NS5A-associated kinase. *Journal of Virology* *71*, 7187–7197.

Reiss, S., Rebhan, I., Backes, P., Romero-Brey, I., Erfle, H., Matula, P., Kaderali, L., Poenisch, M., Blankenburg, H., Hiet, M.-S., et al. (2011). Recruitment and Activation of a Lipid Kinase by Hepatitis C Virus NS5A Is Essential for Integrity of the Membranous Replication Compartment. *Cell Host and Microbe* *9*, 32–45.

Romero-Brey, I., Merz, A., Chiramel, A., Lee, J.-Y., Chlanda, P., Haselman, U., Santarella-Mellwig, R., Habermann, A., Hoppe, S., Kallis, S., et al. (2012). Three-dimensional architecture and biogenesis of membrane structures associated with hepatitis C virus replication. *PLoS Pathogens* *8*, e1003056.

Ross-Thriepland, D., and Harris, M. (2014). Insights into the complexity and functionality of hepatitis C virus NS5A phosphorylation. *Journal of Virology* *88*, 1421–1432.

Ross-Thriepland, D., Amako, Y., and Harris, M. (2013). The C terminus of NS5A domain II is a key determinant of hepatitis C virus genome replication, but is not required for virion assembly and release. *Journal of General Virology* *94*, 1009–1018.

Sainz, B., Barretto, N., Martin, D.N., Hiraga, N., Imamura, M., Hussain, S., Marsh, K.A., Yu, X., Chayama, K., Alrefai, W.A., et al. (2012). Identification of the Niemann-Pick C1-like 1 cholesterol absorption

receptor as a new hepatitis C virus entry factor. *Nature Medicine* 18, 281–285.

Sakane, N., Kwon, H.-S., Pagans, S., Kaelin-Lang, K., Mizusawa, Y., Kamada, M., Lassen, K.G., Chan, J., Greene, W.C., Schnoelzer, M., et al. (2011). Activation of HIV transcription by the viral Tat protein requires a demethylation step mediated by lysine-specific demethylase 1 (LSD1/KDM1). *PLoS Pathogens* 7, e1002184.

Scarselli, E., Ansuini, H., Cerino, R., Roccasecca, R.M., Acali, S., Filocamo, G., Traboni, C., Nicosia, A., Cortese, R., and Vitelli, A. (2002). The human scavenger receptor class B type I is a novel candidate receptor for the hepatitis C virus. *Embo J* 21, 5017–5025.

Scheel, T.K.H., and Rice, C.M. (2013). nm.3248. *Nature Medicine* 19, 837–849.

Schwartz, R.E., Trehan, K., Andrus, L., Sheahan, T.P., Ploss, A., Duncan, S.A., Rice, C.M., and Bhatia, S.N. (2012). Modeling hepatitis C virus infection using human induced pluripotent stem cells. *Proceedings of the National Academy of Sciences* 109, 2544–2548.

Simmonds, P. (2013). The origin of hepatitis C virus. *Curr. Top. Microbiol. Immunol.* 369, 1–15.

Sirinupong, N., Brunzelle, J., Doko, E., and Yang, Z. (2010). Structural Insights into the Autoinhibition and Posttranslational Activation of Histone Methyltransferase SmyD3. *Journal of Molecular Biology* 1–11.

Song, Y., Friebe, P., Tzima, E., Jünemann, C., Bartenschlager, R., and Niepmann, M. (2006). The hepatitis C virus RNA 3'-untranslated region strongly enhances translation directed by the internal ribosome entry site. *Journal of Virology* 80, 11579–11588.

Steenbergen, R.H.G., Joyce, M.A., Thomas, B.S., Jones, D., Law, J., Russell, R., Houghton, M., and Tyrrell, D.L. (2013). Human serum leads to differentiation of human hepatoma cells, restoration of very-low-density lipoprotein secretion, and a 1000-fold increase in HCV Japanese fulminant hepatitis type 1 titers. *Hepatology* 58, 1907–1917.

Tawar, R.G., Maily, L., and Baumert, T.F. (2014). A new HCV mouse model on the block. *Cell Res.* 24, 1153–1154.

Tellinghuisen, T.L., Foss, K.L., and Treadaway, J. (2008a). Regulation of Hepatitis C Virion Production via Phosphorylation of the NS5A Protein. *PLoS Pathogens* 4, e1000032.

Tellinghuisen, T.L., Foss, K.L., Treadaway, J.C., and Rice, C.M. (2008b). Identification of residues required for RNA replication in domains II and III of the hepatitis C virus NS5A protein. *Journal of Virology* 82, 1073–1083.

Tellinghuisen, T.L., Marcotrigiano, J., and Rice, C.M. (2005). Structure of the zinc-binding domain of an essential component of the hepatitis C virus replicase. *Nature* 435, 374–379.

Tellinghuisen, T.L., Marcotrigiano, J., Gorbalenya, A.E., and Rice, C.M. (2004). The NS5A protein of hepatitis C virus is a zinc metalloprotein. *J Biol Chem* 279, 48576–48587.

Tschiersch, B., Hofmann, A., Krauss, V., Dorn, R., Korge, G., and Reuter, G. (1994). The protein encoded by the *Drosophila* position-effect variegation suppressor gene *Su(var)3-9* combines domains of

antagonistic regulators of homeotic gene complexes. *Embo J* 13, 3822–3831.

Tsukiyama-Kohara, K., Iizuka, N., Kohara, M., and Nomoto, A. (1992). Internal ribosome entry site within hepatitis C virus RNA. *Journal of Virology* 66, 1476–1483.

Uhlen, M., Oksvold, P., Fagerberg, L., Lundberg, E., Jonasson, K., Forsberg, M., Zwahlen, M., Kampf, C., Wester, K., Hober, S., et al. (2010). Towards a knowledge-based Human Protein Atlas. *Nat Biotechnol* 28, 1248–1250.

Van Aller, G.S., Reynoird, N., Barbash, O., Huddleston, M., Liu, S., Zmoos, A.-F., McDevitt, P., Sinnamon, R., Le, B., Mas, G., et al. (2012). Smyd3 regulates cancer cell phenotypes and catalyzes histone H4 lysine 5 methylation. *Epigenetics* 7, 340–343.

Van Duynes, R., Easley, R., Wu, W., Berro, R., Pedati, C., Klase, Z., Kehn-Hall, K., Flynn, E.K., Symer, D.E., and Kashanchi, F. (2008). Lysine methylation of HIV-1 Tat regulates transcriptional activity of the viral LTR. *Retrovirology* 5, 40.

Verdegem, D., Badillo, A., Wieruszkeski, J.M., Landrieu, I., Leroy, A., Bartenschlager, R., Penin, F., Lippens, G., and Hanouille, X. (2011). Domain 3 of NS5A Protein from the Hepatitis C Virus Has Intrinsic α -Helical Propensity and Is a Substrate of Cyclophilin A. *Journal of Biological Chemistry* 286, 20441–20454.

Vidalain, P.-O., and Tangy, F. (2010). Virus-host protein interactions in RNA viruses. *Microbes and Infection* 12, 1134–1143.

Wagner, E.F., and Nebreda, A.R. (2009). Signal integration by JNK and p38 MAPK pathways in cancer development. *Nat Rev Cancer* 9, 537–549.

Wakita, T., Pietschmann, T., Kato, T., Date, T., Miyamoto, M., Zhao, Z., Murthy, K., Habermann, A., Kräusslich, H.-G., Mizokami, M., et al. (2005). Production of infectious hepatitis C virus in tissue culture from a cloned viral genome. *Nature Medicine* 11, 791–796.

Waterhouse, A.M., Procter, J.B., Martin, D.M.A., Clamp, M., and Barton, G.J. (2009). Jalview Version 2--a multiple sequence alignment editor and analysis workbench. *Bioinformatics* 25, 1189–1191.

West, L.E., and Gozani, O. (2011). Regulation of p53 function by lysine methylation. *Epigenomics* 3, 361–369.

Windisch, M.P., Frese, M., Kaul, A., Trippler, M., Lohmann, V., and Bartenschlager, R. (2005). Dissecting the interferon-induced inhibition of hepatitis C virus replication by using a novel host cell line. *Journal of Virology* 79, 13778–13793.

Woerz, I., Lohmann, V., and Bartenschlager, R. (2009). Hepatitis C virus replicons: dinosaurs still in business? *Journal of Viral Hepatitis* 16, 1–9.

Xu, S., Wu, J., Sun, B., Zhong, C., and Ding, J. (2011). Structural and biochemical studies of human lysine methyltransferase Smyd3 reveal the important functional roles of its post-SET and TPR domains and the regulation of its activity by DNA binding. *Nucleic Acids Research* 39, 4438–4449.

Yanagi, M., Purcell, R.H., Emerson, S.U., and Bukh, J. (1999). Hepatitis C virus: an infectious molecular

clone of a second major genotype (2a) and lack of viability of intertypic 1a and 2a chimeras. *Virology* 262, 250–263.

You, S., and Rice, C.M. (2008). 3' RNA elements in hepatitis C virus replication: kissing partners and long poly(U). *Journal of Virology* 82, 184–195.

Zhao, Q., and Lee, F.S. (1999). Mitogen-activated protein kinase/ERK kinase kinases 2 and 3 activate nuclear factor-kappaB through IkappaB kinase-alpha and IkappaB kinase-beta. *J Biol Chem* 274, 8355–8358.

Zhou, Z., Ren, X., Huang, X., Lu, L., Xu, M., Yin, L., Li, J., and Sha, J. (2005). SMYD3-NY, a novel SMYD3 mRNA transcript variant, may have a role in human spermatogenesis. *Ann Clin Lab Sci* 35, 270–277.

7. APPENDIX

NS5A K240 Consensus sequence alignment

```

Ref.1a.US.77.H77.NC_004102      RGSPSSMASSASQLSAPSLKATCTANHDSP-DAELIEANL
Ref.1a.US.77.HCV-H.M67463      RGSPSSMASSASQLSAPSLKATCTANHDSP-DAELIEANL
Ref.1a.US.x.5003.EF407419      RGSPSSVASSASQLSAPSLKATCTTNHDSP-DAELIEANL
Ref.1a.x.x.LTD6-2-XF224.AF511950  RGSPSSSEASSASQLSAPSLKATCTANHDSP-DAELIEANL
Ref.1b.BR.03.BR1427_P1_10-7-03.EF032892  RGSPSSLASSASQLSAPSLKATCTTHHDSP-DADLIEANL
Ref.1b.CN.x.AY587016.AY587016    RGSPSSLASSASQLSAPSLKATCTTHHGAP-DTDLIEANL
Ref.1b.JP.x.JT.D11355          RGSPSSLASSASQLSAPSLKATCTTHHDSP-DADLIEANL
Ref.1c.ID.x.HC-G9.D14853       RGSPSSLASSASQLSAPSLKATCTTHHDSP-DADLITANL
Ref.1c.IN.x.AY051292.AY051292    RGSPSSLASSASQLSAPSLKATCTTHHDSP-DADLIEANL
Ref.1g.ES.x.1804.AM910652      RGSPSSLASSASQLSAPSLKATCTTHHDSP-DADLIEANL
Ref.2a.JP.x.AY746460.AY746460    RGSPSEASSASQLSAPSLRATCTTYGRAH-DVDMVDANL
Ref.2a.JP.x.HC-J6.D00944       RGSPSEASSASQLSAPSLRATCTTHGKAY-DVDMVDANL
Ref.2a.JP.x.JFH-1.AB047639     RGSPSEASSASVSQLSAPSLRATCTTHSNTY-DVDMVDANL
Ref.2b.JP.x.HC-J8.D10988       RGSPSQASSASQLSAPSLKATCTTHKTAY-DCDMVDANL
Ref.2b.x.x.JPUT971017.AB030907  RGSPSQASSASQLSAPSLKATCTTHKTAY-DCDMVDANL
Ref.2b.x.x.MD2B-1.AF238486     RGSPSQASSASQLSAPSLKATCTTHKMAY-DCDMVDANL
Ref.2c.x.x.BEBE1.D50409       RGSPSAASSASQLSAPSLRATCTTHAKCP-DIDMVDANL
Ref.2i.VN.x.D54.DQ155561      RGSPSEASSASQLSAPSLRATCTTHARNM#HIDMVDANL
Ref.2j.VE.05.C1292.HM777359    RGSPSEASSASQLSAPSLRATCTTHGGGP-DIDMVDANL
Ref.2j.VE.06.C1799.HM777358    RGSPSEASSASQLSAPSLRATCTTHGRGP-DIDMVDANL
Ref.2k.MD.x.VAT96.AB031663     RGSPSEASSASQLSAPSLRATCTAHAKNY-AVEMVDANF
Ref.2q.ES.01.852.FN666429     RGSPSEASSASQLSAPSLRATCTTHGKNY-DIDMVDANL
Ref.2q.ES.02.963.FN666428     RGSPSEASSASQLSAPSLRATCTTHGKNY-DIDMVDANL
Ref.3a.DE.x.HVCENS1.X76918     RGSPSEASSASQLSAPSLKATCQTHRPHP-DAELVDANL
Ref.3a.x.x.CB.AF046866        RGSPSEASSASQLSAPSLKATCQTHRPHP-DAELVNANL
Ref.3a.x.x.NZL1.NC_009824     RGSPSEASSASQLSAPSLKATCQTHRPHP-DAELVDANL
Ref.3b.JP.x.HCV-Tr.D49374      RGSPSEASSASQLSAPSLKATCQTHRPHP-DAELIDANL
Ref.3i.IN.02.IND-HCV-3i.FJ407092  RGSPSEASSASQLSAPSLKATCETHGPH-DVELIDANL
Ref.3k.ID.x.JK049.D63821      RGSPSSLASSASQLSAPSLKATCTTHGRHP-DAELITANL
Ref.4a.EG.x.ED43.Y11604       RGSPSSLASSASQLSAPSLKATCTAPHDSP-GTDLLEANL
Ref.4a.US.x.F7157.DQ418788     RGSPSSLASSASQLSAPSLKATCTAHDSP-GTDLLEANL
Ref.4b.CA.x.QC264.FJ462435     RGSPSSLASSASQLSAPSLKATCTAHDSP-DADLIEANL
Ref.4b.PT.x.P026.FJ025854     RGSPSSLASSASQLSAPSLKATCTAHDSP-DADLIEANL
Ref.4b.PT.x.P212.FJ025855     RGSPSEASSASQLSAPSLKATCTTNHHSX-DADLIEANL
Ref.4b.PT.x.P245.FJ025856     RGSPSEASSASQLSAPSLKATCTTNHHSX-DADLIEANL
Ref.4c.CA.x.QC381.FJ462436     RGSPSSLASSASQLSAPSLKATCAA#DSP-GTDLLEANL
Ref.4d.CA.x.QC382.FJ462437     RGSPSSLASSASQLSAPSLKATCTDHKDSP-GVDLLEANL
Ref.4d.ES.x.24.DQ516083       RGSPSSLASSASQLSAPSLKATCAHXHYSL-GVDLLEANL
Ref.4d.US.x.03-18.DQ418786     RGSPSSLASSASQLSAPSLKATCTDHKDSP-GVDLIESNL
Ref.4d.x.x.PS2.EU392172       RGSPSSLASSASQLSAPSLKATCTDHKDSP-GVDLLEANL
Ref.4f.FR.x.IFBT84.EF589160    RGSPSSLASSASQLSAPSLKATCPAHHSSP-GQDLLEANL
Ref.4f.FR.x.IFBT88.EF589161    RGSPSSLASSASQLSAPSLKATCTAHHSSP-GQDLLEANL
Ref.4f.x.x.CM.DAV9905.EU392169  RGSPSSLASSASQLSAPSLKATCTAHHSSP-GQDLLEANL
Ref.4f.x.x.CM.SP1578.EU392170  RGSPSSLASSASQLSAPSLKATCTAHHSSP-GQDLLEANL
Ref.4f.x.x.PS4.EU392174       RGSPSSLASSASQLSAPSLKATCTAHHSSP-GLDLLEANL
Ref.4f.x.x.PS6.EU392175       RGSPSSLASSASQLSAPSLKATCAAHDSP-GQDLLEANL
Ref.4g.CA.x.QC193.FJ462432     RGSPSSLASSASQLSAPSLKATCTAHQDSP-DADLIEANL
Ref.4k.CA.x.QC383.FJ462438     RGSPSSLASSASQLSAPSLKATCTTHHESP-DADLIEANL
Ref.4k.x.x.PB65185.EU392171    RGSPSSLASSASQLSAPSLKATCTTHHESP-DADLIEANL
Ref.4k.x.x.PS3.EU392173       RGSPSSLASSASQLSAPSLKATCTTHHESP-DADLIEANL
Ref.4l.CA.x.QC274.FJ839870     RGSPSSLASSASQLSAPSLKATCAAHDSP-GNDLIEANL
Ref.4m.CA.x.QC249.FJ462433     RGSPSSLASSASQLSAPSLKATCPADHDS-GADLIEANL
Ref.4n.CA.x.QC97.FJ462441     RGSPSSLASSASQLSAPSLKATCAXHDS-GTDLIESNL
Ref.4o.CA.x.QC93.FJ462440     RGSPSSLASSASQLSAPSLKATCAAHD#A#-GSDLIEANL
Ref.4p.CA.x.QC139.FJ462431     RGSPSSLASSASQLSAPSLKATCPANHDS-GTDLIEANL
Ref.4q.CA.x.QC262.FJ462434     RGSPSSLASSASQLSAPSLKATCTQHDS-GTDLIEANL
Ref.4r.CA.x.QC384.FJ462439     RGSPSSLASSASQLSAPSLKATCTAHDSP-DADLIEANL
Ref.4t.CA.x.QC155.FJ839869     RGSPSSLASSASQLSAPSLKATCPADHDS-GTDLIEANL
Ref.4v.CY.05.CYHCV048.HQ537008  RGSPSSLASSASQLSAPSLKATCTAHDSP-GADLIEANL
Ref.4v.CY.06.CYHCV073.HQ537009  RGSPSSLASSASQLSAPSLKATCTAHXDS-GAXLIEANL
Ref.5a.GB.x.EUH1480.NC_009826   RGSPSSLANSSASQLSAPSLKATCTIQGHHP-DADLIKANL
Ref.5a.ZA.x.SA13.AF064490     RGSPSSLASSASQLSAPSLKATCTTQGHHP-DADLIEANL
Ref.6.CN.x.GZ52557.DQ278892    RGSPSSLASSASQLSAPSLKATCTSTNCVHP-DAELISANL
Ref.6a.HK.x.6a33.AY859526     RGSPSSLASSASQLSAPSLKATCTTSKDH-DMELIEANL
Ref.6a.HK.x.6a35.DQ480513     RGSPSSLASSASQLSAPSLKATCTTSKDH-DMELIEANL

```


NS5A K378 Consensus sequence alignment

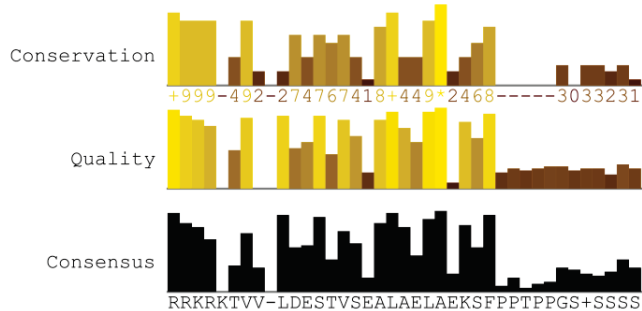
```

Ref.1a.US.77.H77.NC.004102      RKKR-TVV-LTESTLSTALAEELATKSF-----GSSSTSG
Ref.1a.US.77.HCV-H.M67463       RKKR-TVV-LTESTLPTALAEELATKSF-----GSSSTSG
Ref.1a.US.x.5003.EF407419       RKKR-TVV-LTESTVSTALAEELATKSF-----GSSSTSG
Ref.1a.x.x.LTD6-2-XF224.AF511950 RKKR-TVV-LTESTVSTALAEELATKSF-----GSSSTSG
Ref.1b.BR.03.BR1427.P1.10-7-03.EF032892 RRRK-TVV-LTESTVSSALAEELATKTF-----GSSESSA
Ref.1b.CN.x.AY587016.AY587016   RRRK-TVV-LTESTVSSALAEELATKTF-----GSSGSSA
Ref.1b.JP.x.JT.D11355           RKKR-TVV-LTESTVSSALAEELATKTF-----GSSGSSA
Ref.1c.ID.x.HC-G9.D14853        RRRK-TVV-LDESTVSSALAEELATKTF-----GSSTTSG
Ref.1c.IN.x.AY051292.AY051292   RRRK-TVV-LDESTVSSALAEELATKTF-----GSSTTSG
Ref.1g.ES.x.1804.AM910652       RRRK-QVI-LTESTVSAALAEELAEKSF-----GQSTTSG
Ref.2a.JP.x.AY746460.AY746460   RRRR-TVG-LSESVVAEALQQLAIKSFQ-PPPSGNSGL
Ref.2a.JP.x.HC-J6.D00944        RRRR-TVG-LSESSIADALQQLAIKSFQ-PPPSGDSGL
Ref.2a.JP.x.JFH-1.AB047639      RRRR-TVG-LSESTISEALQQLAIKTFQ-PPSSGDAGS
Ref.2b.JP.x.HC-J8.D10988        RRRR-AKV-LTQDNVEGVIREMADKVLSP-LQDNDSGH
Ref.2b.x.x.JPUT971017.AB030907  RRRR-ARV-LTQDNVEGVIREMADKVLSP-LQDTNDSGH
Ref.2b.x.x.MD2B-1.AF238486       RRRR-AKV-LTQDNVEGVIREMANKVLSP-LQDHNDSGH
Ref.2c.x.x.BEBE1.D50409         RRRR-AVV-LDQSNVGEALKEELAIKSGC-PPPSGDPGH
Ref.2i.VN.x.D54.DQ155561        RRRR-TVA-LDQSTVGEALRELAIKAF-----GQPPPSG
Ref.2j.VE.05.C1292.HM777359     RRRR-AIV-LDQSTVGEALKEELAIKSF-----GQPPPSD
Ref.2j.VE.06.C1799.HM777358     RRRR-AIV-LDQSNVGEALKEELAIKSF-----GQPPPSD
Ref.2k.MD.x.VAT96.AB031663       RRRR-ALV-LSQSNVGEALQALAIKSFQ-LPPSCDSGR
Ref.2q.ES.01.852.FN666429       RRRR-AIV-LSQDNVGGALMDLARRSF-----GHPPPSG
Ref.2q.ES.02.963.FN666428       RRRR-AIV-LDQSNVGEALMQLAHQSF-----GQSLPSG
Ref.3a.DE.x.HCVCENS1.X76918     RRRK-TIQ-LDGSNVSAALAEELAKKSFPSVNPQDENSSS
Ref.3a.x.x.CB.AF046866          RRRK-TIQ-LDGSNVSAALRALAEKSFPSLKPQEENSSS
Ref.3a.x.x.NZL1.NC.009824       RRRK-TIQ-LDGSNVSAALAEELAKKSFPSKPKQEENSSS
Ref.3b.JP.x.HCV-Tr.D49374       RRRK-TIK-LDGSNVSAALAEELAEKSFSTKPEGTSSS
Ref.3i.IN.02.IND-HCV-3i.FJ407092 RKKR-TVQ-LDGSNVSAALRALAEKSF-----PSSGLQE
Ref.3k.ID.x.JK049.D63821        RRRK-TIV-LSESTVSKALASLAEKSFQPTCSAEDEST
Ref.4a.EG.x.ED43.Y11604         RRRK-TVQ-LTESVSVSTALAEELAAKTFGQ--SEPSDRD
Ref.4a.US.x.F7157.DQ418788       RRRK-TVQ-LTESVSVSTALAEELAAKTFGQ--SELGSDSG
Ref.4b.CA.x.QC264.FJ462435       RRRK-MVA-LTESNVSEALAEELAIKXF-----GQPAADA
Ref.4b.PT.x.P026.FJ025854       RRRK-VVA-LSESNVSSALAEELAAKTF-----GQPDAD
Ref.4b.PT.x.P212.FJ025855       RRRK-AIV-LTESXVSSALADLAAKVL-----SQPDADV
Ref.4b.PT.x.P245.FJ025856       RRRK-AIA-LTESNVSSALADLAAKAF-----SQPSADV
Ref.4c.CA.x.QC381.FJ462436       RRRK-VVA-LDGSNISNALADLAVKTF-----GQSGLSG
Ref.4d.CA.x.QC382.FJ462437       RRRK-AVA-LSESNISAALASLADKTF-----XQPAVSS
Ref.4d.ES.x.24.DQ516083         RRRK-TVA-LSESNISAALASLADKTFGQ--PAASSDSG
Ref.4d.US.x.03-18.DQ418786       RRRK-AVV-LSESNISAALASLADKTFSQ--PGVSSDSG
Ref.4d.x.x.PS2.EU392172         RRRK-AVA-LSESNISAALASLADKTF-----GQPVVSS
Ref.4f.FR.x.IFBT84.EF589160      RKKK-TVV-LSEATVSDALADLAAKSF-----GRPESEP
Ref.4f.FR.x.IFBT88.EF589161      RKKK-TVV-LSESTVSDALADLAAKSF-----GRPESEP
Ref.4f.x.x.CM.DAV9905.EU392169   RKKK-TVV-LSESTVSEALADLAAKSF-----GRPESES
Ref.4f.x.x.CM.SP1578.EU392170    RKKK-TVV-LSESTVSEALADLAAKSF-----GCPSESEP
Ref.4f.x.x.PS4.EU392174         RKKK-TVV-LSESTVSDALADLAAKSF-----GRPESET
Ref.4f.x.x.PS6.EU392175         RKKK-TVV-LSESTVSEALADLAAKSF-----GHPESEP
Ref.4g.CA.x.QC193.FJ462432       RRRK-TVV-LTESVSEALAEELATKSF-----GSSTQDT
Ref.4k.CA.x.QC383.FJ462438       RRRK-AVV-LTESSVSSALAEELAAKSF-----GTTXPSA
Ref.4k.x.x.PB65185.EU392171      RRRK-AVV-LTESSVSSALAEELAAKSF-----GTTEPSA
Ref.4k.x.x.PS3.EU392172         RRRK-AVV-LTESSVSNALAEELAAKSF-----GTTEPSA
Ref.4l.CA.x.QC274.FJ839870       RRRK-AIV-LTESNVAGALADLAAKTF-----GEPELSS
Ref.4m.CA.x.QC249.FJ462433       RRRK-AVV-LSESVISSALADLAAKSF-----SQSGAES
Ref.4n.CA.x.QC97.FJ462441       RRRK-TVV-LSESTVSSALAEELAEKSF-----SSASPDS
Ref.4o.CA.x.QC93.FJ462440       RRRK-TVI-LDESTVSNALADLAVKAF-----GRSEPDS
Ref.4p.CA.x.QC139.FJ462431       RRRK-MVA-LSESVISSALADLAAKSF-----GQQAES
Ref.4q.CA.x.QC262.FJ462434       RRRK-TVV-LTESKVAEALSDLAAKTF-----SQAESSH
Ref.4r.CA.x.QC384.FJ462439       RRRK-TVV-LSESSVSDALAEELAAKSF-----GRSEPDT
Ref.4t.CA.x.QC155.FJ839869       RRRK-TVV-LSESVISDTLADLAVKSF-----GPPKAET
Ref.4v.CY.05.CYHCV048.HQ537008  RKRT-VVP--TESSVAQAPSDLAKTSF-----SRGPPTS
Ref.4v.CY.06.CYHCV073.HQ537009  RKRT-VVL--TDSNVARALSDLAEASF-----NRGPPTS
Ref.5a.GB.x.EUH1480.NC.009826    RRRKRPME-LSDSTVSVQVMDLADARFKV-DTPSIEGQD
Ref.5a.ZA.x.SA13.AF064490        RRRKRPVV-LSDSNVSVQLADLAHAREKA-DTQSIQD
Ref.6.CN.x.GZ52557.DQ278892     RRRK-LIR-LDES RVAQALAEELASRAF-STPPEQPDNS
Ref.6a.HK.x.6a33.AY859526       RRRK-LVH-LDESTVSRALAQADKVFVEGSDPSPSSD
Ref.6a.HK.x.6a35.DQ480513       RRRK-LVH-LDESTVSHALAQADKVFVEGSDPSPSSD

```

Ref. 6a.HK.x.EUHK2.Y12083
 Ref. 6b.x.x.Th580.NC 009827
 Ref. 6c.TH.x.Th846.EF424629
 Ref. 6d.VN.x.VN235.D84263
 Ref. 6e.CN.x.GX004.DQ314805
 Ref. 6e.US.x.537798.EU408326
 Ref. 6e.VN.x.D42.EU246931
 Ref. 6e.VN.x.D88.EU246932
 Ref. 6f.TH.x.C-0044.DQ835760
 Ref. 6f.TH.x.C-0046.DQ835764
 Ref. 6f.TH.x.TH52.EU246936
 Ref. 6g.HK.x.HK6554.DQ314806
 Ref. 6g.ID.x.JK046.D63822
 Ref. 6h.VN.x.VN004.D84265
 Ref. 6i.TH.x.C-0159.DQ835762
 Ref. 6i.TH.x.TH24.EU246935
 Ref. 6i.TH.x.TH602.DQ835770
 Ref. 6j.TH.x.C-0667.DQ835761
 Ref. 6j.TH.x.Th553.DQ835769
 Ref. 6k.CN.x.KM41.DQ278893
 Ref. 6k.CN.x.KM45.DQ278891
 Ref. 6k.VN.x.VN405.D84264
 Ref. 6l.US.x.537796.EF424628
 Ref. 6l.VN.x.D33.EU246933
 Ref. 6m.TH.x.C-0185.DQ835765
 Ref. 6m.TH.x.C-0192.DQ835766
 Ref. 6m.TH.x.C-0208.DQ835763
 Ref. 6n.CN.x.KM42.AY878652
 Ref. 6n.TH.x.TH22.EU246937
 Ref. 6n.TH.x.TH31.EU246938
 Ref. 6o.CA.x.QC227.EF424627
 Ref. 6o.US.x.535318.EU408327
 Ref. 6o.VN.x.D85.EU246934
 Ref. 6p.CA.x.QC216.EF424626
 Ref. 6q.CA.x.QC99.EF424625
 Ref. 6r.CA.x.QC245.EU408328
 Ref. 6s.CA.x.QC66.EU408329
 Ref. 6t.VN.x.D49.EU246939
 Ref. 6t.VN.x.TV241.EF632069
 Ref. 6t.VN.x.TV249.EF632070
 Ref. 6t.VN.x.VT21.EF632071
 Ref. 6u.CN.x.DH012.EU408330
 Ref. 6u.CN.x.DH014.EU408331
 Ref. 6u.CN.x.DH028.EU408332
 Ref. 6u.VN.x.D83.EU246940
 Ref. 6v.CN.04.NK46.EU158186
 Ref. 6v.CN.x.KM046.EU798761
 Ref. 6v.CN.x.KM181.FJ435090
 Ref. 6v.CN.x.KMN-02.EU798760
 Ref. 6w.TW.x.HCV-6-D140.EU643834
 Ref. 6w.TW.x.HCV-6-D370.EU643836
 Ref. 7a.CA.x.QC69.EF108306

RRKR-LVH-LDESTVSHALQQLADKVFVESSNDPGPSSD
 RRRK-LIQ-LDESAVSQALQQLADKVFVEDTSTSEPSGG
 RRRK-VVK-LDEATAEKVLADLAKKAFTPSSQSSQEESG
 RRRK-VVQ-LDEGSAKRALAELAQTSFPPSTATLSEDSG
 RRRK-VVK-LDESAAAEALAEARKSF-PLNPSEPEESG
 RRRK-VIQ-LDESAAVEALAKMAQKSF-----PSXPSEP
 RRRK-VVQ-LDESAAAEALAEARKSF-----PPDPSKS
 RRRK-VVR-LDESTAAEALAEARKSF-----PSDPSEP
 RRRK-TVL-LDSSTVSQLAELAQKSFPEGSTASXAESG
 RRRK-TVL-LDSSTVSQLAELAQKSFPEGSTASRAESG
 RRRK-TVL-LDSSTVSQLAELAQKSF-----PEGSTAS
 RRRK-LVQ-LDDSVVGHVLAQLAEKSF-PATPDQPHNS
 RRRK-LVQ-LDDSVVGHVLAQLAEKSF-PATPDQPQNS
 RRRK-LVQ-LDSSNVSAALQLAAKTF-ETPSSPTTGYG
 RRRK-VVQ-LDASNVTVLAQLAEKTF-PQPASLTGCG
 RRRK-VVQ-LDASNVTVLAQLAEKTF-----PQPASLT
 RRRK-VVQ-LDASNVTVLAQLAEKTF-PQPASLTGTYG
 RRRK-MXQ-LDSSNVTTVLAQLAEKTX-PQPVSSTGYG
 RRRK-LXQ-XDSSNVSTVLAQLAEKTF-PQPVSSTGYG
 RRRK-VVR-LDESSVVEALADLAKKSF-PTQPSPSTDSD
 RRRK-VVH-LDDSSVAEALAEARKSF-PTQPSPSTDSD
 RRRK-VVH-LDDSTVQALAEKSF-PTPSTSTDPD
 RRRK-VVH-LDDSTVQALAEKSF-----PTPSTTA
 RRRK-VVQ-LDQSTVALAQLAEKTF-PASSLPSTDQD
 RRRK-VVQ-LDRSTVALAQLAEKTF-----PASPPPS
 RRRK-VVQ-LDQSTVTLAQLAEKTF-PASSPPSTDQD
 RRRK-TIH-LDQSTLALAEKSF-PTPSSSTDPD
 RRRK-TIH-LDQSTLPLAQLAEKSF-----PTPSSSS
 RRRK-TIH-LDQSTLSLAQLAEKSF-----PTPSSSS
 RRRK-VVR-LNESSVSTALAEARKSFPPPSAQSQESSG
 RRRK-VVR-LDESSVSSALAEARKSF-----PPPSTQS
 RRRK-VVR-LDESSVSTALAEARKSF-----PPPSAQ
 RRRK-VVQ-LDESSVQALAEKTFPSSSASSQGDG
 RRRK-VVQ-LDESSASAAALAEKAFPPDGSQSQAESG
 RRRK-MVQ-LDSSTVQVLAELAQKSF-----PESSAAS
 RRRK-MVX-LDESSVSAALAEKSF-----PPETTSS
 RRRK-VVQ-LDSSAAAAALAEARKSF-----PPEPLDS
 RRRK-VVQ-XNDSAAAAALAEARKSF-----PPXXLDS
 RRRK-VVQ-LDSSAAAAALAEARKCF-----PSETIDS
 RRRK-VVQ-LDSSAAAAALAEARKSF-----PPEPLDS
 RRRK-LVR-LDESTVAAALAEKSF-----PTTSTGS
 RRRK-LVR-LDESTVAAALAEKSF-----PTTSTGS
 RRRK-LVR-LDESTVAAALAEKSF-----PTTSTGS
 RRRK-VVQ-LDESTASAAALAEARKLF-----PSGPSEE
 RRRK-LIR-LDDSTVQALAEKPF-----SHSDTTP
 RRRK-LIR-LDDSTVQALAEKPF-----SHSDTTP
 RRRK-PIR-LDDSTVQALAEKTF-----SRSDTTP
 RRRK-PIR-LDDSTVQALAEKTF-----SRSDTTP
 RRRK-LIR-LDESVAQALAEKSF-----QPSPEQA
 RRRK-LIR-LDESSVAQALAEKSF-----QTTPEQA
 RRRK-AVIQLTESAVSTALAEKSF---PKEEAPPSD



NS5A P417 P418 Consensus sequence alignment

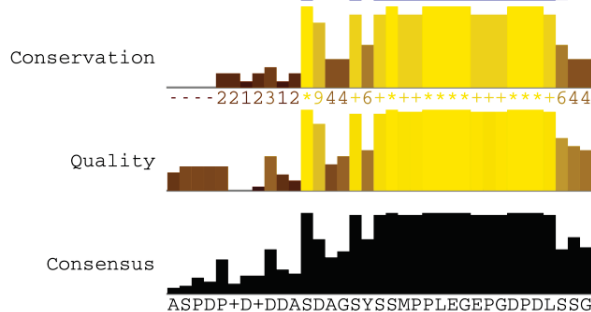
```

Ref. 1a.US.77.H77.NC_004102      ----PSGCPPDSDVESYSSMPLEGEFGDPLSDG
Ref. 1a.US.77.HCV-H.M67463      ----PSGCPPDSDVESYSSMPLEGEFGDPLSDG
Ref. 1a.US.x.5003.EF407419      ----PSDRSPDSDAGSCSSMPLEGEFGDPLSDG
Ref. 1a.x.x.LTD6-2-XF224.AF511950 ----PSGCPPDSDTESYSSMPLEGEFGDPLSDG
Ref. 1b.BR.03.BR1427_P1_10-7-03.EF032892 ----SNNGDTGSDVESYSSMPLEGEFGDPLSDG
Ref. 1b.CN.x.AY587016.AY587016 ----SAEGDAGSDAESYSSMPLEGEFGDPLSDG
Ref. 1b.JP.x.JT.D11355          ----SDDGDKESDVESYSSMPLEGEFGDPLSDG
Ref. 1c.ID.x.HC-G9.D14853       ----SCDGELDSEAESYSSMPLEGEFGDPLSDG
Ref. 1c.IN.x.AY051292.AY051292 ----SCGGELDSEAESYSSMPLEGEFGDPLSDG
Ref. 1g.ES.x.1804.AM910652      ----PREADAGSEAESYSSMPLEGEFGDPLSDG
Ref. 2a.JP.x.AY746460.AY746460 ----PPDELALSETGSTSSMPLEGEFGDPLEPE
Ref. 2a.JP.x.HC-J6.D00944       ----PPDELALSETGSTSSMPLEGEFGDPLEPE
Ref. 2a.JP.x.JFH-1.AB047639     ----SPGEPAPSETGSASSMPLEGEFGDPLESD
Ref. 2b.JP.x.HC-J8.D10988       ----PSDETAASEAGSLSSMPLEGEFGDPLEFE
Ref. 2b.x.x.JPUT971017.AB030907 ----PSGETAASDAGSLSSMPLEGEFGDPLEFE
Ref. 2b.x.x.MD2B-1.AF238486     ----PSDETAASDTGSLSSMPLEGEFGDPLEFD
Ref. 2c.x.x.BEBE1.D50409        ----PPDEPDDSEAGSVSSMPLEGEFGDPLEPE
Ref. 2i.VN.x.D54.DQ155561       ANQTTSNESADSETGSMSSMPLEGEFGDPLEPG
Ref. 2j.VE.05.C1292.HM777359   TNQTIPEESIDSETDSLSSMPLEGEFGDPLENE
Ref. 2j.VE.06.C1799.HM777358   TNQTIPEESIDSETDSLSSMPLEGEFGDPLENG
Ref. 2k.MD.x.VAT96.AB031663     ----ALKESTDSEAGSDSSMPLEGEFGDPLESG
Ref. 2q.ES.01.852.FN666429     PGDIPTGESVDSETGVSMPLEGEFGDPLEPE
Ref. 2q.ES.02.963.FN666428     PRDIPDES DAS ETGSISSMPLEGEFGDPLEXEPE
Ref. 3a.DE.x.HCVCENS1.X76918   ----PPSPGGESDSESCSSMPLEGEFGDPLSCD
Ref. 3a.x.x.CB.AF046866        ----PPSPGGESDSESCSSMPLEGEFGDPLSCD
Ref. 3a.x.x.NZL1.NC_009824     ----PPSPGGESDSESCSSMPLEGEFGDPLSCD
Ref. 3b.JP.x.HCV-Tr.D49374     ----SPETGEESDVESYSSMPLEGEFGDPLDAD
Ref. 3i.IN.02.IIND-HCV-3i.FJ407092 ----GSTDLPKADGGSDTESCSSMPLEGEFGDPLSCD
Ref. 3k.ID.x.JK049.D63821      ----VQLDDDDSDNESHSMPLEGEFGDPLSSG
Ref. 4a.EG.x.ED43.Y11604       ----PIVVDDASDDGSYSSMPLEGEFGDPLTSD
Ref. 4a.US.x.F7157.DQ418788     ----PITVDDASDDGSYSSMPLEGEFGDPLTSD
Ref. 4b.CA.x.QC264.FJ462435    -TPDSPDAXDKSDDGSFSSMPLEGEFGDPLTSD
Ref. 4b.PT.x.P026.FJ025854     -#GSFHRGR*#SDDGSFSSMPLEGEFGDPLTSD
Ref. 4b.PT.x.P212.FJ025855     -TPDPPIADDRSDDGSFSSMPLEGEFGDPLTSD
Ref. 4b.PT.x.P245.FJ025856     -TPDPPIADDRSDDGSFSSMPLEGEFGDPLTSD
Ref. 4c.CA.x.QC381.FJ462436    -DSGPFVVDDQSDDGSYSSMPLEGEFGDPLTSD
Ref. 4d.CA.x.QC382.FJ462437    -EPDPPIVDDKSDDGSYSSMPLEGEFGDPLTSD
Ref. 4d.ES.x.24.DQ516083       ----SIIVDDKSEDFCLSKPPEGEFGDPLTSD
Ref. 4d.US.x.03-18.DQ418786    ----PIIVDDKSEDFSSMPLEGEFGDPLTSD
Ref. 4d.x.x.PS2.EU392172       -EPDPPIADDDKSDDESYSMPLEGEFGDPLTSD
Ref. 4f.FR.x.IFBT84.EF589160   -DSSPPIADDDKSDDGSYSSMPLEGEFGDPLTSD
Ref. 4f.FR.x.IFBT88.EF589161   -DSGPIVADDDKSDDGSYSSMPLEGEFGDPLTSD
Ref. 4f.x.x.CM_DAV9905.EU392169 -DSGPIVADDDKSDDGSYSSMPLEGEFGDPLTSD
Ref. 4f.x.x.CM_SP1578.EU392170 -ESDPPIVDDKSDDGSYSSMPLEGEFGDPLTSD
Ref. 4f.x.x.PS4.EU392174       -DSGPIVADDDKSDDGSYSSMPLEGEFGDPLTSD
Ref. 4f.x.x.PS6.EU392175       -DSGPIVADDDKSDDGSYSSMPLEGEFGDPLTSD
Ref. 4g.CA.x.QC193.FJ462432    -KPDSSSEADNQSDDGSYSSMPLEGEFGDPLTSD
Ref. 4k.CA.x.QC383.FJ462438    -EPDPPIADDDQSDGESYSSMPLEGEFGDPLTSD
Ref. 4k.x.x.PB65185.EU392171   -EPDPLIADDDQSDGESYSSMPLEGEFGDPLTSD
Ref. 4k.x.x.PS3.EU392173       -EPDPPNADDQSDGESYSSMPLEGEFGDPLTSD
Ref. 4l.CA.x.QC274.FJ839870     -GPEPEIIDDKSDNESFSSMPLEGEFGDPLASD
Ref. 4m.CA.x.QC249.FJ462433    -EPDPPIVDDRSDDESYSSMPLEGEFGDPLGSD
Ref. 4n.CA.x.QC97.FJ462441     -EPDPVIVDDRSDDGSFSSMPLEGEFGDPLTAD
Ref. 4o.CA.x.QC93.FJ462440     -DPGPIVDDQSDDGSYSSMPLEGEFGDPLTTD
Ref. 4p.CA.x.QC139.FJ462431    -DPAPIVDDASDDGSYSSMPLEGEFGDPLTSD
Ref. 4q.CA.x.QC262.FJ462434    -RPDPPIVDDASDDGSYSSMPLEGEFGDPLTSD
Ref. 4r.CA.x.QC384.FJ462439    -QGPSPTEESDKESYSSMPLEGEFGDPLTED
Ref. 4t.CA.x.QC155.FJ839869    -DPGFTTVDDASDDGSYSSMPLEGEFGDPLTSD
Ref. 4v.CY.05.CYHCV048.HQ537008 -EPDPPIVDDRSDDGSFSSMPLEGEFGDPLTSD
Ref. 4v.CY.06.CYHCV073.HQ537009 -EPDPPIVDDKSDDGSFSSMPLEGEFGDPLTSD
Ref. 5a.GB.x.EUH1480.NC_009826   ----EKRDDNSDAASYSSMPLEGEFGDPLSSG
Ref. 5a.ZA.x.SA13.AF064490     ----EKRDDDDSDAASYSSMPLEGEFGDPLSSG
Ref. 6.CN.x.GZ52557.DQ278892   ----HDAEGETSDVDSYSSMPLEGEFGDPLSSG
Ref. 6a.HK.x.6a33.AY859526     ----TTPDDACSEAESYSSMPLEGEFGDPLSSG
Ref. 6a.HK.x.6a35.DQ480513     ----TTPDDACSEAESYSSMPLEGEFGDPLSSG

```

Ref. 6a.HK.x.EUHK2.Y12083
 Ref. 6b.x.x.Th580.NC_009827
 Ref. 6c.TH.x.Th846.EF424629
 Ref. 6d.VN.x.VN235.D84263
 Ref. 6e.CN.x.GX004.DQ314805
 Ref. 6e.US.x.537798.EU408326
 Ref. 6e.VN.x.D42.EU246931
 Ref. 6e.VN.x.D88.EU246932
 Ref. 6f.TH.x.C-0044.DQ835760
 Ref. 6f.TH.x.C-0046.DQ835764
 Ref. 6f.TH.x.TH52.EU246936
 Ref. 6g.HK.x.HK6554.DQ314806
 Ref. 6g.ID.x.JK046.D63822
 Ref. 6h.VN.x.VN004.D84265
 Ref. 6i.TH.x.C-0159.DQ835762
 Ref. 6i.TH.x.TH24.EU246935
 Ref. 6i.TH.x.Th602.DQ835770
 Ref. 6j.TH.x.C-0667.DQ835761
 Ref. 6j.TH.x.Th553.DQ835769
 Ref. 6k.CN.x.KM41.DQ278893
 Ref. 6k.CN.x.KM45.DQ278891
 Ref. 6k.VN.x.VN405.D84264
 Ref. 6l.US.x.537796.EF424628
 Ref. 6l.VN.x.D33.EU246933
 Ref. 6m.TH.x.C-0185.DQ835765
 Ref. 6m.TH.x.C-0192.DQ835766
 Ref. 6m.TH.x.C-0208.DQ835763
 Ref. 6n.CN.x.KM42.AY878652
 Ref. 6n.TH.x.TH22.EU246937
 Ref. 6n.TH.x.TH31.EU246938
 Ref. 6o.CA.x.QC227.EF424627
 Ref. 6o.US.x.535318.EU408327
 Ref. 6o.VN.x.D85.EU246934
 Ref. 6p.CA.x.QC216.EF424626
 Ref. 6q.CA.x.QC99.EF424625
 Ref. 6r.CA.x.QC245.EU408328
 Ref. 6s.CA.x.QC66.EU408329
 Ref. 6t.VN.x.D49.EU246939
 Ref. 6t.VN.x.TV241.EF632069
 Ref. 6t.VN.x.TV249.EF632070
 Ref. 6t.VN.x.VT21.EF632071
 Ref. 6u.CN.x.DH012.EU408330
 Ref. 6u.CN.x.DH014.EU408331
 Ref. 6u.CN.x.DH028.EU408332
 Ref. 6u.VN.x.D83.EU246940
 Ref. 6v.CN.04.NK46.EU158186
 Ref. 6v.CN.x.KM046.EU798761
 Ref. 6v.CN.x.KM181.FJ435090
 Ref. 6v.CN.x.KMN-02.EU798760
 Ref. 6w.TW.x.HCV-6-D140.EU643834
 Ref. 6w.TW.x.HCV-6-D370.EU643836
 Ref. 7a.CA.x.QC69.EF108306

---TTPEDAGSEAEYSMPPLEGEPPDLSSG
 ---TTADDTCS DAGSFSSMPPLEGEPPDLSTG
 ---LEGADGVSDDGSYDMPPPLEGEPPDLDSA
 ---READRASDDGSYSSMPPLEGEPPDLSSG
 ---SDEPDAHSDAGSYSSMPPLEGEPPDLSSG
 ETPTSDKPDHSDAGSYSSMPPLEGEPPDLSSG
 ESPVSDGPDSESDAGSYSSMPPLEGEPPDLSSG
 ETPTSDEPDAHSDAGSYSSMPPLEGEPPDLSSG
 ---LGEDDAGSEAGSFSSMPPLEGEPPDLSSG
 ---LGEDDAGSEAGSFSSMPPLEGEPPDLSSG
 VVPSLGEDDAGSEAGSFSSMPPLEGEPPDLSSG
 ---SAEDDDASDADSYSSMPPLEGEPPDLSEG
 ---SAEDDDASDADSYSSMPPLEGEPPDLSDG
 ---DRDDGVASEAEYSMPPLEGEPPDLSSG
 ---SEEDGAASEADSYSSMPPLEGEPPDLSSG
 SGEQSEEDGAASEADSYSSMPPLEGEPPDLSSG
 ---SEEDGAASEADSYSSMPPLEGEPPDLSSG
 ---SEDDGAASEADSYSSMPPLEGEPPDLSSG
 ---SEDDGAASEADSYSSMPPLEGEPPDLSSG
 ---DEADAASDAGSYSSMPPLEGEPPDLSSG
 ---VEKADAGSDAGSYSSMPPLEGEPPDLSSG
 ---DEGEDTPEAGSYSSMPPLEGEPPDLSSG
 ---GEDAGAASDVEYSMPPLEGEPPDLSSG
 PDDSGEDAGAASDVEYSMPPLEGEPPDLSSG
 ---AGDAERLSEAEYSMPPLEGEPPDLSSG
 SEEAAGDAERLSEAEYSMPPLEGEPPDLSSG
 ---AGDADRLSEAEYSMPPLEGEPPDLSSG
 ---KGDVETFS DAGSYSSMPPLEGEPPDLSSG
 SSEAKGDVETLSDAGSYSSMPPLEGEPPDLSSG
 SSEAKGDVETLSDAGSYSSMPPLEGEPPDLSSG
 ---PNEADTASDAEYSMPPLEGEPPDLSSG
 SPEPPNEADTASDAEYSMPPLEGEPPDLSSG
 SPESPNEADTASDAGSYSSMPPLEGEPPDLSSG
 ---SDDXETASDAGSYSSMPPLEGEPPDLSSG
 ---PDEEDATSEAGSYSSMPPLEGEPPDLSSG
 AVLSPGEDDAGSEAGSFSSMPPLEGEPPDLSSG
 SAVADGPCSDASDDSDCSSMPPLEGEPPDLSSG
 AXPSQVDDIESDAGSYSSMPPLEGEPPDLSSG
 AAXSQVEDDTGSDAGSYSSMPPLEGEPPDLSSG
 AASSQVEDDIESDAGSYSSMPPLEGEPPDLSSG
 AASSQVEDDTESDAGSYSSMPPLEGEPPDLSSG
 PSTPPGDDEAASDAGSYSSMPPLEGEPPDLSSG
 PSTPPGDDEETASDAGSYSSMPPLEGEPPDLSSG
 PPTPPGDDEETASDAGSYSSMPPLEGEPPDLSSG
 ETPTSGEHDAQSDAGSYSSMPPLEGEPPDLSSG
 ASEPDASDGAASDVEYSMPPLEGEPPDLSSG
 ASEPDASDGAASDVEYSMPPLEGEPPDLSSG
 ASEPDASDGATSDVEYSMPPLEGEPPDLSSG
 ASEPDASDGAXSDVEYSMPPLEGEPPDLSSG
 ESPDHDAEEETS DVEDCSSMPPLEGEPPDLSSG
 ESVDHDAEEEPSDADSYSSMPPLEGEPPDLSSG
 ---PSDCDQCSI - SFSSMPPLEGEPPDLSSG



Carol-Ann Eberle

Curriculum Vitae

Personal details:

Address: 101 Chemin de la Salade Ponsan
Contact: Tel: +33 750 820 154; email: eberlec@tcd.ie
Date of Birth: 29.09.1986, Munich, Germany
Nationality: Irish-German joint nationality

Education:

Spring. 2015 (expected) **PhD in molecular biology/virology**
Medical University of Vienna, Austria
As part of the Cell Communication in Health and Disease (CCHD) PhD Program
Thesis title: *Investigating the interaction of the methyltransferase SMYD3 and the HCV non-structural protein NS5A*
Supervisor: Prof. Dr. Giulio Superti-Furga

June 2010 **BA (hons.) in natural science, moderatorship molecular medicine**
University of Dublin, Trinity College, Ireland
Bachelor thesis title: *SAMHD1 – A novel regulator of the innate immune response to DNA?*
Supervisor: Prof. Dr. Andrew Bowie and Dr. Sinéad Keating

Research experience:

June 2014 – now **Post-doctoral researcher, Marie Curie Infection Biology Training Network (INBIONET)**
Sanofi - Therapeutic Strategic Unit for Infectious Disease
Toulouse, France

June 2010 – June 2014 **Doctoral Student in the laboratory of Prof. Dr. Giulio Superti-Furga**
CeMM - Centre for Molecular Medicine of the Austrian academy of Science,
Vienna, Austria

April 2012 – Oct. 2012 **Visiting Scientist at the laboratory of Prof. Ralf Bartenschlager**
Molecular Virology, Department of Infectious Diseases
University of Heidelberg, Germany

Nov. 2009 – Feb. 2010 **Undergraduate Student in the laboratory of Prof. Andrew Bowie**
School of Biochemistry and Immunology
University of Dublin, Trinity College, Ireland

Technical skills:

Molecular Biology:

- *Nucleic acid-based*: PCR, cloning (conventional and gateway recombination cloning), site-directed mutagenesis, in vitro transcription, phenol-chloroform extraction of nucleic acids, mRNA extraction and reverse transcription, agarose gel electrophoresis
- *Protein-based*: In vitro translation, protein precipitation, basic knowledge on expression and

purification of recombinant protein from *E.Coli* using affinity chromatography, SDS PAGE and western blot

- *Protein-protein interactions*: Co-immunoprecipitations, tandem-affinity purification and colocalization studies using immunofluorescence and confocal microscopy
- *Functional assays*: ELISA, firefly-reporter assays, methyltransferase assays, gene expression analysis by qPCR using SYBR Green and Taqman

Cell biology:

- Transient transfection of plasmid DNA or siRNA by lipofection and electroporation
- Generation of stable cell lines
- Generation of isogenic expression cell lines using the Flp-In system from Invitrogen
- Dose – response curves and cell viability assays
- Training in working with radioactive material, in particular tritium and some experience with associated quantification methods such as fluorography and liquid scintillation counting

Virology:

- Experience working in biosafety level 2 and 3 containment facilities
- *HCV*: Experience working with various types of cell culture models of HCV (subgenomic reporter replicons, full-length infectious reporter and non-reporter strains), HCV titer determination by histocytochemistry,
- Methods to quantify HCV
- Viruses used and associated methods for quantification: TCID₅₀ (VSV, EMCV, HSV1, RVFV-Clone 13), focus-forming assays for non-cytolytic viruses (LCMV) and HCV core ELISA
- Flu Minireplicons
- Generation of retroviral and lentiviral particles for stable protein overexpression or shRNA-mediated gene knockdown

Other:

- Languages: fluent German and English (bilingual education), very basic french
- Very good knowledge of Microsoft Office
- Other software: Graphpad, Cytoscape, Inkscape, Gimp, ImageJ, Serial Cloner

Administrative experience:

- Oct. 2013 – Feb. 2014** **Organising committee of the annual CCHD “Bridging the Gap” PhD Symposium**
Responsibilities: Invitation and correspondence with Speakers, distribution and coordination of tasks, organisation of social events
- April 2012 – now** **Member of the sports council at CeMM**
Responsibilities: Organising the participation of CeMM at various team running events, including the annual Vienna City Relay Marathon 2011-2014
- Sept. 2011 – Sept. 2012** **PhD student representative at CeMM**
Responsibilities: Mediating communication between students and principal investigators, assisting first year PhD students

Poster presentations:

- Jan. 2014** **Keystone Symposium “Innate immunity to viral infection”**, Keystone Resort, Colorado, USA
Title: *Investigating the interaction of the methyltransferase SMYD3 with HCV NS5A*
- May 2013** **Gordon Research Conference “Viruses and Cells”**, Barga, Italy
Title: *Investigating the interaction of the methyltransferase SMYD3 with HCV NS5A*
- Jan. 2012** **Keystone Symposium “Chromatin Dynamics”**, Keystone Resort, Colorado, USA
Title: *The role of Chromatin modulators in viral infection*
- May 2011** **Toll2011**, Riva del Garda, Italy
Title: *Epigenetic modulators involved in viral infection*

Publications:

1. **Eberle CA**, Zayas M, Stukalov A, Pichlmair A, Alvisi G, Müller AC, Bennett KL, Bartenschlager R, Superti-Furga G. (2014) The lysine methyltransferase SMYD3 interacts with hepatitis C virus NS5A and is a negative regulator of viral particle production. *Virology*. 2014 Aug;462-463:34-41
2. Pichlmair A, Kandasamy K, Alvisi G, Mulhern O, Sacco R, Habjan M, Binder M, Stefanovic A, **Eberle CA**, Goncalves A, Bürckstümmer T, Müller AC, Fauster A, Holze C, Lindsten K, Goodbourn S, Kochs G, Weber F, Bartenschlager R, Bowie AG, Bennett KL, Colinge J, Superti-Furga G. (2012) Viral immune modulators perturb the human molecular network by common and unique strategies. *Nature*. 26;487(7408):486-90.
3. Pichlmair A, Lassnig C, **Eberle CA**, Górna MW, Baumann CL, Burkard TR, Bürckstümmer T, Stefanovic A, Krieger S, Bennett KL, Rüllicke T, Weber F, Colinge J, Müller M, Superti-Furga G. (2011) IFIT1 is an antiviral protein that recognizes 5'-triphosphate RNA. *Nat Immunol*. 12(7):624-30.